

MRG-1/MRG15 is a barrier for germ cell to neuron reprogramming in *Caenorhabditis elegans*

Martina Hajduskova^{*†1}, Glkiz Baytek^{*†1}, Ena Kolundzic^{*†1}, Alexander
Godschan^{*†}, Marlon Kazmierczak^{*†}, Andreas Ofenbauer^{*†}, Maria Lena Beato
del Rosal^{*†}, Sergej Herzog^{*†}, Nida ul Fatima^{*†}, Philipp Mertins^{*}, Stefanie
Seelk-Mthel^{*†2}, Baris Tursun^{*†2}

* Max Delbrck Center for Molecular Medicine in the Helmholtz Association, Berlin,
Germany.

† Berlin Institute for Medical Systems Biology, Germany

¹ These authors contributed equally to this work.

² Corresponding authors: Stefanie.Muethel@mdc-berlin.de and
Baris.Tursun@mdc-berlin.de (lead)

Keywords: Automated Reverse Genetics; Reprogramming; Epigenetics; *C. elegans*;
MRG15; Germline; Protein Network

Corresponding author address: Max Delbrck Center for Molecular Medicine in the
Helmholtz Association, Berlin Institute for Medical Systems Biology, Robert-
Roessle-Strasse 10, 13125 Berlin, Germany

Abstract

Chromatin regulators play important roles in the safeguarding of cell identities by opposing the induction of ectopic cell fates and, thereby, preventing forced conversion of cell identities by reprogramming approaches. Our knowledge of chromatin regulators acting as reprogramming barriers in living organisms needs improvement as most studies use tissue culture. We used *C. elegans* as an *in vivo* gene discovery model and automated solid-phase RNAi screening, by which we identified 10 chromatin-regulating factors that protect cells against ectopic fate induction. Specifically, the chromodomain protein MRG-1 safeguards germ cells against conversion into neurons. MRG-1 is the ortholog of mammalian MRG15 (MORF-related gene on chromosome 15) and is required during germline development in *C. elegans*. However, MRG-1's function as a barrier for germ cell reprogramming has not been revealed previously. Here, we further provide protein-protein and genome interactions of MRG-1 to characterize its molecular functions. Conserved chromatin regulators may have similar functions in higher organisms and, therefore, understanding cell fate protection in *C. elegans* may also help to facilitate reprogramming of human cells.

Introduction

Epigenetic regulators can act as barriers for cellular reprogramming

To successfully reprogram cellular identities using transcription factors (TFs), the expression of genes that are usually repressed, need to be activated. In some contexts, forced expression of a cell fate-inducing TF is sufficient for the activation of ectopic gene expression. One classic example is the mammalian TF MyoD, which, when mis-expressed in fibroblasts, induces muscle gene expression leading to the conversion of fibroblasts into muscle cells (Davis *et al.* 1987). However, aside from fibroblasts, many cell types are less efficiently converted into muscle-like cells due to cell fate safeguarding mechanisms, that prevent ectopic gene expression based on repressive epigenetic signatures (reviewed in (Pasque *et al.* 2011; Gifford and Meissner 2012; Brumbaugh and Hochedlinger 2013; Becker *et al.* 2016)). Epigenetic regulators, including histone modifiers and chromatin remodelers, as well as a variety of different factors such as kinases and RNA-binding proteins, contribute to establishing a repressive chromatin signature and, may therefore act as barriers for cellular reprogramming.

RNAi screens in *C. elegans* to identify reprogramming barriers

The nematode *C. elegans* allows *in vivo* interrogation of such regulators for their role in safeguarding cellular identities using RNAi-mediated gene expression knockdown (Tursun *et al.* 2011; Kolundzic *et al.* 2018b). In contrast to knocking-out a gene by mutagenesis or gene editing (CRISPR/Cas9), RNAi generally leads to a partial knockdown thereby allowing the assessment of essential genes, which cause lethality when fully depleted. We applied RNAi post-embryonically to avoid early lethality, which limited a previous RNAi screen where we identified the highly conserved histone chaperone LIN-53 (CAF-1^{p48}/RBBP7 in humans) as a barrier for direct reprogramming of germ cells into neurons (Tursun *et al.* 2011).

In this study, we aimed to reveal additional factors acting like LIN-53 and identified the conserved chromodomain-containing factor MRG-1 (MORF-related gene on chromosome 15 = MRG15 in human) (Olgun *et al.* 2005; Takasaki *et al.* 2007) as a novel barrier for TF-induced germ cell conversion. In mammals, MRG15 is required for proliferation of neural precursor cells, regulation of pre-mRNA splicing during spermatogenesis (Chen *et al.* 2009; Iwamori *et al.* 2016), DNA repair and protection against genotoxic stress (Hayakawa *et al.* 2010; Bleuyard *et al.* 2017). In *C. elegans*,

MRG-1 plays a role in chromosome pairing, maintaining genomic integrity, repressing X-linked genes, and regulating proliferation in the germline (Fujita *et al.* 2002; Takasaki *et al.* 2007; Dombecki *et al.* 2011; Xu *et al.* 2012; Gupta *et al.* 2015). While MRG-1's role in germline development and differentiation to produce mature germ cells, are well described (Fujita *et al.* 2002; Takasaki *et al.* 2007; Dombecki *et al.* 2011; Xu *et al.* 2012; Gupta *et al.* 2015), its function in safeguarding germ cells against TF-induced conversion was unknown. Furthermore, MRG-1-interacting proteins and its genomic DNA-binding sites in *C. elegans* were not described previously. We performed an in-depth analysis of MRG-1's interactions with proteins and DNA using immunoprecipitations combined with mass spectrometry (IP-MS) and ChIP-seq. Interestingly, MRG-1 interacts with SET-26, which mediates repressive histone H3K9 methylation (Greer *et al.* 2014). Conversely, we found that MRG-1 associates predominantly with genomic loci carrying active histone marks, including H3K36me3 and H3K4me3. Yet, our study indicates that MRG-1 and SET-26 might cooperate to prevent conversion of germ cells into neurons.

Overall, understanding mechanisms that safeguard cell fates in *C. elegans* could help to identify conserved reprogramming barriers, as exemplified by the previously identified reprogramming barriers LIN-53 and FACT in *C. elegans* (Tursun *et al.* 2011; Kolundzic *et al.* 2018a), which could be targeted to facilitate the generation of tissues for future replacement therapies.

Results

Setup for automated chromatin RNAi sub-library screening

To perform RNAi screens for chromatin factors that safeguard cell fates, we used a previously described transgenic strain carrying the *gcy-5p::gfp* reporter, which specifically labels the ASER neuron, and the *hsp::che-1* (heat-shock promoter controlled *che-1*) transgene that allows broad mis-expression of the TF CHE-1. CHE-1 induces the fate of specific neurons termed ASER/L, but its broad overexpression does not lead to reprogramming of other cells in wild-type or control backgrounds (Figure 1A). However, RNAi against the histone chaperone gene *lin-53* allows germ cell reprogramming to ASE neurons upon *che-1* overexpression as previously described (Figure 1A) (Tursun *et al.* 2011; Kolundzic *et al.* 2018a; b). We aimed to screen for more factors that prevent *che-1*-induced reprogramming by exposing

animals to RNAi only after embryonic development (P0 RNAi) (Figure 1A).

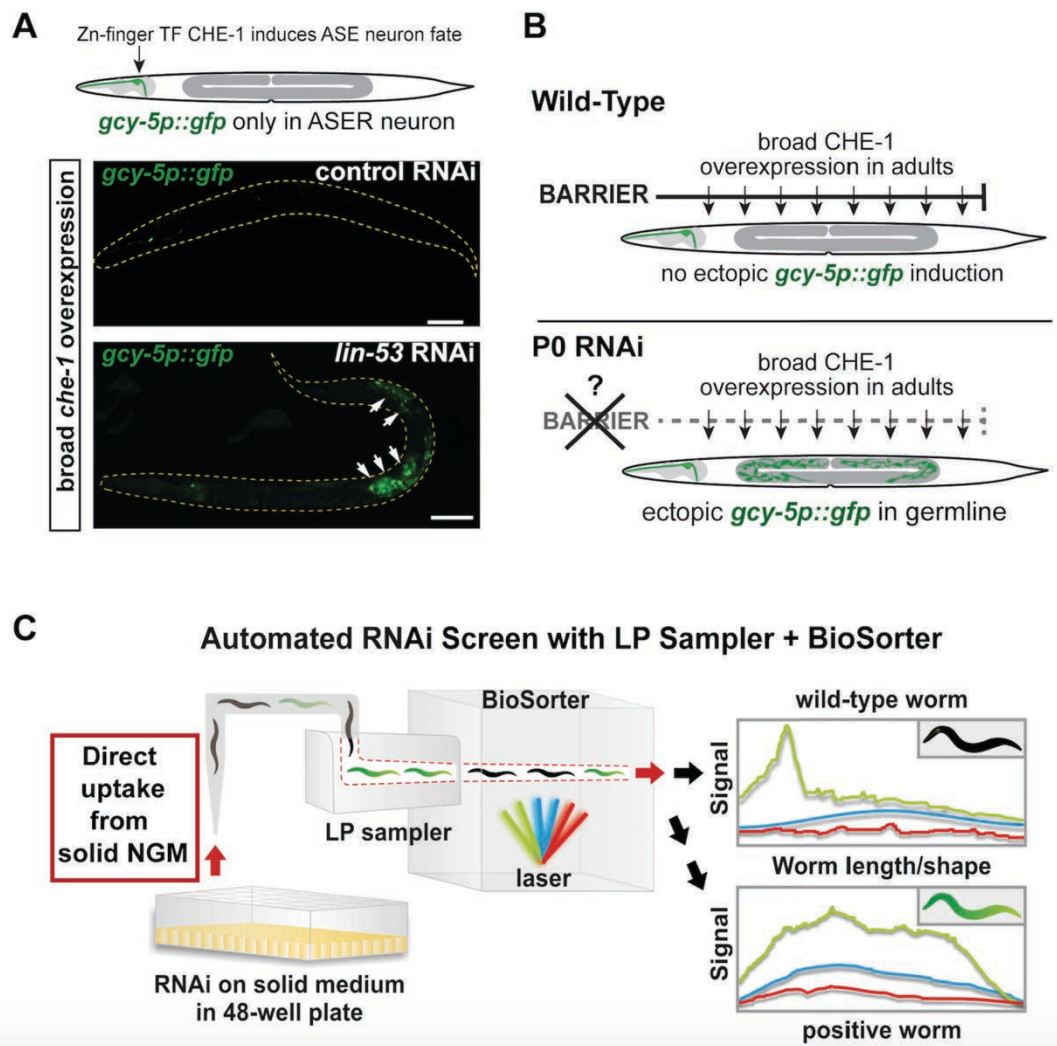


Figure 1 Automated RNAi screen for epigenetic reprogramming barriers.

(A) Mis-expression of CHE-1 and F1 RNAi against the histone chaperone gene *lin-53* (Caf1p48/RBBP4/7) on solid worm growth media allows germ cell conversion (GeCo) to ASE neuron-like cells as visualized by *gcy-5p::gfp* expression in the germline (white arrows). Scale bars = 50 μ m. (B) Ubiquitously mis-expressed TF CHE-1 is blocked by reprogramming barriers to induce the glutamatergic ASE neuron fate visualized by the ASE-specific reporter *gcy-5p::gfp*. P0 RNAi screening to identify epigenetic barrier factors, which block germ cell conversion. (C) A solid media-based automated RNAi screening system by combining the BioSorter with a robotic large-particle sampling system (LP sampler, both Union Biometrica). The LP sampler collects worms from solid RNAi medium by repeated flushing and aspiration and directly transfers worms to the BioSorter for fluorescence-intensity scanning. Detailed analysis of aspiration and sorting efficiency is shown in Table S2. Scale bars = 20 μ m.

This strategy allows the assessment of factors that cause embryonic lethality, or developmental arrest, when animals are treated with RNAi during embryogenesis by exposing their mothers to RNAi (F1 RNAi). We generated an RNAi sub-library targeting all known factors (approximately 800) that have been implicated in

chromatin regulation (Cui and Han 2007; Shaye and Greenwald 2011; Lai and Wade 2011; Wenzel *et al.* 2011) including a variety of different protein families (Figure S1A, Table S1). Since germ cell reprogramming efficiency drops significantly in liquid RNAi compared to solid media RNAi (Figure S1B), we had to establish a solid phase-based RNAi screening pipeline by combining a large-particle sorter (BioSorter) with an automated sampling system (LPsampler) (Figure 1C, Figure S2).

A previously described automated RNAi screening procedure from solid media requires manual transfer of worms to the sorting unit (Squiban *et al.* 2012). In contrast, the new setup allows a fully automated transfer of worms, which are then automatically analyzed for changes in the pattern of fluorescence (approx.20 worms/sec) (Figure S2, Table S2). The high sensitivity of this system allows for the detection of increased GFP derived from only one additional cell (Figure S2) thereby making it a sensitive and powerful tool to screen for factors that block induction of ectopic GFP expression.

The chromodomain protein MRG-1 is a barrier for germ cell reprogramming

By performing a P0 RNAi screen to identify factors that prevent germ cell to neuron conversion, in combination with the BioSorter, we detected increased GFP expression derived from the *gcy-5p::gfp* transgene upon RNAi against 10 target genes (Figures 2A-E). Depletion of different target factors create permissiveness for *gcy-5p::gfp* induction by CHE-1 in distinct tissues such as the intestine and epidermis (Figures 2A-E). We focused on the target *mrg-1* because closer examination revealed that RNAi against *mrg-1* yields a phenotype resembling the germ cell to neuron conversion (Figure 2B) as seen before for *lin-53* F1 RNAi (Figure 1A). MRG-1 is orthologous to the mammalian chromodomain-containing MRG15 – a component of the NuA4 histone acetyltransferase (HAT) complex (Chen *et al.* 2009) and has recently been shown to regulate the differentiation of germ cells in *C. elegans* (Gupta *et al.* 2015). Assessment of the ectopic *gcy-5p::gfp* induction in *mrg-1* RNAi animals, revealed that germ cells undergo conversion into neuron-like cells (Figures 3A-B) as previously observed when targeting the Polycomb Repressive Complex 2 (PRC2) genes, including *lin-53*, by RNAi (Patel *et al.* 2012).

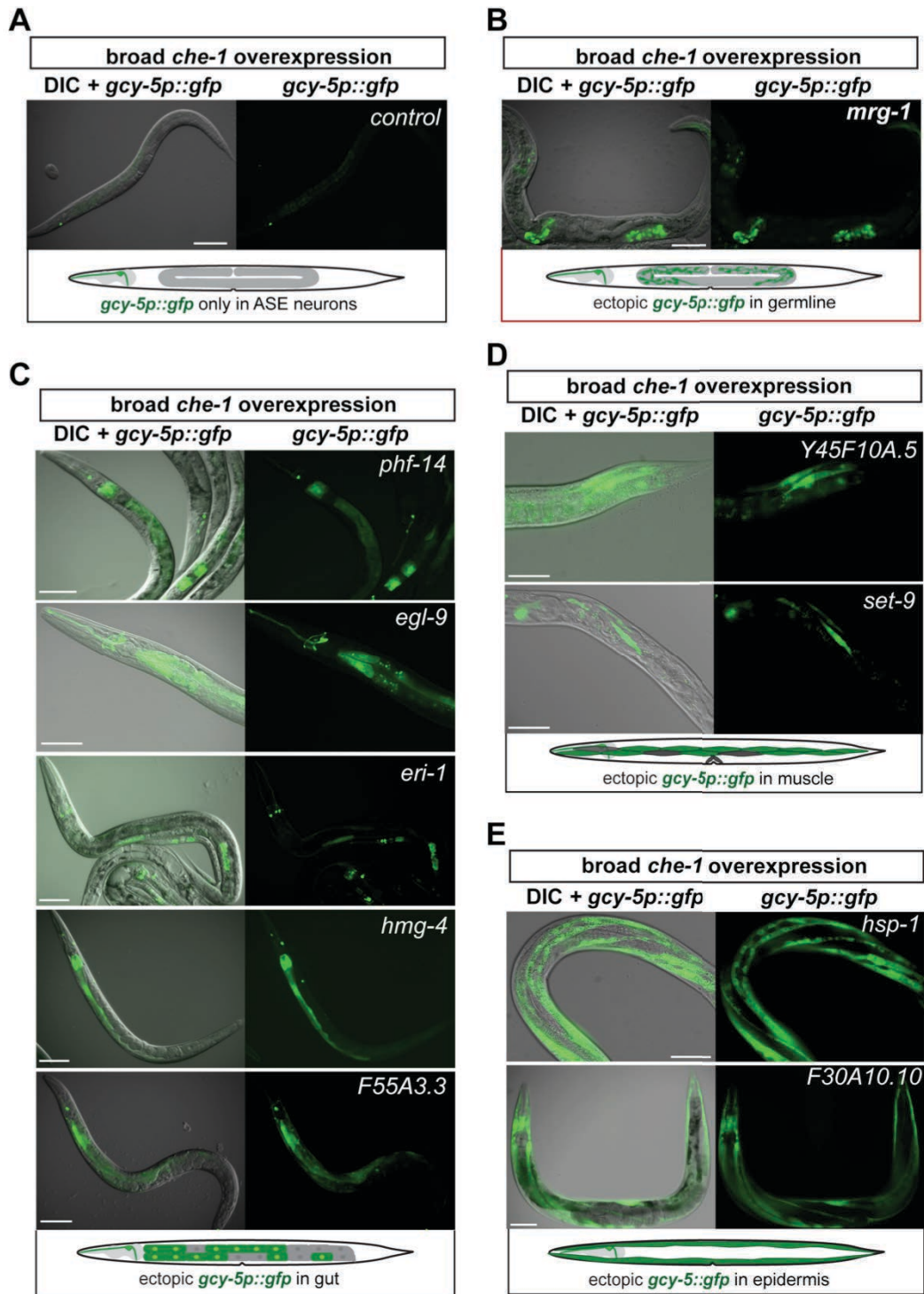


Figure 2 Ectopic expression of *gcy-5p::gfp* observed in an automated P0 RNAi screen. (A) Transgenic background *hsp::che-1*, *gcy-5p::gfp* used for screening. RNAi control worms show expression of *gcy-5* only in the ASER head neuron. (B-E) Ectopic induction of *gcy-5p::gfp* is detectable in different tissues including germline (B), gut (C), muscle (D), and epidermis (E) depending on the RNAi target. Only depletion of *mrg-1* encoding a chromodomain-containing protein (orthologous to human Mortality factor 4-like protein 1/MRG15) shows ectopic *gcy-5p::gfp* in the germline. Scale bars = 20 μ m.

RNAi against *mrg-1* without overexpressing *che-1* is not causing any ectopic *gcy-5p::gfp* induction or loss of germ cell characteristics (Figures S3A-B), which excludes the possibility that germ cells converted due to teratoma formation, as previously described (Ciosk *et al.* 2006). The converted germ cells show morphological changes with neuronal characteristics including projection-like extensions (Figure 3A) and start expressing neuron subtype-specific, as well as pan-neuronal marker genes, such as *ceh-36* (ASE/AWC glutamatergic), *osm-6* (pan-sensory), *rab-3* (pan-neuronal) and *unc-119* (pan-neuronal) (Figure 3C) (Tursun *et al.* 2011; Patel *et al.* 2012). To assess whether the neuronal reporter transgenes reflect expression of transcripts derived from endogenous genes, we performed single molecule fluorescent *in situ* hybridization (smFISH) (Figures 3D-E, Figures S3B-D). smFISH revealed that GFP-positive germ cells turn on endogenous expression of *gcy-5*, *ceh-36*, *rab-3*, the pan-neuronal RIM homolog *unc-10*, and *unc-119* with comparable levels as authentic neurons (Figure 3D-E, Figures S3B-D). Endogenous expression of these neuronal genes further corroborates that germ cells faithfully converted to neuron-like cells.

Converted germ cells upon *mrg-1* RNAi lose germline characteristics

RNAi against *mrg-1* permits germ cells to adopt neuronal characteristics by changing their morphological appearance, and turning on expression of neuronal genes upon induction of *che-1* overexpression. However, it is possible that germ cell characteristics are still preserved in cell expressing *gcy-5p::gfp*. To address this, we assessed expression of the germline-specific *pie-1* reporter (*pie-1::RFP::histone*) (Figure 4A-B) and immunostained for germline-specific P-Granules. Both germ cell-specific characteristics are lost in GFP-positive cells upon conversion (Figure 4A-B). Hence, adoption of neuronal gene expression accompanied by the loss of germ cell fate features further substantiates the notion that germ cells can be reprogrammed into ASE neuron-like cells upon RNAi against *mrg-1*. Notably, we did not observe expression of genes that belong to other neuronal fates such as interneurons or GABAergic motor neurons (Figure S4A) indicating the specificity of ASE neuron fate induction in reprogrammed germ cells by CHE-1. Hence, germ cells that fail to show *gcy-5p::gfp* but have lost germ cell characteristics may not express other ectopic cell fates.

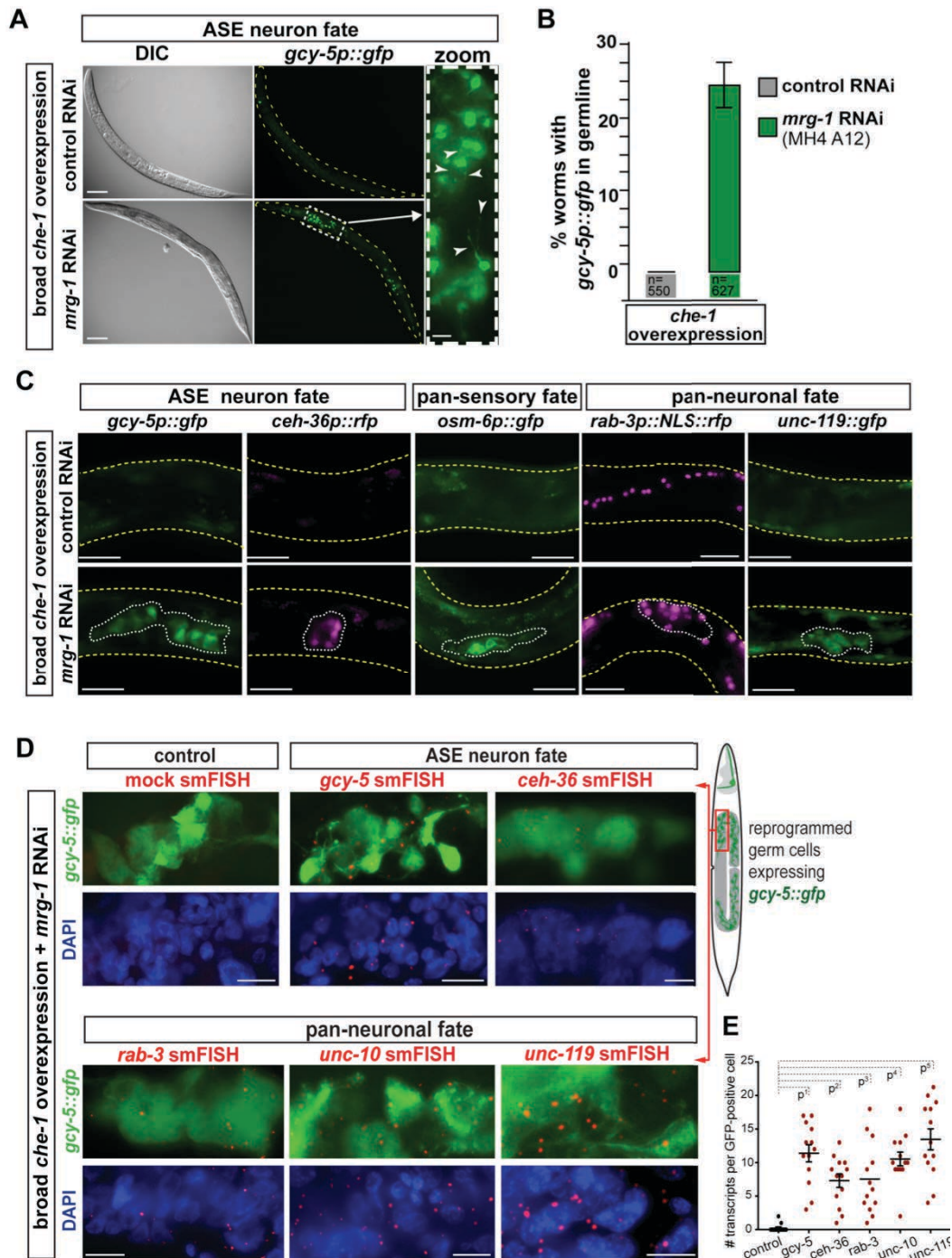


Figure 3 RNAi against *mrg-1* results in conversion of germ cells into neurons.

(A) RNAi control animals show *gcy-5p::gfp* expression only in head neurons. RNAi against *mrg-1* allows mis-expressed *che-1* to induce *gcy-5p::gfp* expression in the germline. Magnification (white stippled box) reveals that GFP-positive cells adopt neuronal morphology by showing axo-dendritic outgrowths and protrusions (white arrow heads). Scale bars = 20 μ m. (B) Quantification of animals that show GFP in the germline when treated with *mrg-1* RNAi and *che-1* mis-expression. Number of animals (n) quantified are indicated. Error bars represent SEM. (C) RNAi against *mrg-1* allows *che-1* to induce expression of additional neuronal gene reporters. *ceh-36p::rfp* is specific for glutamatergic ASE and AWC neurons, *osm-6p::gfp* is specific to pan-sensory neurons such as ASE, *rab-3p::nls::rfp* and *unc-119p::gfp* are pan-neuronally expressed genes. White lines outline areas of the germline with

GeCo. Yellow lines outline worm body. Scale bar = 10 μm . (D) Single molecule fluorescent in situ hybridizations (smFISH) to detect transcripts derived from endogenous neuronal genes in GFP-positive (*gcy-5p::gfp*) germ cells. mRNA molecules are visible as red dots. Control was incubated with mock hybridization. Scale bars, 2 μm . (E) Quantification of smFISH detections based on counts of hybridization signals (red dots) per GFP-positive cells. For each condition 20 GFP-positive cells were counted for smFISH-derived transcript detection based on fluorescence signals as exemplified in (D). p-values based on ANOVA with Dunnett's multiple comparison test: p1 = 0,0001; p2 = 0,0003; p3 = 0,0002; p4 = 0,0001; p5 = 0,0001.

MRG-1 safeguards germ cell identity independently of LIN-53 and PRC2

We wondered whether the germ cell conversion in *mrg-1* RNAi animals might be due to a loss of the previously identified germ cell reprogramming barrier LIN-53 (Tursun *et al.* 2011; Kolundzic *et al.* 2018b). LIN-53 acts with the Polycomb Repressive Complex 2 (PRC2), which represses chromatin by catalyzing methylation of histone H3K27, to counteract CHE-1-induced germ cell conversion (Patel *et al.* 2012). We examined whether *mrg-1* depletion affects *lin-53* expression in the germline. However, *mrg-1*-depleted animals with or without *che-1* overexpression, do not show obvious alterations of LIN-53 levels in the germline as assessed by immunostainings (Figure 4D). Interestingly, MRG-1 proteins only partially colocalize with LIN-53 in germ cell nuclei (Figure 4E), indicating that both proteins might have little functional overlap to protect the germline. Furthermore, RNAi against *lin-53* and other PRC2 subunits causes global loss of the PRC2-mediated histone modification H3K27me3 in the germline (Patel *et al.* 2012), which we did not observe upon *mrg-1* depletion in whole worms (Figure 4F) or specifically in the germline (Figure 4G). Overall, these findings indicate that *mrg-1* safeguards germ cells through mechanisms that are not related to PRC2-mediated regulation. Notably, *mrg-1* RNAi animals show a slight increase of the constitutive heterochromatin mark H3K9me3, as well as an increase of H3K14ac (Figures 4F-G), which has been implicated in DNA damage checkpoints in yeast (Wang *et al.* 2012). However, it is unknown which genomic DNA-binding sites are occupied by MRG-1, and, whether MRG-1 is directly linked to regulating histone modifications.

DNA-binding sites of MRG-1 in the germline and soma

To provide clues as to how MRG-1 contributes to safeguarding germ cells against reprogramming, we sought to reveal the genome-wide DNA-binding patterns of MRG-1 by performing chromatin immunoprecipitation with sequencing (ChIP-Seq).

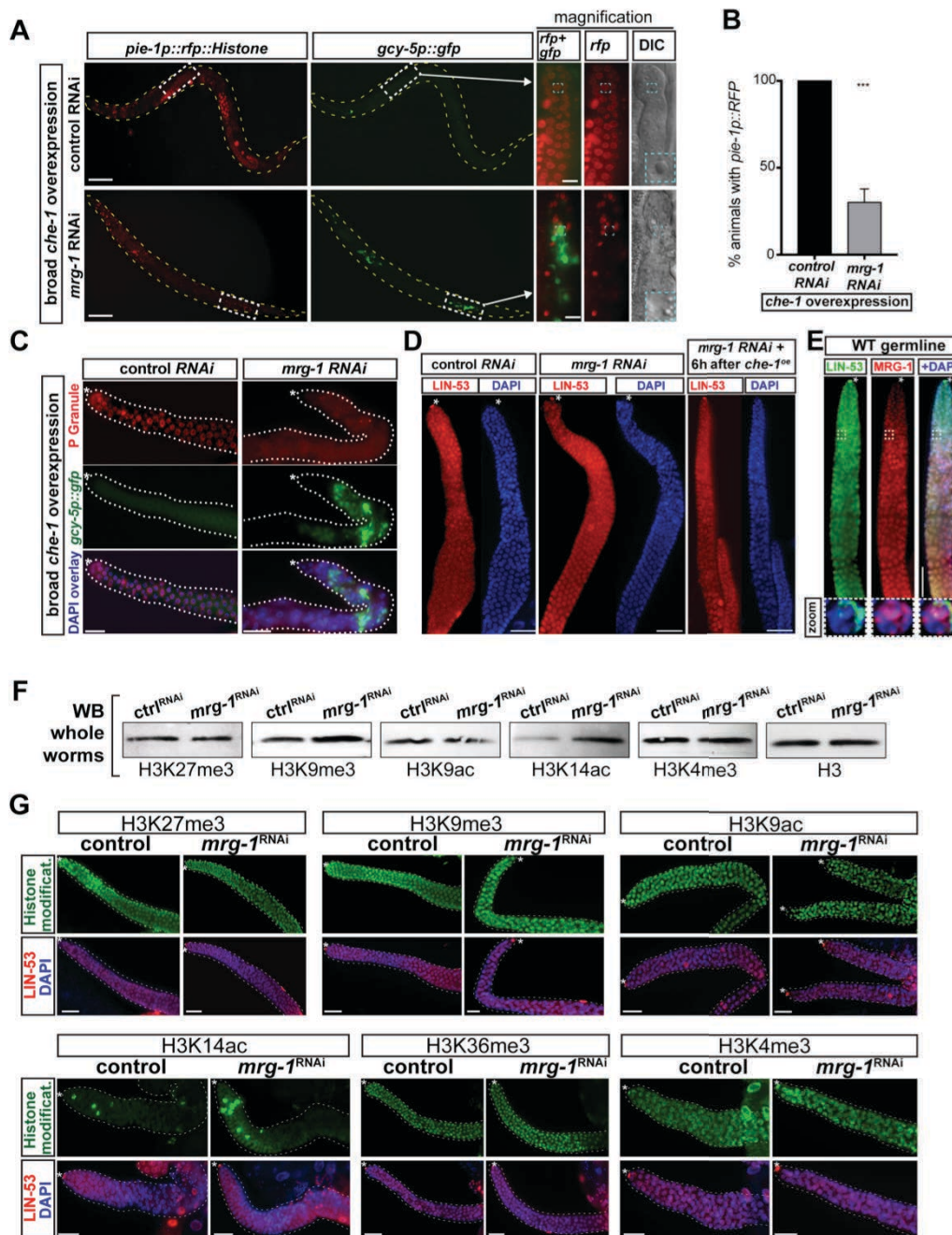


Figure 4 Changes of germline fate and histone modifications upon *mrg-1* RNAi.

(A) Induction of *gcy-5p::gfp* in *mrg-1* RNAi-treated worms leads to loss of germ cell characteristics. Expression of the germline-specific reporter *pie-1p::rfp* diminishes in cell with ectopic *gcy-5p::gfp* expression as revealed upon magnification of the germline area with germ cell conversion (white stippled box). The blue stippled boxes highlight a control and a reprogrammed germ cell that has lost the typical fried egg-shaped appearance of the nucleus and now displays a rather speckled nucleus typical for neurons. Scale bars = 50 μ m (5 μ m in magnification). (B) Quantification of *pie-1p::RFP* reporter loss in reprogrammed germ cells upon *mrg-1* RNAi. 150 animals in triplicate experiments were assessed. Error bars represent SEM. (C) Antibody staining for germline-specific P Granules upon *mrg-1* RNAi-mediated conversion of germ cells to ASE neuron-like cells. Scale bars = 5 μ m. (D) LIN-53 antibody immunostaining of young adult hermaphrodite germlines from control and *mrg-1* RNAi treated animals with and without *che-1* overexpression. Asterisk indicates distal tip of the

gonad. Scale bar = 5 μ m (E) Antibody staining of MRG-1 and LIN-53 proteins in the distal wild-type germline of a young adult hermaphrodite. The magnified germ cell nucleus in the zoom is indicated with a white stipple-line box. Asterisk indicates distal tip of the gonad. Scale bar = 5 μ m (F) Western Blot analysis of whole worm lysates from control and *mrg-1* RNAi treated worms without *che-1* overexpression using the indicated antibodies against specific histone modifications. Detection of histone H3 serves as the loading control. (G) Immunostaining of gonads from control and *mrg-1* RNAi treated worms using the indicated antibodies against specific histone modifications. Staining for LIN-53 (shown as overlay with DAPI) serves as a control for staining efficiency. Scale bars = 5 μ m.

Importantly, MRG-1 proteins can be detected in the germline, as well as in somatic cells including neurons and intestinal cells (Figure 5A, Figure S4B). To distinguish between germline-specific and somatic MRG-1 genome binding sites, we used wild-type animals and *glp-4* temperature-sensitive mutants (*bn2*) which lose the germline when grown at 25°C (Beanan and Strome 1992) (Figure 5B). Subsequent comparison of DNA-binding patterns from these two backgrounds provided information about MRG-1 DNA-binding sites in all tissues versus the germline in a highly reproducible manner (Figure 5C, Figures S5A-B, Table S3).

Overall we identified around 6723 DNA-binding sites for MRG-1 in the genome of the WT (N2) background (Figure 5A, Table S3) of which 1183 are differential peaks when compared to the germline-less *glp-4* background (Figure S5B, Table S3). Gene set enrichment analysis using PANTHER (Mi *et al.* 2013) revealed that MRG-1 target genes, in the soma and germline, are predominantly involved in the regulation of translation, RNA processing, as well as DNA replication and recombination (Figure 5D). Genes that are bound by MRG-1 exclusively in the germline regulate cell cycle and contribute to DNA metabolic processes (Figure 5D). These enriched biological processes of MRG-1 targets concur with findings from previous studies that have implicated MRG-1 and MRG15 in genome integrity, DNA recombination, mRNA processing, germline regulation and proliferation (Takasaki *et al.* 2007; Luco *et al.* 2010; Dombecki *et al.* 2011; Xu *et al.* 2012; Gupta *et al.* 2015; Iwamori *et al.* 2016). Furthermore, human MRG15 associates with the specific histone modification H3K36me3 (Zhang *et al.* 2006; Luco *et al.* 2010), which has also been proposed for MRG-1 in conjunction with the SET domain-containing H3K36 methyltransferase MES-4 in *C. elegans* (Rechtsteiner *et al.* 2010). In order to test which histone modifications are enriched at MRG-1 DNA-binding sites in *C. elegans* we made use of available modENCODE data sets (Gerstein *et al.* 2010) and analyzed the overlap of

MRG-1 peaks with different histone modifications (Figures 5E-F, Figures S6A-B).

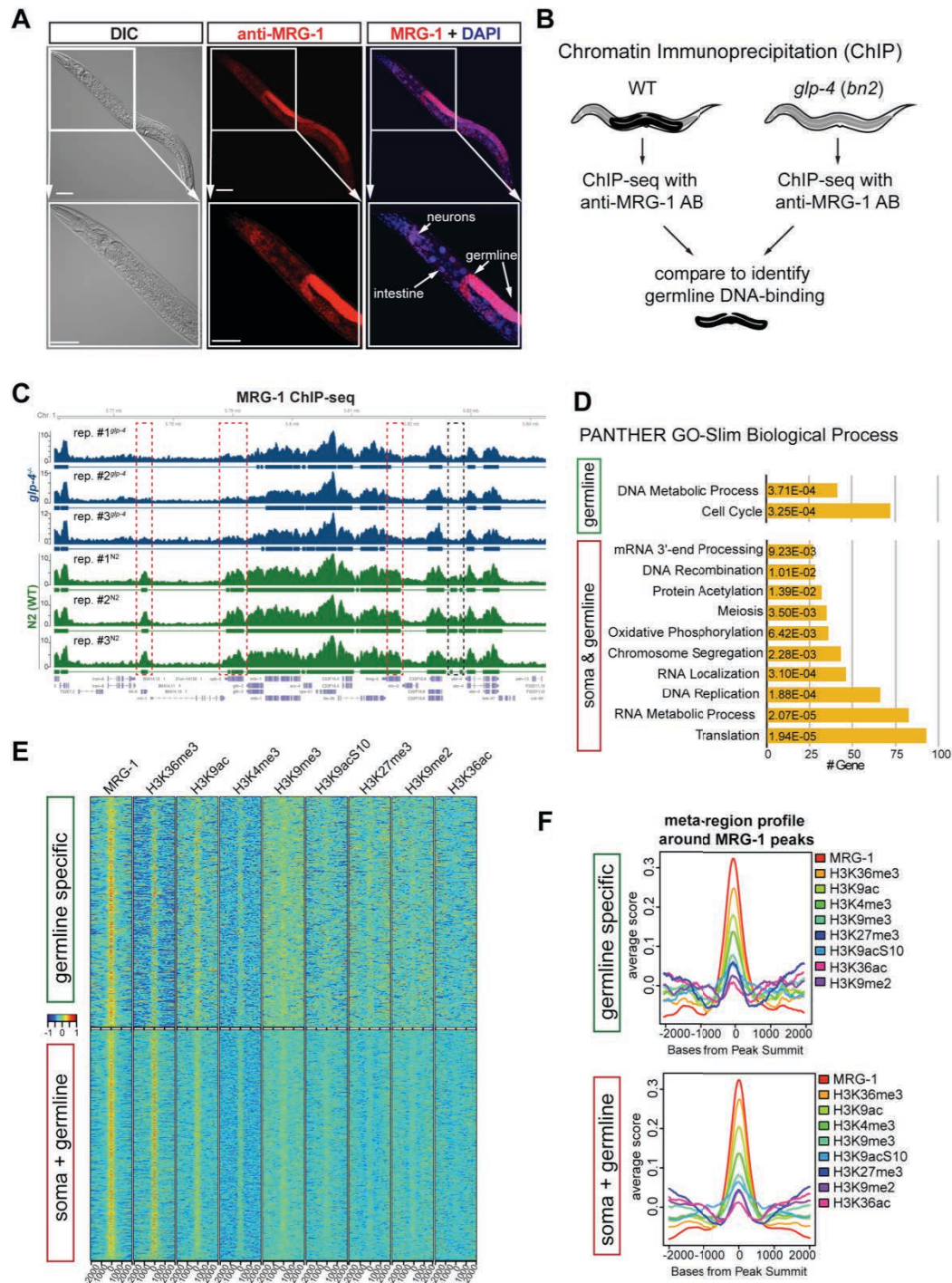


Figure 5 MRG-1 ChIP-seq in soma versus germline.

(A) Immunostaining of wild-type young adult hermaphrodite with MRG-1 antibody. MRG-1 proteins are detectable in the germline and predominantly in neurons and the intestine. Co-staining for LIN-53 is shown in S5 Figure. Scale bars = 20 μ m. (B) In order to distinguish genome-wide DNA-binding sites in the soma and germline, MRG-1 ChIP-seq was performed in WT and the germline-lacking *glp-4 (bn2)* background. (C) Browser-shot of a representative genomic region on Chromosome 1 illustrating MRG-1 ChIP-seq peaks from all three replicates for WT and *glp-4 (bn2)* background. Red boxes mark genes that cannot be detected as MRG-1 bound in the germline-less background. The black box marks an

intergenic region that cannot be detected as MRG-1 bound in the germline-less background. (D) GO-Term analysis using PANTHER of gene loci bound by MRG-1. (E) Heatmaps showing enrichment of histone modifications at MRG-1 ChIP-seq peaks overlapping in at least two of the WT samples (5141) and peaks which were only identified in WT but not in *glp-4(bn2)* background (521). The scale bar is the scaled centered peak score. (F) Meta-region profile showing the overall distribution averaged over all peaks for MRG-1 ChIP-seq peaks overlapping in at least two of the WT samples and peaks which were only identified in WT but not in the *glp-4(bn2)* background.

Soma and germline-shared MRG-1 binding sites correlate predominantly with H3K36me3, H3K9ac, and H3K4me3 while association with genomic loci carrying the repressive histone modifications H3K9me3 or H3K27me3 is rather low (Figures 5E-F, Figures S6B-C). The correlation pattern does not change drastically for germline-exclusive MRG-1-binding sites except for H3K27me3-carrying loci, which become slightly more pronounced (Figures 5E-F, Figures S6B-C). Such genes bound by MRG-1 carrying H3K9me3 or H3K27me3 may be direct targets of MRG-1 for repression (Table S4). Overall, MRG-1 predominantly binds genomic loci carrying H3K36me3, H3K9ac, and H3K4me3 which are histone modifications that mark active genes (reviewed by (Bannister and Kouzarides 2011; Tessarz and Kouzarides 2014; Hyun *et al.* 2017)), suggesting that MRG-1 might protect germ cells against conversion to neurons, not by acting as a repressive chromatin regulator, but by maintaining the genomic integrity and expression of germline components as previously demonstrated (Wu *et al.* 2012; Xu *et al.* 2012).

Protein interaction network of MRG-1

Next, we asked whether MRG-1 protects the germline fate in complex with other proteins. We therefore investigated the protein interaction network of MRG-1 by performing ‘Immunoprecipitations in combination with Mass Spectrometry’ (IP-MS). IP-MS was performed in the wild-type background using anti-MRG-1 antibodies and, in order to reduce the identification of false-positive protein interactions, we also generated a CRISPR/Cas9-mediated 3xHA knock-in to perform IP-MS using HA antibodies and compared enriched proteins from both experiments (Figure 6A). IP-MS using anti-MRG-1 yielded 100 enriched proteins while IP-MS with HA antibodies in the *mrg-1::3xHA^{CRISPR}* strain yielded 44 proteins (Figure 6B-C, Table S5). Proteins enriched in both IP-MS experiments, which we considered as the most reliable interacting proteins, were ATHP-1, F54D11.4, F59E12.1, Y14H12B.1,

and is predicted to associate with another newly identified MRG-1-interacting protein: the β -linked N-acetylglucosamine (O-GlcNAc) transferase OGT-1 (Yang *et al.* 2002; Choy *et al.* 2007; She *et al.* 2009). OGT-1 is the ortholog of the human O-GlcNAc transferase OGT and plays a role in nutrient sensing and insulin signaling pathways both of which are involved in lifespan regulation in *C. elegans* (Hanover *et al.* 2005; Love *et al.* 2010; Mondoux *et al.* 2011; Radermacher *et al.* 2014). In addition, OGT-1 can be part of histone acetyltransferase-containing protein complexes (Hoe and Nicholas 2014) (reviewed by (Gambetta and Müller 2015)) suggesting a direct involvement in chromatin regulation. In summary, our IP-MS identified novel MRG-1 interactions and excludes the possibility of direct MRG-1 association with PRC2 or MES-4. Since the newly identified interactors SIN-3, SET-26 and OGT-1 mediate chromatin regulation, they could potentially contribute to MRG-1's function in protecting the germ cell fate.

SET-26 and OGT-1 might cooperate with MRG-1 to protect germ cells

To examine whether the protein-protein interactions of SIN-3, SET-26 or OGT-1 with MRG-1 are relevant for MRG-1's function in protecting the germline fate we tested whether the mutant backgrounds *sin-3 (tm1276)*, *set-26 (tm2467)*, and *ogt-1 (ok430)* affect the *mrg-1* RNAi-mediated conversion of germ cells into ASE neuron-like cells (Figure 7A). We quantified the number of *gcy-5p::gfp*-positive cells in gonads showing germ cell to neuron conversion (Figures 7B-C). While the *sin-3 (tm1276)* mutant background showed no changes in the number of reprogrammed germ cells when compared to the control wild-type (WT) background, *set-26 (tm2467)*, and *ogt-1 (ok430)* mutations yielded an increase in reprogramming efficiency upon *mrg-1* RNAi. On average, the *set-26 (tm2467)* mutant background allowed an approximately 2-fold increase in the number of germ cells that convert to neurons, while the quantified increase in the *ogt-1 (ok430)* background by around 1.5-fold, is less pronounced (Figures 7B-C). These observed enhancements in the number of *gcy-5p::gfp*-positive cells in the reprogrammed germlines of *mrg-1* RNAi animals suggest that the newly identified interaction of MRG-1 with SET-26 and OGT-1 could be relevant for MRG-1's role in protecting germ cells against being converted to neurons (Figure 7D).

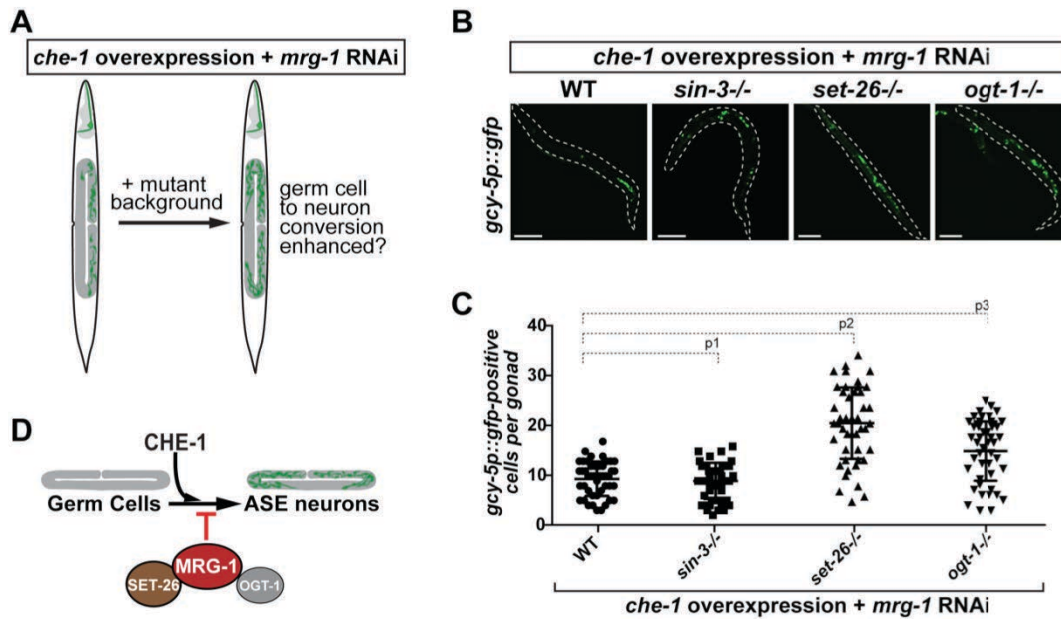


Figure 7. Enhancement of *mrg-1* RNAi-mediated germ cell reprogramming

(A) Rationale for testing animal carrying mutations of newly identified MRG-1 interactors for involvement in MRG-1's role in safeguarding germ cells. (B) The mutant backgrounds of *sin-3* (*tm1276*), *set-26* (*tm2467*), and *ogt-1* (*ok430*) were tested for enhancement of *mrg-1* RNAi-mediated germ cell reprogramming. Scale bars = 20 μ m (C) Quantifications of converted germ cells upon *mrg-1* RNAi in *sin-3* (*tm1276*), *set-26* (*tm2467*), and *ogt-1* (*ok430*) backgrounds. Number of *gcy-5p::gfp*-positive cells in individual gonads were counted. One-way ANOVA multiple comparison: $p^1 = 0,7083$; $p^2 < 0.0001$; $p^3 < 0.0001$. (D) Model illustrating that MRG-1 associates with SET-26 and OGT-1 to counteract the conversion of germ cells to ASE neuron-like cells by the Zn-finger TF CHE-1.

Discussion

Automated screening with solid-phase RNAi identified new safeguarding factors

In order to identify factors that play a role in protecting *C. elegans* cells against reprogramming to neurons, we aimed to setup an automated RNAi screening system. Because we encountered a decrease in germ cell conversion when depleting LIN-53 in liquid versus solid culture, we established an automated screening pipeline allowing worm growth on solid RNAi media. Compared to a previous procedure described by the Ewbank group (Squiban *et al.* 2012), our setup bypasses the requirement for manual transfer of animals from solid RNAi medium to the screening unit. Using our complemented Chromatin 2.0 library for a P0 RNAi screen, we identified 10 factors that prevent ectopic induction of *gcy-5p::gfp*. Interestingly, ectopic *gcy-5p::gfp* induction occurs in distinct tissues suggesting that different cell identities are protected by specific mechanisms. The investigation of such tissue-

specific mechanisms can provide further knowledge about the different modes of cell fate maintenance and protection.

MRG-1 safeguards the germ cell fate independently of PRC2

We focused on examining MRG-1, which allowed a germ cell to neuron conversion upon RNAi as recently described for components of the PRC2 complex. MRG-1 is orthologous to the mammalian Mortality Factor 4 Like 1 (MORF4L1) also known as MRG15 (Yochum and Ayer 2002; Olgun *et al.* 2005; Takasaki *et al.* 2007; Chen *et al.* 2009). We used RNAi to deplete *mrg-1* because animals carrying the *hsp::che-1* (*otIs305*) transgene in combination with balanced *mrg-1* mutants (*ok1262*, *qa6200*, and *tml227*) were not viable. Since we previously showed for *lin-53* and *mes-2* (PRC2) that homozygous mutants (M+Z-) derived from heterozygous mothers could not recapitulate the RNAi-based germ cell reprogramming due to maternal rescue effects (Tursun *et al.* 2011; Patel *et al.* 2012), we speculate that such maternal rescue is a likely scenario also for *mrg-1* (M+Z-) mutants.

Recently, MRG-1 was shown to be involved in regulating gene expression and antagonizing the germline fate in the intestine, as well as differentiating the mitotic germline to meiotic and mature germ cells in *C. elegans* (Takasaki *et al.* 2007; Petrella *et al.* 2011; Gupta *et al.* 2015). Additionally, an interplay of MRG-1 with the PRC2 complex during germ cell development has been proposed (Rechtsteiner *et al.* 2010). Since our ChIP-seq results revealed MRG-1 binding to H3K27me3-carrying genes, a cooperation of MRG-1 with PRC2 and LIN-53 could be possible. However, other findings argue against interplay between MRG-1 and PRC2 / LIN-53 in protecting germ cells against reprogramming. MRG-1 showed very limited colocalization with LIN-53 in germ cell nuclei and we could not detect protein-protein interactions with LIN-53 or any of the PRC2 subunits. Furthermore, loss of *lin-53* and other PRC2 subunits causes global H3K27me3 decrease in the germline (Patel *et al.* 2012), which we did not observe upon *mrg-1* depletion. Hence, our findings suggest that MRG-1 safeguards the germ cell fate independently of PRC2 and LIN-53.

MRG-1 and the H3K36 methyltransferase MES-4 do not physically interact

Because MRG-1 preferentially associates with DNA loci that carry the histone modification H3K36me3, which is catalyzed by MES-4 (Rechtsteiner *et al.* 2010), we hypothesized that MRG-1 and MES-4 might directly interact with each other. Interestingly, the MRG-1 ortholog Mrg15 in *Drosophila* promotes the methylation of H3K36 by reinforcing chromatin association of the methyltransferase Ash1 (Huang *et*

al. 2017) and such an interaction during chromatin recruitment has also been proposed for MRG-1 and MES-4 (Rechtsteiner *et al.* 2010). However, we did not detect an interaction of MES-4 with MRG-1 by any of the IP-MS experiments. Hence, it remains to be determined whether MRG-1 and MES-4 may indirectly cooperate in protecting the germ cell fate. Previously, MRG-1 was found to be required for X-chromosomal silencing and an indirect mechanism for its repressive effect has been suggested (Takasaki *et al.* 2007). It is possible that MRG-1 contributes to repressing chromatin in an indirect manner similar to MES-4, by helping to focus PRC2-mediated methylation of H3K27 (Gaydos *et al.* 2012). Since MRG-1 depletion does not lead to a detectable loss of H3K36me3, we speculate that the genomic distribution of H3K36me3 might be altered upon *mrg-1* RNAi that, in turn, could affect gene repression.

MRG-1 binds to genes that regulate metabolism, replication, and cell cycle

Overall, genes bound by MRG-1 are enriched for functions in DNA metabolism, replication, and cell cycle as well as chromosome segregation which is in line with recent findings that MRG-1 and its ortholog MRG15 are implicated in chromosomal break repair and homologous pairing (Garcia *et al.* 2007; Hayakawa *et al.* 2010; Dombecki *et al.* 2011). Therefore, it is possible that a lack of MRG-1 leads to DNA damage thereby causing the observed increase of H3K14ac in the *mrg-1* RNAi germline - an effect that has previously been shown in yeast and mouse (Kim *et al.* 2008; Wang *et al.* 2012). An increase in H3K14ac might lead to a decreased efficiency of H3K9 methylation, as previously suggested (Alvarez *et al.* 2011), which results in lowering or redistributing repressive chromatin marks in the germline. Nevertheless, how such negative crosstalk between these histone modifications might be regulated remains to be determined.

MRG-1 associates with different chromatin-regulating factors

The interaction of MRG-1 with different chromatin-regulating complexes could provide clues as to how MRG-1 functions at the molecular level. As shown for its mammalian ortholog MRG15 (Yochum and Ayer 2002; Doyon *et al.* 2004; Chen *et al.* 2009), we found an interaction of MRG-1 with SIN-3, the ortholog of the mSin3A histone deacetylase complex (HDAC) subunit. Notably, we also identified the ortholog of the human O-GlcNAc transferase (OGT) OGT-1 as a novel MRG-1-interacting protein. OGT has been shown to interact with Sin3A in mammalian cells and is thereby being recruited to promoters of repressed genes (Yang *et al.* 2002),

indicating that MRG-1 might form a complex with an OGT-1-containing Sin3 HDAC. Yet, the *Drosophila* ortholog of OGT-1 was initially identified as a member of Polycomb group (PcG) class proteins, which are repressive chromatin regulators (Ingham 1984). Additional studies suggest that OGT-1 can be part of histone acetyltransferase-containing protein complexes (Hoe and Nicholas 2014)(reviewed by (Gambetta and Müller 2015)). As one of the most consistent MRG-1-interacting proteins we identified the H3K9 methyltransferase SET-26 (Greer *et al.* 2014). SET-26 plays a role in the transgenerational sterility of *spr-5* mutants and a *set-26* mutation suppresses developmental defects seen in animals lacking the NuRD and MEC complex subunit LET-418 (Mi2) (Greer *et al.* 2014; Erdelyi *et al.* 2017). Interestingly, we observed a slight increase in H3K9 methylation in *mrg-1* RNAi animals, which has previously been reported for *mrg-1* mutants (Xu *et al.* 2012). This effect is counterintuitive because we assumed that *mrg-1* depletion causes more open chromatin based on the observed permissiveness for reprogramming. Furthermore, association of MRG-1 with H3K9 methylated genomic sites, even though to a limited degree, indicated that SET-26 might be directly involved in MRG-1's role as a barrier for germ cell reprogramming. Interestingly, the *set-26* mutant background significantly increased germ cell reprogramming upon *mrg-1* RNAi, while a modest enhancement could also be observed for the *ogt-1*, but not for *sin-3*, mutant background. Based on the high reproducibility of the protein interaction data we therefore suggest that MRG-1 forms a complex with SET-26 and OGT-1 in order to counteract the conversion of germ cells to neuron-like cells. However, we cannot exclude the possibility that SET-26 and OGT-1 contribute to germ cell protection also in parallel to their interaction with MRG-1.

Overall, we demonstrate the value of enhanced RNAi screens for identifying factors that safeguard cellular identities and the use of *C. elegans* as a gene discovery tool. In light of recent findings illustrating conservation of reprogramming barriers from worms to mammalian tissues (Tursun *et al.* 2011; Cheloufi *et al.* 2015), further genetic screens using different cell fate-inducing backgrounds in *C. elegans* have the potential to identify other context-specific factors that regulate cellular reprogramming, both in *C. elegans* and other species.

Acknowledgments

We thank Alina El-Khalili, Oliver Popp, and Tim Wolfram for technical assistance and Mei He for support with immunostainings. We also thank the CGC, supported by the NIH, for providing strains and Holger Richly as well as Giono Poulin for providing RNAi clones. We thank Anna Reid for discussion and comments on the manuscript and Rico Bongaarts and Francis Smet for technical support with the BioSorter. This work was partly sponsored by the ERC-StG-2014-637530 and ERC CIG PCIG12-GA-2012-333922 and is supported by the Max Delbrueck Center for Molecular Medicine in the Helmholtz Association. All procedures conducted in this study were approved by the Berlin State Department for Health and Social (LaGeSo). The authors declare that they have no competing interests.

Authors' contributions

MH, SS, GB, and EK conducted the experiments, analyzed the data, and helped with the experimental design. AG used bioinformatics to analyze IP-MS and ChIP-Seq data, GB, MK, NF, and AO conducted experiments, SH conducted experiments and maintained the animals. PM helped with IP-MS experiments. BT conceptualized and designed the project, and finalized the manuscript. All authors read and approved the final manuscript.

Methods

Worm strains

The wild type *C. elegans* Bristol strain (N2) and strains without heat-shock constructs were maintained according to the standard protocol (Stiernagle 2006) at 20°C. Transgenic lines carrying heat-shock constructs were grown at 15°C unless indicated otherwise. The following strains were used in this study: BAT28 *otIs305[hsp-16.2p::che-1::3xHA, rol-6(su1006)] ntIs1[gcy-5p::gfp, lin-15(+)] V*, BAT29 *otIs284[hsp-16.2p::che-1::3xHA, rol-6(su1006)] ntIs1[gcy-5p::gfp, lin-15(+)] V*, BAT30 *otIs264[ceh-36p::tagRFP]*, OH3192 *ntIs1[gcy-5p::gfp, lin-15(+)] V*, BAT326 *otIs263[ceh-36p::tagRFP]; otIs305[hsp-16.2p::che-1::3xHA] ntIs1[gcy-5p::gfp, lin-15(+)] V*, BAT483 *ogt-1(ok430) III.; otIs305[hsp-16.2p::che-1::3xHA, rol-6(su1006)] ntIs1[gcy-5p::gfp, lin-15(+)] V*, BAT522 *otIs305[hsp-16.2p::che-1::3xHA, rol-6(su1006)] ntIs1[gcy-5p::gfp, lin-15(+)] V; otIs393[ift-20p::NLS::tagRFP]*, BAT527 *otIs355[rab-3p::NLS::tagRFP] IV?; otIs305[hsp-16.2p::che-1::3xHA, rol-6(su1006)] ntIs1[gcy-5p::gfp, lin-15(+)] V*; BAT606 *edIs6[unc-119p::GFP, rol-6(su1006)]; otIs305[hsp-16.2p::che-1::3xHA, rol-6(su1006)] V*, RB653 *ogt-1(ok430) III.* (obtained from Gene Knockout project at OMRF); *otIs305[hsp-16.2p::che-1::3xHA, rol-6(su1006)] ntIs1[gcy-5p::gfp, lin-15(+)] V*; BAT32 *glp-1(ar202) III, ntIs1 otIs305 V*, BAT1940 *sin-3(tm1276); otIs305 ntIs1 V*, BAT1939 *set-26(tm2467); otIs305 ntIs1 V*, BAT483 *ogt-1(ok430); otIs305 ntIs1 V*, , SS104 *glp-4(bn11)*. BAT2019 *mrg-1(bar33[mrg-1::3xHA]) III* (CRISPR/Cas9).

Synchronized worm population

Synchronized worms were obtained by two standard techniques: bleaching or harvesting early hatched L1 worms. For bleaching, gravid hermaphrodites were treated with sodium hypochlorite solution as previously described (Ahringer 2006). Household bleach (5% sodium hypochlorite) was mixed with 1M NaOH and water in the 3:2:5 ratio. Worms were washed from NGM plates with M9 buffer containing gelatin (0.05% w/v), incubated in bleaching solution for 5 minutes in a 1:1 ratio, vortexed and following worm lysis, eggs were washed three times with M9 buffer. For harvesting L1 worms, plates containing shortly starved adults and freshly hatched L1 larvae were used. Worms were collected into 1.5-ml tubes by washing twice with 800 µl of M9 buffer + gelatin. Tubes containing worms were left to stand for 2

minutes to allow the separation of the two stages. Adult stage worms sink faster in a solution compared to larvae because they are heavier. Within 2 minutes, adult worms are pelleted at the bottom of the tube, whereas L1 larvae are still swimming near the surface of the solution. The top two thirds of M9 buffer, containing mostly larvae worms, was transferred into a fresh 1.5-ml tube and L1 larvae were collected by centrifugation at 900 g for 1 minute. Harvested L1 larvae or eggs obtained by bleaching were either applied directly onto RNAi plates or regular NGM plates for further maintenance of synchronized population.

Generating the chromatin RNAi sub-library

Candidate genes for the chromatin RNAi sub-library were chosen based on the presence of characteristic protein domains (<http://www.uniprot.org>), known function in chromatin modifications and remodeling, and any direct or indirect link to chromatin function. The RNAi sub-library was generated by compiling existing RNAi clones from the Ahringer and Vidal RNAi libraries. The list of RNAi clones in the library can be found in the S1 Table. The identity of all RNAi clones was verified by sequencing. Clones that did not exist in the RNAi libraries or clones for which sequence was incorrect, were replaced by newly built RNAi clones (S1 Table). Primers were designed to amplify a unique sequence for each gene of interest (preferably cDNA). PCR products were cloned into the L4440 vector followed by transformation into HT115 (DE3) bacteria. Resulting clones were verified by sequencing. All RNAi clones were grown on plates containing 12.5 µg/ml tetracycline (selection for presence of T7 polymerase and RNase III mutation) and 50 µg/ml carbenicillin (selection for L4440 plasmid) to ensure RNAi efficiency in future experiments. Correct RNAi clones (730 in total) were compiled into the 96-well-plate format S1 Table. Deep-well plates containing 1 ml of LB medium with 50 µg/ml carbenicillin per well were prepared using an automated dispensing machine (MultidropTM Combi Reagent Dispenser, Thermo Scientific). Inoculated RNAi bacteria were grown by shaking overnight at 37°C. Grown bacterial cultures were mixed with glycerol (13% final concentration) and stored at -80°C for further use.

RNAi screening

We used the strain BAT28 to screen for ectopic expression of the glutamatergic neuronal marker *gcy-5p::gfp* upon induction of the transcription factor CHE-1.

Conditions for both automated and manual RNAi have been optimized for solid media to allow precise and fast control of the right developmental stage for *che-1* mis-expression. RNAi screening of the chromatin sub-library was performed using the feeding technique, as described previously with slight modifications (Kamath *et al.* 2001). As indicated in the screen workflow in Figure S2B, we aimed to automate as many steps as possible. L1 worms were grown on solid RNAi medium in 48-well plates at 15°C until the L4 stage and heat shocked for inducing ubiquitous mis-expression (Tursun *et al.* 2011) of the ASE neuron fate-inducing TF CHE-1. 16 h later the BioSorter + Large Particle (LP) sampler setup was used to automatically screen for ectopic *gcy-5p::gfp* expression. We performed the P0 screen, where synchronized L1 larvae were applied on RNAi plates, and scored adults of the same generation (P0). Standard NGM agar medium, supplemented with 50 µg/ml carbenicillin and 1 mM IPTG, was used to pour 48-well or 6-well RNAi feeding plates. The 6-well RNAi plates were dried overnight at room temperature, and then stored at 4°C until use. Because the 48-well RNAi plates tend to dry out quickly, freshly-poured plates were directly turned upside-down, transferred into a humid chamber (plastic box with wet paper towels) and stored at 4°C. The 96-deep-well plates containing 1.2 ml of LB medium with 50 µg/ml carbenicillin/well were poured using the automated dispensing machine (Multidrop™ Combi Reagent Dispenser, Thermo Scientific) and then inoculated with RNAi clones of the sub-library and grown by shaking at 37°C. For the manual screen, bacteria grown for sixteen hours were centrifuged for 5 min at 300 g, 800 µl of the supernatant was removed and the bacterial pellet resuspended in the remaining LB medium. Resuspended bacteria were seeded in duplicates on 6-well-RNAi plates (30 µl/well) and dsRNA synthesis was induced overnight at 37°C. The following day, synchronized worms at the L1 stage were added to RNAi plates (100 - 200 larvae/well) that had been pre-cooled to 15°C to avoid heat shock. To minimize the co-transfer of OP50 bacteria, worms were washed three times with M9 buffer prior to plating. Worms on RNAi plates were kept at 15°C until they reached the L4 stage, at which time they were heat-shocked at 37°C for 26 minutes to induce expression of CHE-1. Following heat shock, RNAi plates were shifted to 25°C and scored approximately sixteen hours later. To check for ectopic expression of the *gcy-5p::gfp* reporter, we used the Olympus MVX10 and Leica M205 FA dissecting microscopes. For the automated screen, the liquid cultures of RNAi bacteria were centrifuged as described above and the majority of the

supernatant was discarded by quickly inverting the 96-well plates. Bacterial pellets were resuspended by vortexing in the remaining medium and from this suspension, 10 μ l was used for seeding the 48-well plates. Seeded 48-well plates were placed under the fume hood for one hour to dry the bacterial lawn. Subsequently, plates were incubated in humid chamber at 37°C overnight. The following day, seeded plates were cooled-down to 15°C before applying synchronized worm populations. If necessary, seeded 48-well plates could be stored at 4°C for maximum three days. The concentration of worm eggs or L1 larvae in M9 medium was adjusted to 100 individuals/5 μ l and this volume was pipetted on each well of the RNAi plates. Worms on RNAi plates were incubated under the fume hood for five minutes to let the M9 medium be absorbed. Afterwards, worms on RNAi plates were kept in a humid chamber at 15°C until they reached the L4 stage. For the heat-shock treatment, 48-well plates were sealed in plastic bags and floated with the agar side up in a water bath at 37°C for 8 minutes. After heat shock, worms on RNAi plates were placed back into the humid chamber and kept at 25°C for approximately sixteen hours. The following day, we screened worms for ectopic *gcy-5p::gfp* signal using the Large Particle (LP) Sampler in combination with the BioSorter Large Particle Flow Cytometer (Union Biometrica). Before BioSorter analysis, RNAi plates were incubated at 4°C for one hour to immobilize worms and straighten their body. This step eliminates artifacts during fluorescence acquisition caused by worm bending and clustering. The LP sampler aspirated worms from each well of the 48-well plates containing solid RNAi media. Worms were individually passed through the BioSorter system. Measurement of axial length and optical density allowed exclusion of young animals from the analysis. Worms were scored positive based on the GFP profile along the body length. Red fluorescence was used to subtract the autofluorescent background of worms. We used FlowPilot software for the BioSorter screen and data analysis. Subsequent data processing was performed using Excel.

Antibody Staining

Antibody staining was performed using a freeze-crack protocol on whole worms (Duerr 2006; Hadwiger *et al.* 2010) (Duerr, 2006). After washing worms were placed between two SuperFrost Plus slides and frozen on dry ice for 30 minutes. Worms were cracked by quickly breaking up the slides and immersed in PFA or ice-cold methanol for 5 minutes at RT. After washing once in PBS, worms were incubated for

30 minutes in blocking solution (1x PBS, 0.25% Triton X-100, 0.2% Gelatine, 0.04% NaN₃, ddH₂O) at 25°C. Primary antibody incubations were performed at 4°C for 4 h – 12h and secondary antibody incubations for 2 h at room temperature. Primary and secondary antibodies were diluted in PGT (1x PBS, 0.25% Triton X-100, 0.1% Gelatine, 0.04% NaN₃, ddH₂O). After washing off the secondary antibodies, worms were mounted on glass microscopy slides in DAPI-containing mounting media.

Histone modifications were detected with rabbit polyclonal anti-H3K27me₃ antibody (Cat.# 07-449, Milipore), rabbit polyclonal anti-H3K9me₃ (Cat.# ab8898, Abcam) rabbit polyclonal anti-H3K4me₃ (Cat.# ab8580, Abcam), rabbit polyclonal anti-H3K9ac (Cat.# ab4441, Abcam), rabbit monoclonal anti-H3K14ac (Cat.# ab52946), and mouse monoclonal anti-H3K36me₂ (gift from Dr. Hiroshi Kimura; Graduate School of Frontier Biosciences Osaka University). We co-stained with monoclonal guinea pig anti-LIN-53 (Pineda). All primary antibodies were diluted at 1:200.

Secondary antibodies were AlexaFlour488 Goat Anti-Guinea Pig (Cat.# A11073, Mol Probes), AlexaFlour568 Goat Anti-Rabbit (Cat.# A21069, Mol. Probes), and AlexaFlour488 Goat Anti-rabbit (Cat.# A11070, Mol. Probes, All secondary antibodies were diluted at 1:1500.

Single molecule fluorescent in situ hybridizations (smFISH)

smFISH probes against *gcy-5*, *ceh-36*, *rab-3*, *unc-199*, and *unc-10* transcripts were custom ordered from Stellaris and used according to the manual provided by Stellaris for hybridizing FISH probes. smFISH probe set sequences:

gcy-5

cattcggatgctccaagaac; caattccaactcgaagcgtc; caattggaagagtccacca;
tatecattcggatattcc; tccactacaacatctacat; tattggtatcagccaactgg;
tgccactcgatcaaattgga; tttacagtagtcttggtcgt; ctttaaggtgcctcaacatc;
atccgactggatagatc; cgatcttgtaatgcctcat; tacgagctcgactctttaca;
ggaccactaattgcgcataa; ccaatactcctcattgtcaa; tcttcccaaactgttgt;
tggagtagtccattgcaa; ctactgtgaatgactcccaa; atttctaacagcatccgcaa;
tgccatcccgtataagtaaa; tagtaaccattgcccgcata; gcggtagagatttgaccaa;
tcatgttaactagtccact; ccgtgacaattgcgaagacg; cgttttcttttgggcat;
gtgactctcgactattggc; actttctccggttatagttg; gctatgatgttgggtgta;
atttctcttctcttcttta; ggtccatcgatagataatcc; gatatcctgaagtgatectc;
aaagttcataccctctgcaa; ggcaagtagctgaacgtaga; ctcccaatccaaaatctgtt;

tacgatttctccttttttc; aagtattaactccggtcgga; acttgcaaattgctcagct;
gtctgcaacttgtttggga; tctccaattgattccacttt; tgcggttaaccagaaacac;
ggaacctgaagetcttaca; gcccactattaattccaatt; atggatagaccaacgacacc;
gtatcccaaataggcaata; ttccacttcttccattct; tgtgcagcttctgacatatg;
tctcctcttgaactgtttc; tgtttccattacaccttttc; gattttgtgtcactgtcagt;

ceh-36

gtgtagaagttggtggcat; ggataagcagtgtagccgag; tgcggcagcaaatgcaaatt;
atgtaagactgggtgccgtg; cattgtcgttgagcttggg; ttcactgtttggagccattg;
ctctgttgaacgaggtacgt; tttccagctgatcagttg; gatactgtgtttcgcggaaa;
gcttcttctgtgcacatc; caaattgattgccttcgcca; ttactgtacccttccatca;
cgattttgaaccaaaccgt; gttgtttctatccttggctc; gatggactccatccatttt;
gatcttgatgaagtcttcc; cgttgtgtggagaaccattg; gtgatttagtatcaggcttt;
tgtcctggatgtgaattc; cactgtgtcattgaattcc; gagttgcctcatattggc;
ttgcagttgactcaagactg; agtctccagttcactttt; atttggtatctgcaagtggg;
cttgagcctgaggaagaagt; agttgcgtaggatgcatatg; tagttgtacgggtaaggagc;
gtttgatgggaagtagctgt; tgcttccatattgttgtag; aggcagtaaatattggggtg;

rab-3

caaagtctgatcgggtgt; atcaggagcttgaacatgta; tccaactgatgaattccga;
catcacagtaacggaagagg; gtagagacgaaggcagaagt; cactttgaaatcgattccga;
ttgtctccacggaacacag; ggtatcccagattgaagt; gatagtaggcgggtggtgatg;
cagaatgaatccattgctc; actcttcattagtgatgtca;gcaccaatcctgaacactat;
ttccatgagtatgtctg; ccaacaaaacaactgagc; ttcagagtccatatacatt;
ccctatccatagatacaact; aagttgatcagcaagttggc; ggctgatgtttcgaagaatt;
cctttacattaatgttctcc; tctccaccaacttctcaaaa; tctgccatcttatacaaat;
ctgtgggtccttatccaaac; ttcgagcttctgtcctttg; aattgcattgctgttgagca;
attgcgtttggaattggga; agagctacgcgcttttagaa; cctagatgttgagagaggga;
ttacgatccatatactgg; taattaaaccaactacgcc; ggggaatatgattgaacgtt;
gctctgggaattgttggaa; ggcgactatgattagttaga; tgggaactgggaagtcacta;
aatcaatcttccagcgggtg; cctcgaataaatttctcc

unc-10

taaatccggcatcatcgacg; ttacgttcttctgcagata; ccgtgatctgtttgtctaac;

agatttgacagatcgctca; caattccgtccgcaaatttg; cagattgccttatttttgc;
gattttgactcattggctgt; catattctgattgtggctct; tttgtcctttgttggtttg;
aggcgtttgttcatagttc; tctgttggtccatgttgatt; attctctctcattctgtgt;
tctcggaattccagtgtag; ggttgttttgggtctgattc; ggttcaaatggctcgtcagta;
tcgaagttgcctatgcaate; cgagttttatgatcgccat; atggtgacaaggacagcgat;
ccctgttccaaaatgatcat; tggctgcagaattttcagtt; gtaatgaatgcaccgagctt;
atgtggcattttgcagagac; ttgcagc gatgctatcatat; gaatacgcggaggatgacat;
gatggatatgcagatggcac; ggctgattgtgaatgtggta; gatgtcgaacgattgcgtga;
gagcaactgagagttgtcga; aaactggcatgagtgctct; ggttcagtaagccattata;
tcgtaatcccagacagttag; gtcatttggggcaagatgat; tcgtcgtcgtcaatgtattc;
atgatcagatgtgtagcctg; tgttgatcgtacatacct; tccatcactataatcctt;
cattgtagtggcatgctat; aaacttttcttctcctt; cctcagatctagcaaaaccg;
gtgagccgatctgaagacaa; cttgcttcagaaaggagga; gcaaactgtctgagtgagc;
aagcacttgacgaccgacaa; cttttacataggagctgga; tttggcaatgcattgtttgc;
ttccatacagaccgtaatac; tttcgaaatccccatgaat; cagttataaccacctatta;

unc-119

cgatcgattgttgttggc; catctgagacgggaagggtg; gttatagcctgttcggttac;
tgatttttcgcgagaagctc; agagctagcacatcatttgg; gcataggaatccttgagtga;
ttatagacgtttgccgatgg; cgaggtcacggatttggat; gcaatttcgaagagcacgtg;
attctcttccgtctcatttt; gatatcggacatatcttggc; aatgtgtgatcggcacatcg;
aagtgcggttcaatcattcg; gcatttcaataaacgatcct; ggcatacagaatccaaattc;
tgttcacagttgttctcga; gttgtgtgaaagttgtgga; attattgatcatgtcgtcca;
aatagaagctatcggagcgg; gtgcattacgagcttattct; tgcatacagagtagtcgg ;

Western Blot

Control and *mrg-1* RNAi treated worms were washed off, collected in SDS/PAGE Sample buffer and frozen at -20°C. Immediately before loading, samples were boiled for 10 minutes and centrifuged. Histone modifications were detected with rabbit polyclonal anti-H3K27me3 antibody (Cat.# 07-449, Milipore) at a dilution of 1:1000, rabbit polyclonal anti-H3K9me3 (Cat.# ab8898, Abcam) at 1:1000, rabbit polyclonal anti-H3K4me3 (Cat.# ab8580, Abcam) at 1:1000, rabbit polyclonal anti-H3K9ac (Cat.# ab4441, Abcam) at 1:500, and rabbit monoclonal anti-H3K14ac (Cat.# ab52946) at 1:2000.

As a standard loading control, we used the rabbit polyclonal anti-histone 3 (Cat.

#ab1791, Abcam) at 1:5000 dilution and the secondary anti-mouse HRP antibody (Cat.#sc-2005, Santa Cruz) at 1:5.000 dilution or anti-rabbit HRP antibody (Cat.#sc-2357, Santa Cruz). The Lumi Light detection kit (Roche) and the ImageQuant LAS4000 system (GE Healthcare Life Sciences) were used for the signal detection.

Generation of CRISPR alleles. CRISPR engineering was performed by microinjection using a PCR repair template containing the 3xHA tag sequence. The injection mix contained Cas9 protein (0,3mg/μl), as well as a crRNA targeting *mrg-1* (100ng/μl). Overall, we used a recently described procedure (Dokshin *et al.* 2018).

Sequences of the crRNA are: 5'GGATCTCTCGCCGCCGACGA3', 5'GTTCGCTCCAACCTCCGTCGT3'.

Immunoprecipitations coupled with Mass Spectrometry (IP-MS)

Each immunoprecipitation was performed in triplicate. L4 staged wild type and *mrg-1::3xHA^{CRISPR}* worms were collected by M9 buffer, washed 4 times with M9 to get rid of bacteria and concentrated into worm pellet after the last wash. The worms were added into liquid nitrogen, drop-by-drop by paying attention that the resulting “worm beads” did not exceed size of a black pepper to achieve even grinding afterwards. The frozen worms were then cryo-fractured by using a pulverizer. In order to obtain a fine powder, worms were further ground using a mortar and pestle on dry ice. The worm powder was resuspended in 1.5x of lysis buffer (20mM Hepes pH 7.4, 150mM NaCl, 2mM MgCl₂, 0.1% Tween20 and protease inhibitors), dounced with tight douncer 30 times and sonicated using a Biorupter (6 times 30 sec ON, 30 sec OFF; high settings) followed by centrifugation at 16,000g at 4°C for 10 min. The supernatant was removed to 2 mL Eppendorf tubes and incubated with following antibodies: N2 lysates with anti-MRG-1 (Novus) or with preimmune serum for control samples; *mrg-1::3xHA^{CRISPR}* and N2 lysates (negative control) with HA antibodies (Roche) for 30 min on a rotator at 4°C. Next, μMACS ProteinA beads (Milteny Biotec) were added into samples as instructed in the kit and samples were incubated for 30 min at 4°C rotating. Meanwhile, the μMACS columns were placed to magnetic separator to be equilibrated and ready for sample application. Samples were diluted 5x of their volume with lysis buffer before being applied to columns and the columns with bound proteins were washed 3 times with lysis buffer to remove background binders. The proteins were eluted with elution buffer (100mM TrisCl pH 6.8, 4 % SDS, 20mM

DTT) heated at 95°C. Eluted samples were prepared for mass spec measurements by using SP3 (Hughes et al. 2014) before they were analyzed on a Q Exactive Plus (Thermo Scientific) connected to a Proxeon HPLC system (Thermo Scientific). Label-free quantification (LFQ) was performed using Max Quant as described below.

IP-MS Analysis

The raw mass spectrometry data was first analyzed using MaxQuant Software {Cox and Mann:2008; Nature Biotechnology} and the resulting “proteinGroups.txt” was then processed using the Bioconductor R package DEP v1.0.1 following the section “Differential analysis” of the vignette (<https://bioconductor.org/packages/release/bioc/vignettes/DEP/inst/doc/DEP.html#differential-analysis>, version from 17 November 2017) with minor adjustments. First we set the random seed to the number 123 in order to receive reproducible results and then we followed the paragraphs on “Loading of the Data” and “Data Preparation” of the vignette to create our raw protein table. Then we extracted the associated UniProt IDs from the raw protein table and queried them on the UniProt ID mapping tool (<http://www.uniprot.org/uploadlists/>) to generate a mapping from “UniProtKB AC/ID” to “Gene name”, which was downloaded as a mapping table in tsv format. The unmapped IDs were manually curated by a search in the UniProt Knowledgebase (UniProtKB) and then appended to the mapping table. This mapping table was loaded into R, where we first removed all rows of the table containing duplicated UniProt IDs, next we created unique gene names by appending to each duplicated gene name its number of occurrence separated by a dot, then we merged the raw protein table with the mapping table based on ID and UniProt ID respectively while keeping all rows of the raw protein table and updated those entries in the names column where a gene name was available in the mapping table. Next we loaded the table specifying the experimental design of the IP-MS analysis {table experimentDesign}, followed the instructions of the paragraph “Generate a SummarizedExperiment object” and “Filter on missing values”, where we decided to performed the less stringent filtering approach to keep those proteins that are identified in 2 out of 3 replicates of at least one condition. Then we performed the steps described in the “Normalization” and imputed the missing data using random draws from a manually defined left-shifted Gaussian distribution with a shift of 1.8 and a scale of 0.3 as proposed in the “Impute data for missing values” paragraph. Next we followed the paragraph “Differential

enrichment analysis” to identify proteins being significantly enriched in comparison to the control coIP with a minimum log₂ fold change of 2 plus t-test with an adjusted p-value (*alpha*) below 0.05 (see Table S5).

ChIP-seq

The ChIP experiment was carried out as previously described (Seelk *et al.* 2016). In brief, worms (wt and *glp-4(bn2)*) at L4 stage were washed off plates using M9 buffer and flash-frozen as “worm popcorn” in liquid nitrogen. The popcorn was pulverized using a biopulverizer before further grinding to a fine powder using a mortar. The powder was dissolved in 10 vol 1,1 % formaldehyde in PBS+1 mM PMSF and fixed for 10 min with gentle rocking. Quenching was achieved by adding 2,5 M Glycine to a final concentration of 125 mM and gently rocking for 5 min. After centrifugation the pellet was washed with ice-cold PBS+1 mM PMSF, before it was resuspended in FA-buffer (50 mM HEPES/KOH pH 7,5, 1mM EDTA, 1% Triton X-100, 0,1 % sodium deoxycholate, 150 mM NaCl) + 1 % Sarkosyl + protease inhibitor and sonicated twice using a Bioruptor (15 times, 15 sec ON, 15 sec OFF; high settings) followed by 15 min centrifugation at full speed, 4°C. The supernatant was taken off (approx. 2-4 mg protein) and incubated either with MRG-1 antibody (Novus) or with buffer ON at 4°C on a rotator. Next, samples were incubated with μ MACS ProteinA beads (Milteny Biotec) for 1 h on ice before they were applied to μ MACS magnetic M columns that were equilibrated using FA buffer. The columns with bound material were washed 2x using FA buffer followed by washing with FA buffer + 1 mM NaCl and FA buffer + 500 mM NaCl. After further washing with TEL buffer (0,25 mM LiCl, 1 % sodium deoxycholate, 1 mM EDTA) and 2x with TE buffer, the samples were eluted using elution buffer (1 % SDS, 250 mM NaCl, 10 mM Tris pH 8,0, 1mM EDTA). The fixation was reverse crosslinked using 2 μ l of 10 mg/ml Proteinase K at 50°C for 1 h followed by incubation at 65°C ON. The DNA was purified using the QIAquick PCR purification kit in a final volume of 40 μ l. The DNA concentration was measured using Qubit dsDNA HS assay kit and libraries were prepared using the NEXTflex qCHIP-Seq v2 kit according to manufacturer’s instructions. After measuring the DNA quality using Bioanalyzer DNA1000 kit and Qubit dsDNA HS Assay, sequencing was carried out at a HighSeq4000 as paired end sequencing 2x75 bp.

ChIP-seq Analysis

Alignment. ChIP-seq reads were mapped using bowtie2 v2.3.2 (Langmead and Salzberg 2012) in paired end mode with default settings (-D 15 -R 2 -N 0 -L 22 -i S,1,1.15) and allowing up to one alignment per read (-k 1) to version ce10 of the worm genome. Resulting Alignment files were converted from SAM to BAM format, sorted and indexed using samtools v1.5. Additional BigWig tracks were generated from the alignment files using bedtools bamtobed v2.25.0 (Quinlan and Hall 2010) and an in-house R script.

Peak Calling and Differential Analysis. Peaks were called for each replicate of both conditions (“glp-4” an wt) using the MACS v2.1.0.20151222 (Zhang *et al.* 2008) module callpeak with genome size set to the worm genome, skipping of model building process and extension of reads in 5’ to 3’ direction to 300 base pairs (-g ce -keep-dup auto -q 0.05 -nomodel -extsize 300).

The resulting peaks were then analysed using the Bioconductor R package DiffBind v2.66 following the section “Example: Obtaining differentially bound sites” of its vignette (<http://bioconductor.org/packages/release/bioc/vignettes/DiffBind/inst/doc/DiffBind.pdf>, Edited: March 27, 2017; Compiled: January 19, 2018). Within R we defined a sample sheet with a similar structure as the example and used the dba() function to load all peaks, count the total number of unique peaks after merging overlapping ones (8226) and the total number of peaks that overlap in at least two of the samples (6723). Then we calculated a binding matrix with scores based on read counts for every sample using the dba.count() function with the summit argument set to 250, leading to centering of the peaks at their point of highest enrichment (summit) and extending them 250bp up- and downstream from there. Next we established the contrast based on the tissue metadata and performed the differential analysis to detect significantly differentially bound peaks with a minimum fold change of 1 and a maximum adjusted p-value of 0.05 (1183).

Gene Annotation. The peaks identified by MACS were annotated by overlapping with the ENSEMBL assembly annotation WBcel215 version 70. The gene tables S4 and S5 were defined by deriving the set of unique gene names of all overlapping genes.

Correlation with Histone Modifications. Wiggle signal data files created from ChIP-seq experiments were downloaded for a selection of Histone modifications, that shared experimental conditions, from modEncode database (Gerstein *et al.* 2010). The tool CrossMap v0.2.1 (Zhao *et al.* 2013) was used to perform a liftOver of the wiggle tracks from assembly ce6 to assembly ce10 and exporting to BigWig format on the fly. The module multiBigwigSummary of the software deepTools v2.5.1

(Ramírez *et al.* 2016) was used to calculate the average score for equally sized bins of 10 kb size covering the whole genome for all BigWig tracks of the histone modifications and the BigWig tracks of the wt MRG-1 ChIP-seq alignment. The resulting matrix was then used to calculate the Spearman correlation between the histone modifications and the binding profile of MRG-1 (Figure S7 A).

MRG-1 ChIP-seq Peak Heatmaps. The heatmaps were prepared and plotted using the Bioconductor R package *genomation* v1.10.0 (Akalin *et al.* 2015). To define the rows of our heatmap we took the summit centered peaks, fixed the center point and extended them to a total length of 4000bp. Then we used the function `ScoreMatrixList()` from *genomation* to create a matrix (`ScoreMatrix`) for every sample, where we have *m* rows for *m* being the number of peaks and *n* columns for *n* = 50. The columns are constructed by subsetting every peak into *n* bins of equal width and calculating the average read count per million (rpm) per bin from the respective BAM files of the sample. Because the scores per row can have a high dynamic range, it is sometimes convenient to scale the matrix before plotting, so we scale and center each matrix using the function `scaleScoreMatrixList()`. This procedure was performed for all peaks that overlap in at least two of the samples (6723), for all significantly differentially bound ChIP-seq peaks between N2 and *glp-4(bn2)* background with FDR < 0.05 (1183) and for all differentially bound ChIP-seq peaks between N2 and *glp-4(bn2)* background with FDR < 0.05 and fold change >2 (409) to create Figureures S6 A,B and C respectively.

Histone Modifications Peak Heatmap. For the peak heatmaps of the modEncode-based histone modifications we created a `ScoreMatrixList` (explained above) with *n* = 400 bins with the score calculated from the BigWig signal tracks. The “soma + germline” heatmap was based on all peaks that overlap in at least two of the N2 samples (5141) and the “germline specific” heatmap is based on all those peaks which were only identified in N2 background but not in *glp-4(bn2)* background (521).

Meta Region Profile. The meta region profile of the modEncode-based histone modifications was acquired by plotting the `ScoreMatrixList` in a histogram representation to show the column-wise average of the centered and scaled `ScoreMatrix`.

Heatmap of Meta Region Profile. The heat map of the meat region profile represents a set of meta region profiles as a stack of heatmaps.

Genome Browser Shot. The Genome Browser view shows the region “chr10:117,922,301-119,587,630” of the ce10 genome assembly and was created using the Bioconductor R package *Gviz* (Hahne and Ivanek 2016).

Microscopy

Worms were mounted on freshly made 2% agarose pads for fluorescence and Nomarski imaging. 10 mM tetramizole hydrochloride (2,3,3,6 tetrahydro-6-phenylimidasol) in M9 buffer was used to anesthetize animals. Microscopy analyses were performed using the Axio Imager.M2 (Zeiss) equipped with a sensitive CCD camera (Sensicam qe, PCO Imaging). MicroManager was used for image acquisition and processing (Edelstein *et al.* 2010; 2014).

References

- Ahringer, J., ed. Reverse genetics (April 6, 2006), WormBook, ed. The *C. elegans* Research Community, WormBook, doi/10.1895/wormbook.1.47.1, <http://www.wormbook.org>.
- Akalin A., Franke V., Vlahovick K., Mason C. E., Schübeler D., 2015 genomation: a toolkit to summarize, annotate and visualize genomic intervals. *Bioinformatics* **31**: 1127–1129.
- Alvarez F., Muñoz F., Schilcher P., Imhof A., Almouzni G., et al. 2011 Sequential Establishment of Marks on Soluble Histones H3 and H4. *J Biol Chem* **286**: 17714–17721.
- Bannister A. J., Kouzarides T., 2011 Regulation of chromatin by histone modifications. *Cell Research* **21**: 381–395.
- Beanan M., Strome S., 1992 Characterization of a germ-line proliferation mutation in *C. elegans*. *Development* **116**: 755.
- Becker J. S., Nicetto D., Zaret K. S., 2016 H3K9me3-Dependent Heterochromatin: Barrier to Cell Fate Changes. *Trends Genet* **32**: 29–41.
- Bleuyard J.-Y., Fournier M., Nakato R., Couturier A. M., Katou Y., et al. 2017 MRG15-mediated tethering of PALB2 to unperturbed chromatin protects active genes from genotoxic stress. *Proc Natl Acad Sci USA* **114**: 7671–7676.
- Brumbaugh J., Hochedlinger K., 2013 Removing reprogramming roadblocks: Mbd3 depletion allows deterministic iPSC generation. *Cell Stem Cell* **13**: 379–381.
- Checchi P. M., Engebrecht J., 2011 *Caenorhabditis elegans* Histone Methyltransferase MET-2 Shields the Male X Chromosome from Checkpoint Machinery and Mediates Meiotic Sex Chromosome Inactivation (JT Lee, Ed.). *PLoS Genet* **7**: e1002267–16.
- Cheloufi S., Elling U., Hopfgartner B., Jung Y. L., Murn J., et al. 2015 The histone chaperone CAF-1 safeguards somatic cell identity. *Nature* **528**: 218–224.
- Chen M., Takano-Maruyama M., Pereira-Smith O. M., Gaufo G. O., Tominaga K., 2009 MRG15, a component of HAT and HDAC complexes, is essential for proliferation and differentiation of neural precursor cells. *J. Neurosci. Res.* **87**: 1522–1531.
- Choy S. W., Wong Y. M., Ho S. H., Chow K. L., 2007 *C. elegans* SIN-3 and its associated HDAC corepressor complex act as mediators of male sensory ray development. *Biochem. Biophys. Res. Commun.* **358**: 802–807.
- Ciosk R., DePalma M., Priess J., 2006 Translational regulators maintain totipotency in the *Caenorhabditis elegans* germline. *Science* **311**: 851.
- Cui, M. and Han, M.

- Roles of chromatin factors in *C. elegans* development (May 3, 2007), WormBook, ed. The *C. elegans* Research Community, WormBook, doi/10.1895/wormbook.1.139.1, <http://www.wormbook.org>.
- Davis R. L., Weintraub H., Lassar A. B., 1987 Expression of a single transfected cDNA converts fibroblasts to myoblasts. *Cell* **51**: 987–1000.
- Dokshin G. A., Ghanta K. S., Piscopo K. M., Mello C. C., 2018 Robust Genome Editing With Short Single-Stranded and Long, Partially Single-Stranded DNA Donors in *Caenorhabditiselegans*. *Genetics*.
- Dombecki C. R., Chiang A. C. Y., Kang H.-J., Bilgir C., Stefanski N. A., et al. 2011 The Chromodomain Protein MRG-1 Facilitates SC-Independent Homologous Pairing during Meiosis in *Caenorhabditis elegans*. *Dev Cell* **21**: 1092–1103.
- Doyon Y., Selleck W., Lane W. S., Tan S., Côté J., 2004 Structural and functional conservation of the NuA4 histone acetyltransferase complex from yeast to humans. *Mol Cell Biol* **24**: 1884–1896.
- Duerr, J. S. Immunohistochemistry (June 19, 2006), WormBook, ed. The *C. elegans* Research Community, WormBook, doi/10.1895/wormbook.1.105.1, <http://www.wormbook.org>.
- Edelstein A. D., Tsuchida M. A., Amodaj N., Pinkard H., Vale R. D., et al. 2014 Advanced methods of microscope control using μ Manager software. *J Biol Methods* **1**: 10–18.
- Edelstein A., Amodaj N., Hoover K., 2010 Computer control of microscopes using μ Manager. *Current Protocols in*
- Erdelyi P., Wang X., Suleski M., Wicky C., 2017 A Network of Chromatin Factors Is Regulating the Transition to Postembryonic Development in *Caenorhabditis elegans*. *G3* **7**: 343–353.
- Fujita M., Takasaki T., Nakajima N., Kawano T., Shimura Y., et al. 2002 MRG-1, a mortality factor-related chromodomain protein, is required maternally for primordial germ cells to initiate mitotic proliferation in *C. elegans*. *Mech. Dev.* **114**: 61–69.
- Gambetta M. C., Müller J., 2015 A critical perspective of the diverse roles of O-GlcNAc transferase in chromatin. *Chromosoma* **124**: 429–442.
- Garcia S. N., Kirtane B. M., Podlutzky A. J., Pereira-Smith O. M., Tominaga K., 2007 Mrg15null and heterozygous mouse embryonic fibroblasts exhibit DNA-repair defects post exposure to gamma ionizing radiation. *FEBS Lett.* **581**: 5275–5281.
- Gaydos L. J., Rechtsteiner A., Egelhofer T. A., Carroll C. R., Strome S., 2012 Antagonism between MES-4 and Polycomb Repressive Complex 2 Promotes Appropriate Gene Expression in *C. elegans* Germ Cells. *Cell Reports* **2**: 1169–1177.
- Gerstein M. B., Lu Z. J., Van Nostrand E. L., Cheng C., Arshinoff B. I., et al. 2010

- Integrative analysis of the *Caenorhabditis elegans* genome by the modENCODE project. *Science* **330**: 1775–1787.
- Gifford C. A., Meissner A., 2012 Epigenetic obstacles encountered by transcription factors: reprogramming against all odds. *Curr Opin Genet Dev* **22**: 409–415.
- Greer E. L., Beese-Sims S. E., Brookes E., Spadafora R., Zhu Y., Rothbart S. B., Aristizábal-Corrales D., Chen S., Badeaux A. I., Jin Q., Wang W., et al. 2014 A Histone Methylation Network Regulates Transgenerational Epigenetic Memory in *C. elegans*. *Cell Reports* **7**: 113–126.
- Gupta P., Leahul L., Wang X., Wang C., Bakos B., et al. 2015 Proteasome regulation of the chromodomain protein MRG-1 controls the balance between proliferative fate and differentiation in the *C. elegans* germ line. *Development* **142**: 291–302.
- Hadwiger G., Dour S., Arur S., Fox P., Nonet M. L., 2010 A monoclonal antibody toolkit for *C. elegans*. (M Hendricks, Ed.). *PLoS ONE* **5**: e10161.
- Hahne F., Ivanek R., 2016 Visualizing Genomic Data Using Gviz and Bioconductor. *Methods Mol Biol* **1418**: 335–351.
- Hanover J. A., Forsythe M. E., Hennessey P. T., Brodigan T. M., Love D. C., et al. 2005 A *Caenorhabditis elegans* model of insulin resistance: altered macronutrient storage and dauer formation in an OGT-1 knockout. *Proc Natl Acad Sci USA* **102**: 11266–11271.
- Hayakawa T., Zhang F., Hayakawa N., Ohtani Y., Shinmyozu K., et al. 2010 MRG15 binds directly to PALB2 and stimulates homology-directed repair of chromosomal breaks. *J Cell Sci* **123**: 1124–1130.
- Hoe M., Nicholas H. R., 2014 Evidence of a MOF histone acetyltransferase-containing NSL complex in *C. elegans*. *worm* **3**: e982967.
- Huang C., Yang F., Zhang Z., Zhang J., Cai G., et al. 2017 Mrg15 stimulates Ash1 H3K36 methyltransferase activity and facilitates Ash1 Trithorax group protein function in *Drosophila*. *Nature Communications*: 1–13.
- Hyun K., Jeon J., Park K., Kim J., 2017 Writing, erasing and reading histone lysine methylations. **49**: e324–22.
- Ingham P. W., 1984 A gene that regulates the bithorax complex differentially in larval and adult cells of *Drosophila*. *Cell* **37**: 815–823.
- Iwamori N., Tominaga K., Sato T., Riehle K., Iwamori T., et al. 2016 MRG15 is required for pre-mRNA splicing and spermatogenesis. *Proc Natl Acad Sci USA* **113**: E5408–15.
- Kamath R. S., Martinez-Campos M., Zipperlen P., Fraser A. G., Ahringer J., 2001 Effectiveness of specific RNA-mediated interference through ingested double-stranded RNA in *Caenorhabditis elegans*. *Genome Biol* **2**: RESEARCH0002.
- Kim Y.-C., Gerlitz G., Furusawa T., Catez F., Nussenzweig A., et al. 2008 Activation

- of ATM depends on chromatin interactions occurring before induction of DNA damage. *Nature Cell Biology* **11**: 92–96.
- Kolundzic E., Ofenbauer A., Bulut S. I., Uyar B., Baytek G., et al. 2018a FACT Sets a Barrier for Cell Fate Reprogramming in *Caenorhabditis elegans* and Human Cells. *Dev Cell*: 1–47.
- Kolundzic E., Seelk S., Tursun B., 2018b Application of RNAi and Heat-shock-induced Transcription Factor Expression to Reprogram Germ Cells to Neurons in *C. elegans*. *JoVE*: e56889–e56889.
- Lai A. Y., Wade P. A., 2011 Cancer biology and NuRD: a multifaceted chromatin remodelling complex. *Nature Publishing Group* **11**: 588–596.
- Langmead B., Salzberg S. L., 2012 Fast gapped-read alignment with Bowtie 2. *Nat Methods* **9**: 357–359.
- Love D. C., Ghosh S., Mondoux M. A., Fukushige T., Wang P., et al. 2010 Dynamic O-GlcNAc cycling at promoters of *Caenorhabditis elegans* genes regulating longevity, stress, and immunity. *Proc Natl Acad Sci USA* **107**: 7413–7418.
- Luco R. F., Pan Q., Tominaga K., Blencowe B. J., Pereira-Smith O. M., et al. 2010 Regulation of alternative splicing by histone modifications. *Science* **327**: 996–1000.
- Mi H., Muruganujan A., Casagrande J. T., Thomas P. D., 2013 Large-scale gene function analysis with the PANTHER classification system. *Nature Protocols* **8**: 1551–1566.
- Mondoux M. A., Love D. C., Ghosh S. K., Fukushige T., Bond M., W et al. 2011 O-Linked-N-Acetylglucosamine Cycling and Insulin Signaling Are Required for the Glucose Stress Response in *Caenorhabditis elegans*. *Genetics* **188**: 369–382.
- Olgun A., Aleksenko T., Pereira-Smith O. M., Vassilatis D. K., 2005 Functional analysis of MRG-1: the ortholog of human MRG15 in *Caenorhabditis elegans*. *The Journals of Gerontology Series A: Biological Sciences and Medical Sciences* **60**: 543–548.
- Pasque V., Jullien J., Miyamoto K., Halley-Stott R. P., Gurdon J. B., 2011 Epigenetic factors influencing resistance to nuclear reprogramming. *Trends Genet* **27**: 516–525.
- Patel T., Tursun B., Rahe D. P., Hobert O., 2012 Removal of Polycomb Repressive Complex 2 Makes *C. elegans* Germ Cells Susceptible to Direct Conversion into Specific Somatic Cell Types. *Cell Reports*.
- Petrella L. N., Wang W., Spike C. A., Rechtsteiner A., Reinke V., et al. 2011 synMuv B proteins antagonize germline fate in the intestine and ensure *C. elegans* survival. *Development* **138**: 1069–1079.
- Quinlan A. R., Hall I. M., 2010 BEDTools: a flexible suite of utilities for comparing genomic features. *Bioinformatics* **26**: 841–842.

- Radermacher P. T., Myachina F., Bosshardt F., Pandey R., Mariappa D., et al. 2014 O-GlcNAc reports ambient temperature and confers heat resistance on ectotherm development. *Proc Natl Acad Sci USA* **111**: 5592–5597.
- Ramírez F., Ryan D. P., Grüning B., Bhardwaj V., Kilpert F., et al. 2016 deepTools2: a next generation web server for deep-sequencing data analysis. *Nucleic Acids Research* **44**: W160–W165.
- Rechtsteiner A., Ercan S., Takasaki T., Phippen T. M., Egelhofer T. A., et al. 2010 The histone H3K36 methyltransferase MES-4 acts epigenetically to transmit the memory of germline gene expression to progeny. *PLoS Genet* **6**: e1001091.
- Seelk S., Adrian-Kalchhauser I., Hargitai B., Hajduskova M., Gutnik S., et al. 2016 Increasing Notch signaling antagonizes PRC2-mediated silencing to promote reprogramming of germ cells into neurons. *eLife* **5**.
- Shaye D. D., Greenwald I., 2011 OrthoList: a compendium of *C. elegans* genes with human orthologs. *PLoS ONE* **6**: e20085.
- She X., Xu X., Fedotov A., Kelly W. G., et al. 2009 Regulation of Heterochromatin Assembly on Unpaired Chromosomes during *Caenorhabditis elegans* Meiosis by Components of a Small RNA-Mediated Pathway (JD Lieb, Ed.). *PLoS Genet* **5**: e1000624–15.
- Squiban B., Belougne J., Ewbank J., Zugasti O., 2012 Quantitative and automated high-throughput genome-wide RNAi screens in *C. elegans*. *JoVE*: e3448–e3448.
- Stiernagle, T. Maintenance of *C. elegans* (February 11, 2006), WormBook, ed. The *C. elegans* Research Community, WormBook, doi/10.1895/wormbook.1.101.1, <http://www.wormbook.org>.
- Takasaki T., Liu Z., Habara Y., Nishiwaki K., Nakayama J.-I., I et al. 2007 MRG-1, an autosome-associated protein, silences X-linked genes and protects germline immortality in *Caenorhabditis elegans*. *Development* **134**: 757–767.
- Tessarz P., Kouzarides T., 2014 Histone core modifications regulating nucleosome structure and dynamics. *Nat Rev Mol Cell Biol*: 1–6.
- Tursun B., Patel T., Kratsios P., Hobert O., 2011 Direct conversion of *C. elegans* germ cells into specific neuron types. *Science* **331**: 304–308.
- Wang Y., Kallgren S. P., Reddy B. D., Kuntz K., López-Maury L., et al. 2012 Histone H3 lysine 14 acetylation is required for activation of a DNA damage checkpoint in fission yeast. *Journal of Biological Chemistry* **287**: 4386–4393.
- Wenzel D., Palladino F., Jedrusik-Bode M., 2011 Epigenetics in *C. elegans*: Facts and challenges. *Genesis* **49**: 647–661.
- Wu X., Shi Z., Cui M., Han M., Ruvkun G., 2012 Repression of Germline RNAi Pathways in Somatic Cells by Retinoblastoma Pathway Chromatin Complexes (SE Mango, Ed.). *PLoS Genet* **8**: e1002542.

- Xu J., Sun X., Jing Y., Wang M., Liu K., et al. 2012 MRG-1 is required for genomic integrity in *Caenorhabditis elegans* germ cells. *Cell Research* **22**: 886–902.
- Yang X., Zhang F., Kudlow J. E., 2002 Recruitment of O-GlcNAc transferase to promoters by corepressor mSin3A: coupling protein O-GlcNAcylation to transcriptional repression. *Cell* **110**: 69–80.
- Yochum G. S., Ayer D. E., 2002 Role for the mortality factors MORF4, MRGX, and MRG15 in transcriptional repression via associations with Pfl, mSin3A, and Transducin-Like Enhancer of Split. *Mol Cell Biol* **22**: 7868–7876.
- Zhang P., Du J., Sun B., Dong X., Xu G., et al. 2006 Structure of human MRG15 chromo domain and its binding to Lys36-methylated histone H3. *Nucleic Acids Research* **34**: 6621–6628.
- Zhang Y., Liu T., Meyer C. A., Eeckhoute J., Johnson D. S., et al. 2008 Model-based analysis of ChIP-Seq (MACS). *Genome Biol* **9**: R137.
- Zhao H., Sun Z., Wang J., Huang H., Kocher J.-P., et al. 2013 CrossMap: a versatile tool for coordinate conversion between genome assemblies. *Bioinformatics* **30**: 1006–1007.

Supplemental Figures

Figure S1 RNAi library and comparison of liquid vs. solid media RNAi

Figure S2 Automated solid media-based RNAi screening.

Figure S3 Controls for *mrg-1* RNAi and smFISH.

Figure S4 Controls for reprogramming and anti-MRG-1/ LIN-53 immunostainings.

Figure S5 MRG-1 ChIP-seq heatmaps

Figure S6 MRG-1 binding correlation with specific histone modifications sites

Figure S7 MRG-1 immunoprecipitations coupled to mass spectrometry (IP-MS)

Supplemental Tables

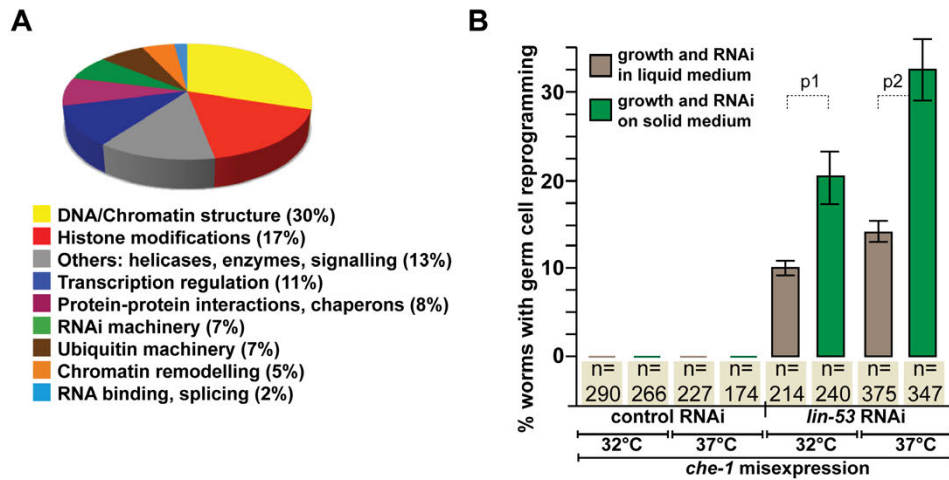
Table S1 Chromatin 2.0 Sub-library. This table lists all RNAi clones in the Chromatin 2.0 library. Color coding is according to functional groups of proteins. Source of clones indicated and explained at the end of the table.

Table S2 Efficiency of worm recovery from individual plates by the LP sampler. Strains expressing different levels of *gfp* in the neurons were mixed according to indicated numbers. *gcy-5p::gfp* is expressed in only one neuron while *unc-119p::gfp* is expressed in all neurons. Aspirated worms were analyzed by the BioSorter.

Table S3 ChIP-seq results. Genes assigned to MRG-1 binding sites from all ChIP-seq experiment (pooled triplicates) backgrounds.

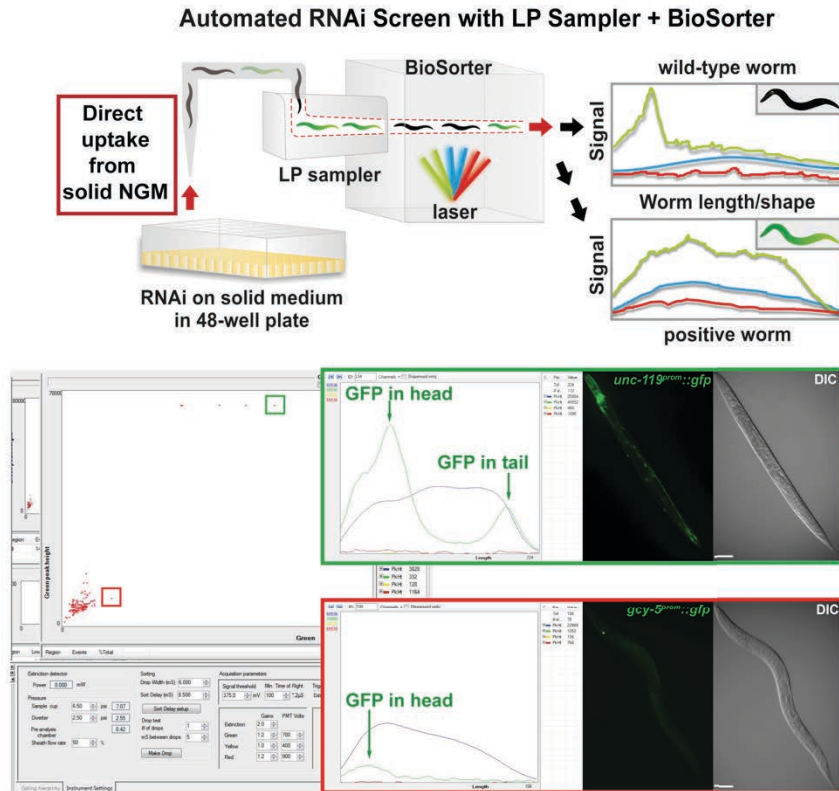
Table S4 Correlation of MRG-1 ChIP-seq peaks with histone modifications. Genes bound by MRG-1 (ChIP-seq peaks) in WT and *glp-4(bn2)* background that also carry H3K27me3 and H3K9me3 based on modEncode datasets

Table S5 Enriched proteins from IP-MS. Spectral values of all proteins enriched by MRG-1 IP-MS from WT, *glp-4(bn2)* and *mrg-1::3xHA^{CRISPR}* backgrounds.

Figure S1**Hajduskova et al.****Figure S1** Chromatin RNAi library and liquid vs. solid media RNAi efficiency.

(A) A detailed breakdown of the targeted factors by the Chromatin RNAi sub-library 2.0 showing that targeted chromatin regulating factors are implicated in a variety of different biological processes. The Chromatin 2.0 sub-library was assembled based on a previously published incomplete collection as described in Tursun et al., 2011. Previously missing clones (82) were generated and added (Table S1). All clones of the Chromatin 2.0 sub-library have been checked by sequencing, corrected and complemented. (B) RNAi against *lin-53* in liquid worm cultures results in a 50% GeCo decrease compared to solid media RNAi. Numbers of animals (n) quantified per condition are indicated below each column. Error bars represent SEM. One-way ANOVA: $p_1 = 0.022$; $p_2 = 0.032$.

A



B

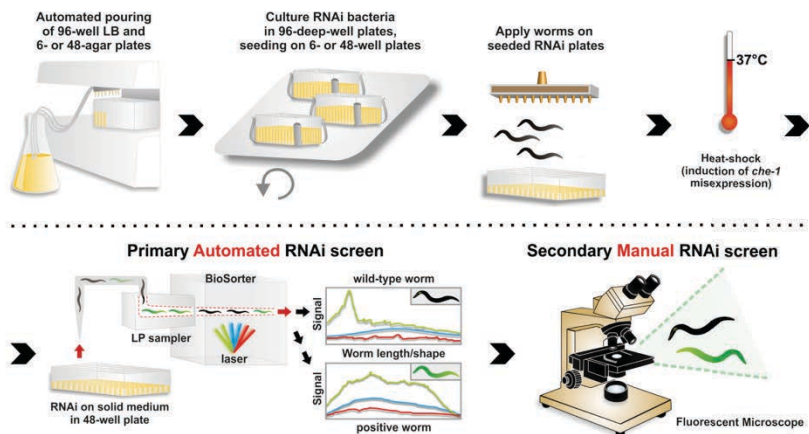


Figure S2. Automated solid media-based RNAi screening.

(A) A solid media-based automated RNAi screening system by combining the BioSorter (UnionBiometrica) with a robotic large-particle sampling system (LP sampler, Union Biometrica). The LP sampler collects worms from solid RNAi medium by repeated flushing and aspiration followed by fluorescence-intensity

scanning in the BioSorter. Screenshot of the BioSorter software after scanning for GFP signal intensity (Green peak height) of mixed worm strains either expressing the pan-neuronal reporter *unc-119p::gfp* or the ASE-specific *gcy-5p::gfp* is shown. Each dot in the scatter plot represents a single worm. The fluorometric analysis reveals worms with high GFP signals (green dashed box, *unc-119p::gfp*) versus low (red stippled box, *gcy-5p::gfp*). The peaks of the green curve reflect GFP intensities along the body axis (blue) of individual worms. Detailed analysis of aspiration and sorting efficiency is shown in S3 Table. Scale bars = 20 μm . (B) Workflow of the automated and manual P0 RNAi screens. The MultidropTM dispenser (Thermo Scientific) is used to prepare LB cultures in 96-deep-well plates and to automatically pour either 6-, 12-, or 48-well RNAi plates. RNAi clones are picked from the 96-well format of the frozen library into the 96-deep-well LB cultures and grown overnight. Concentrated bacteria are seeded on the multi-well RNAi plates where dsRNA synthesis is induced at 37°C overnight. A synchronized worm population (L1 larvae) of a strain carrying *hsp::che-1* and *gcy-5p::gfp* transgenes is applied on seeded RNAi plates. Worms are kept on RNAi plates at 15°C until they reach the L4 larval stage and ubiquitous expression of CHE-1 is induced by heat-shock. Screening for ectopic *gcy-5p::gfp* expression using the BioSorter Large Particle Flow Cytometer (Union Biometrica) is performed within 16-24 hours after heat-shock treatment by aspiration from the 48-well RNAi plates with the Large Particle Sampler. A secondary screen to confirm phenotypes is performed using a fluorescent microscope.

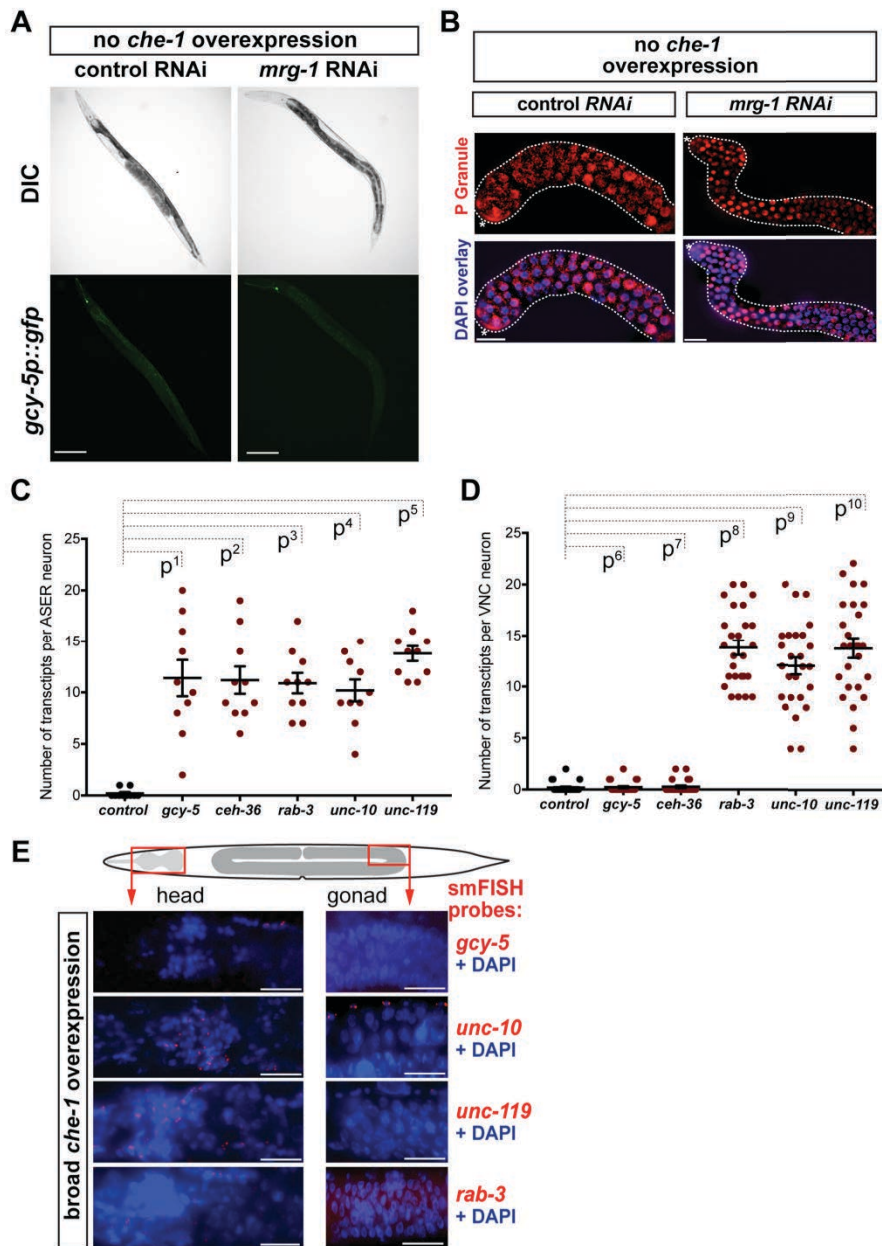


Figure S3. Controls for *mrg-1* RNAi and smFISH.

(A) RNAi against *mrg-1* without overexpression of *che-1* does not lead to ectopic induction of the neuronal reporter. Scale bars = 20 μ m. (B) Antibody staining for germline-specific P Granules upon *mrg-1* RNAi but without *che-1* overexpression. Scale bars = 5 μ m. (C-D) Quantification of smFISH detections based on counts of hybridization signals (red dots) of (C) endogenous ASER neurons and (D) ventral nerve cord neurons, which do not show expression of the ASE neuron-specific genes *gcy-5* and *ceh-36*. For each condition 20 cells were counted for smFISH-derived transcript detection based on fluorescence signals. p-values based on ANOVA with

Dunnett's multiple comparison test: p1 = 0,0001; p2 = 0,0001; p3 = 0,0001; p4 = 0,0001; p5 = 0,0001; p6 = 0,999; p7 = 0,999; p8 = 0,0001; p9 = 0,0001; p10 = 0,0001.

(D) Control for expression of neuronal gene expression by smFISH in germ cells
Upon *che-1* overexpression without any RNAi depletion no transcripts of the tested genes can be detected in germ cells. Scale bars = 5 μ m.

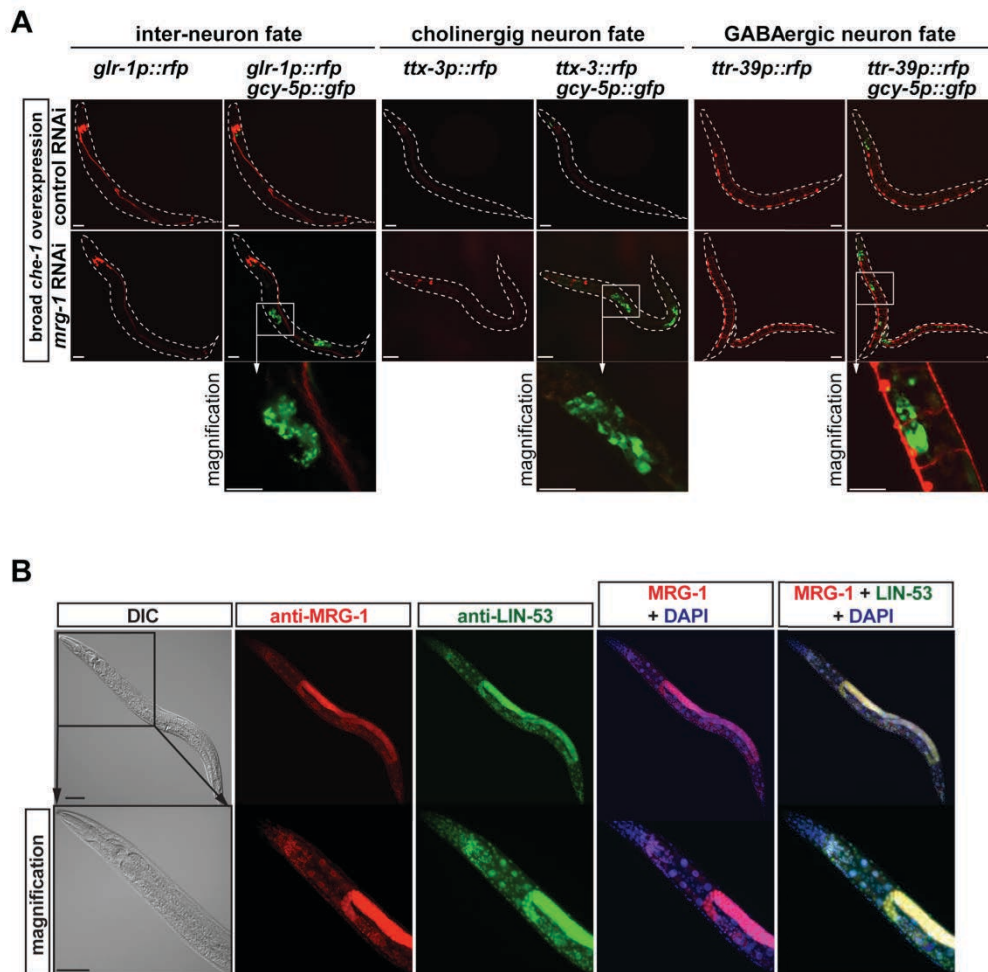


Figure S4. Controls for reprogramming and anti-MRG-1/ LIN-53 immunostainings.

(A) Worms co-expressing together with the ASE neuron fate reporter *gcy-5p::gfp* reporters for different neuronal identities: *glr-1p::rfp* (inter neurons), *ttx-3p::rfp* (cholinergic inter neuron), and *ttr-39p::rfp* (GABAergic neurons) were tested. Upon germ cell reprogramming by *che-1* overexpression and *mrg-1* RNAi no other reporter besides *gcy-5p::gfp* can be detected in the gonad. Scale bars = 10 μ m. (B) Young adult hermaphrodite was co-stained using anti-MRG-1 and anti-LIN-53 antibody.

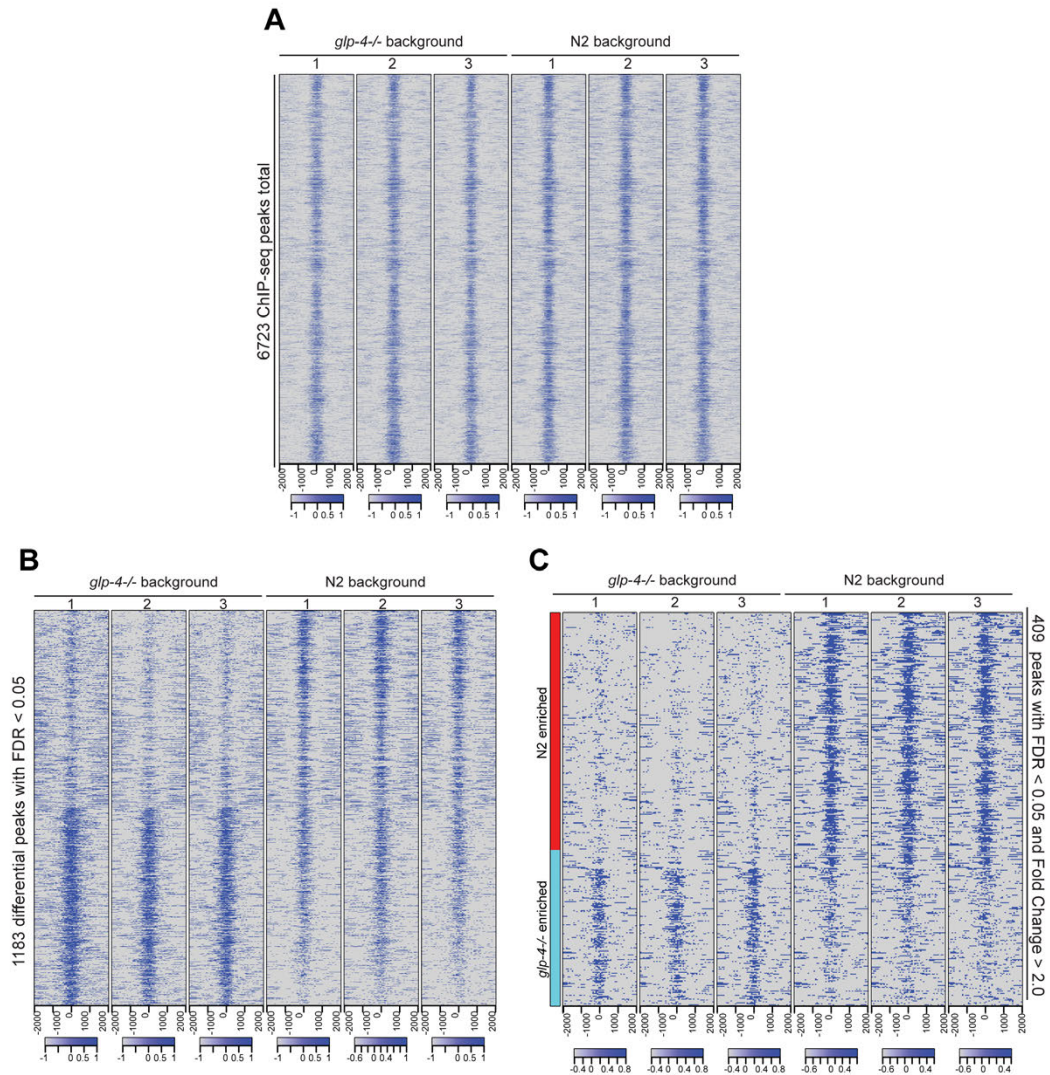


Figure S5. MRG-1 ChIP-seq heatmaps.

(A) Read counts at highest significant ChIP-seq peaks. Only peaks found in at least two replicates are shown. (B) Heatmap of differential ChIP-seq peaks between N2 and *glp-4(bn2)* background with FDR < 0.05. (C) Heatmap of differential ChIP-seq peaks between N2 and *glp-4(bn2)* background with FDR < 0.05 and fold change > 2.

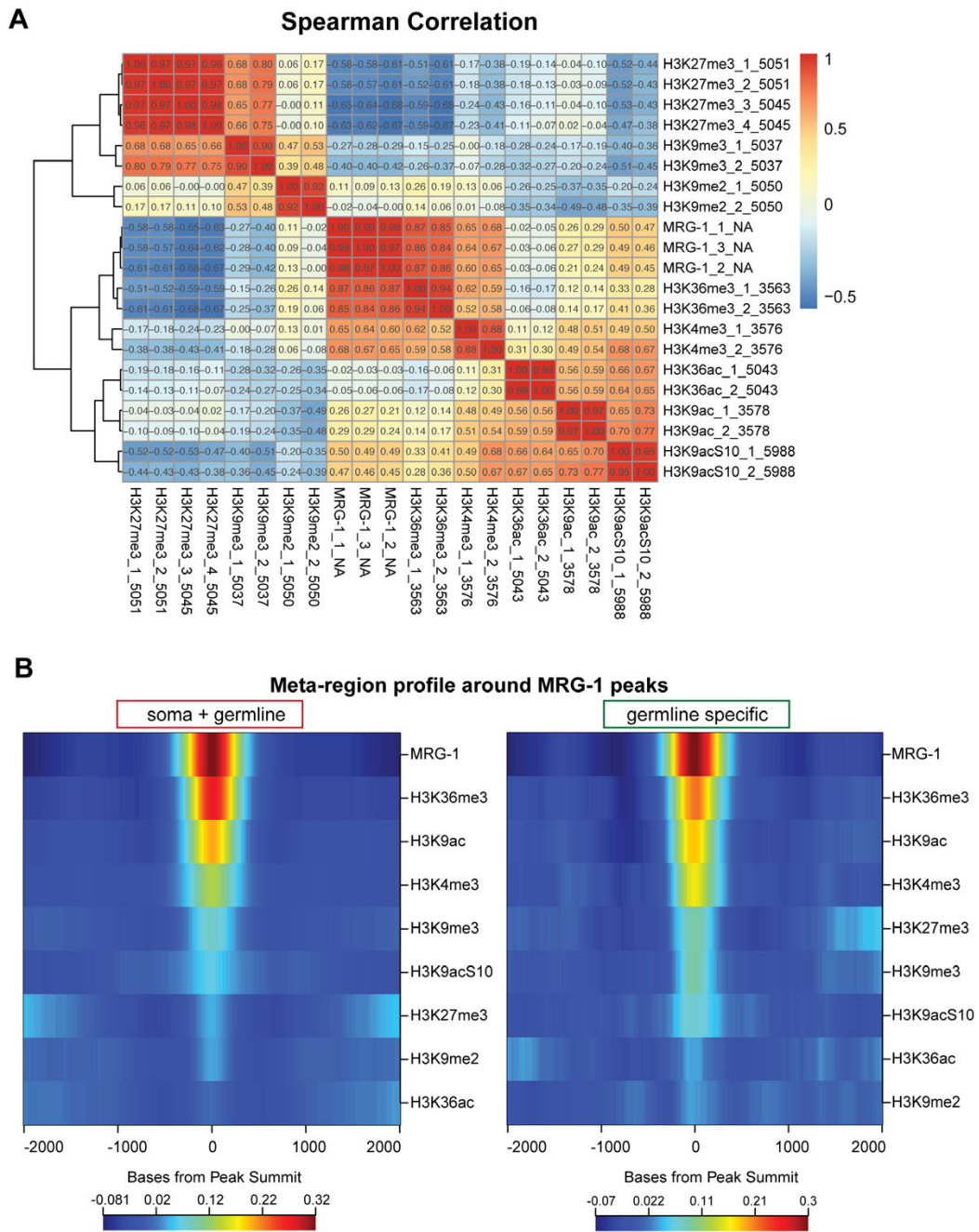


Figure S6. MRG-1 binding correlation with specific histone modifications sites. (A) Heatmap of MRG-1 binding sites correlating (Spearman Correlation) with histone modifications based on modEncode data. (B) Scaled meta-region profile of modEncode-based histone modifications around MRG-1 peaks.

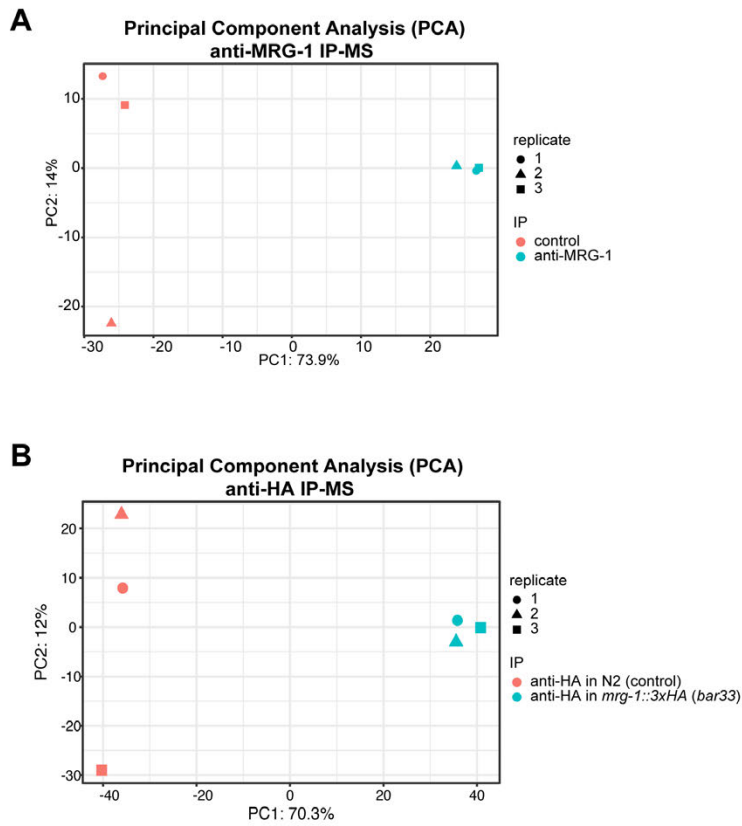


Figure S7 MRG-1 immunoprecipitations coupled to mass spectrometry (IP-MS).

(A) Principal component analysis of IP-MS replicates from N2 background IP-MS experiments with anti-MRG-1 antibodies and unspecific antibodies as control. (B) Principal component analysis of IP-MS replicates from *mrg-1::3xHA^{CRISPR}* (*bar33*) and N2 (control) background IP-MS experiments with anti-HA antibodies.

Table S1. Chromatin 2.0 Sub-library

Plate	Position	Origin	Seq. name	Gene name	Characterization	Category	Domain
MH1	A1	96AL_2A01	F47G6.1	<i>dyb-1</i>	alpha-dystrobrevin	Others	coiled-coil, Zn finger
MH1	A2	96AL_1A12	F53G12.5	<i>mex-3</i>	KH domain-containing RNA binding proteins	RNA binding	KH
MH1	A3	96AL_3B10	T28F2.4	<i>jmjC-1</i>	Isoform 4 of MYC-induced nuclear antigen; abundant spermatogenesis enriched protein copurified with chromatin	chromatin binding	JmjC
MH1	A4	96AL_1C09	R119.6	<i>taf-4</i>	Isoform 1 of Transcription initiation factor TFIID	transcription regulation	
MH1	A5	96AL_3C03	D1037.1		Isoform A of Protein SON. RNA-binding protein that acts as a mRNA splicing cofactor by promoting efficient splicing of transcripts that possess weak splice sites.	RNA binding/ splicing	G-patch
MH1	A6	96AL_1D06	F56A6.1	<i>sago-2</i>	Argonaute homolog that is partially required for the amplification phase of RNAi responses	RNAi machinery	PAZ/PIWI
MH1	A7	96AL_3D03	T12F5.4	<i>lin-59</i>	SET domain-containing protein that is most closely related to the ASH1 group of histone-lysine N-methyltransferases; Essential protein required to maintain expression of homeotic genes <i>egl-5</i> and <i>mab-5</i> . May play an analogous role to the trithorax Group (<i>trxG</i>) proteins. Histone methyltransferase	histone modification; DNA methylation	AWS, SET, PHD-type, Zn finger
MH1	A8	96AL_4D12	C18E3.7	<i>ppw-1</i>	PAZ/PIWI domain-containing protein; mutants are resistant to RNA interference in the germline.	RNAi machinery	PAZ/PIWI
MH1	A9	96AL_4E03	C43E11.1	<i>acin-1</i>	encodes an ortholog of human ACIN1 (OMIM:604562, which induces apoptotic chromatin condensation)	NA binding	
MH1	A10	96AL_4E05	C43E11.3	<i>met-1</i>	histone methyltransferase; <i>met-1</i> is required for normal levels of histone H3K36 and H3K9 trimethylation	histone modification; DNA methylation	SET
MH1	A11	96AL_4E12	C43E11.10	<i>cdc-6</i>	origin complex component (CDC6), AT hook	DNA binding	AT hook
MH1	A12	96AL_2F02	W10C8.2	<i>pap-1</i>	Part of the Wnt signaling pathway. HMG box-containing protein that is the sole <i>C. elegans</i> member of the TCF/LEF family of transcription factors; Represses expression of target genes via its interaction with <i>hda-1</i> histone deacetylase.	transcription regulation	HMG box
MH1	B1	96AL_4F04	C43E11.1	<i>acin-1</i>	encodes an ortholog of human ACIN1 (OMIM:604562, which induces apoptotic chromatin condensation)	NA binding	
MH1	B2	96AL_2G09	C45E1.4		Ubiquitin-like protein which can be covalently attached to target lysines as a monomer. Does not seem to be involved in protein degradation and may function as an antagonist of ubiquitin in the degradation process. Plays a role in a number of cellular processes such as nuclear transport, DNA replication and repair, mitosis and signal transduction.	others	
MH1	B3	96AL_1H07	K12C11.2	<i>smo-1</i>		ubiquitin machinery	Ubiquitin-like protein kinase, ankyrin repeats
MH1	B4	96AL_1H09	K12C11.4	<i>dapk-1</i>	death-associated protein (DAP) kinase	protein kinase	
MH1	B5	96AL_6A02	F54C1.3	<i>mes-3</i>	member of a Polycomb-like chromatin repressive complex that acts via H3K27 methylation	histone modification; DNA methylation	
MH1	B6	96AL_7A04	T05E8.2	<i>his-8</i>	histone H2B	chromatin/nucleosome structure	
MH1	B7	Supp V-14J8	Y59A8A.2	<i>phf-14</i>	PHD finger family	chromatin binding	PHD finger, Zn finger
MH1	B8	Cloned	C06A5.3		PSIP1 protein ortholog	protein-protein interactions	PWWP domain (Pro-Trp-Trp-Pro motif)
MH1	B9	96AL_6D02	F56A3.2	<i>slx-1</i>	Isoform 1 of Structure-specific endonuclease subunit SLX1. Catalytic subunit of a heterodimeric structure-specific endonuclease that resolves DNA secondary structures generated during DNA repair and recombination.	chromatin structure (nucleases)	SLX1-type Zn finger, GIY-YIG
MH1	B10	96AL_6D09	<i>all his-1 (his-2, his-5, his-6, his-24)</i>		H4 histone, coded by histone gene cluster HIS1	chromatin/nucleosome structure	
MH1	B11	96AL_6E09	C01G8.9	<i>let-526</i>	component of the SWI/SNF complex	DNA binding	ARID (AT-rich interaction) domain
MH1	B12	96AL_6E10	C01G8.8/C01G8.9	<i>let-526</i>	component of the SWI/SNF complex	DNA binding	ARID (AT-rich interaction) domain
MH1	C1	96AL_6G02	F55A12.8	<i>nath-10</i>	N-acetyltransferase 10 homolog	histone modification; DNA methylation	N-acetyltransferase; helicase and tRNA binding domain
MH1	C2	96AL_7G08	C32F10.2	<i>lin-35</i>	retinoblastoma protein (Rb) ortholog	Others	Retinoblastoma-associated protein A/B domain
MH1	C3	96AL_7G10	C32F10.5	<i>hmg-3</i>	HMG box-containing protein 3; Facilitates chromatin transcription complex subunit <i>ssrp1-B</i> . Component of the FACT complex, a general chromatin factor that acts to reorganize nucleosomes. The FACT complex is involved in multiple processes that require DNA as a template such as mRNA elongation, DNA replication and DNA repair. During transcription elongation the FACT complex acts as a histone chaperone that both destabilizes and restores nucleosomal structure. It facilitates the passage of RNA polymerase II and transcription by promoting the dissociation of one histone H2A-H2B dimer from the nucleosome, then subsequently promotes the reestablishment of the nucleosome following the passage of RNA polymerase II. Binds specifically to double-stranded DNA	DNA binding	HMG-box domain Tudor (recognizes methylated histones)
MH1	C4	96AL_11A02	F22D6.6	<i>ekl-1</i>	Enhancer of Ksr-1 Lethality; RITS (meiotic/germline H3K9me2 on repetitive heterochromatin)	histone binding	
MH1	C5	96AL_11A11	K10D3.3	<i>taf-11.2</i>	putative TATA binding protein associated transcription factor	transcription regulation	
MH1	C6	96AL_12B03	D2030.9	<i>wdr-23</i>	WD repeat-containing protein 2; DDB1- and CUL4-associated factor 11 homolog	protein-protein interactions	WD repeats
MH1	C7	AL I-3D18	F26A3.3	<i>ego-1</i>	RNA-directed RNA polymerase related EGO-1; regulates germline development and RNA interference	RNAi machinery	
MH1	C8	96AL_9C04	K04F10.6	<i>rde-3 - mut-2</i>	Mutator; RNAi defective <i>rde-3</i> ; nucleotidyltransferase	RNAi machinery	
MH1	C9	96AL_12C03	T23G11.2	<i>gno-2</i>	Phosphoglucosamine acetyltransferase	histone modification; DNA methylation	GNAT domain
MH1	C10	96AL_11C08	C01H6.7	<i>tag-298 = swsn-9</i>	SWI/SNF nucleosome remodeling complex component	chromatin remodelling	bromodomain
MH1	C11	96AL_11C10	C01H6.9		homolog of haploid germ cell-specific nuclear protein kinase (haspin)	protein kinase	
MH1	C12	AL I-3G19	T23H2.3		homolog transcription termination factor RNA polymerase II; helicase	chromatin remodelling	SNF2-related
MH1	D1	AL I-3G24	K02F2.3	<i>teg-4/phi-6/tag-203</i>	homolog of splicing factor 3b	splicing	WD repeats
MH1	D2	96AL_11D05	R06C7.7	<i>lin-61</i>	polycomb-like protein; binds to oocyte chromatin; regulates splicing; recognizes and binds H3K9me2/3 (MBT domain); predicted to function in a transcriptional regulatory complex	splicing/chromatin binding/transcription regulation	MBT repeats
MH1	D3	AL III-4J4	R107.2		PHD-finger containing protein	chromatin binding	PHD finger
MH1	D4	96AL_11D12	F21C3.4	<i>rde-2</i>	RNAi Defective, encoding nematode specific protein required for RNA interference, control of transposon transposition in the germline and proper chromosome segregation.	RNAi machinery	
MH1	D5	96AL_12D12	D2005.5	<i>drh-3</i>	dicer-related helicase, required to maintain chromosome integrity and proper chromosome segregation in the germline; RITS (meiotic/germline H3K9me2 on repetitive chromatin)	DNA binding	
MH1	D6	96AL_12E08	F30F8.8	<i>taf-5</i>	putative TATA binding protein associated transcription factor	transcription regulation	WD repeats
MH1	D7	GP 1C2	H06O01.2	<i>chd-1</i>	chromodomain-helicase-DNA-binding protein	chromatin remodelling	chromodomain
MH1	D8	96AL_12G12	C54G4.1	<i>rskn-2</i>	Putative ribosomal protein S6 kinase alpha-2; Serine/threonine kinase that may play a role in mediating the mitogen- and stress-induced effects on transcription. May repress transcription via phosphorylation of 'Ser-1' of histone H2A. May phosphorylate histone H3	protein kinase	HMG box, bromodomain, Zn finger
MH1	D9	96AL_11H07	C26C6.1	<i>pbrm-1</i>	Putative bromodomain containing protein; predicted to function in chromatin remodeling and transcriptional regulation	chromatin remodelling/transcription regulation	
MH1	D10	96AL_11H11	C26C6.5	<i>dcp-66</i>	a member of the transcriptionally inhibitory nucleosomal remodeling and deacetylase (NuRD) complex	chromatin remodelling	
MH1	D11	96AL_13A10	C09H6.1	<i>spr-4</i>	Suppressor of presenilin protein 4; probable transcriptional regulator	transcription regulation	Zn finger, C2H2-type
MH1	D12	96AL_15A12	W06D4.4	<i>prmt-7</i>	Protein arginine N-methyltransferase 7	histone modification; DNA methylation	SAM domain
MH1	E1	96AL_14B06	F43G9.12		putative GC-rich sequence DNA-binding factor homologue; partial homologies to a transcription repressor and histone-interacting protein	DNA binding activity, transcription regulation	GCFC domain
MH1	E2	96AL_15B02	W06D4.6	<i>rad-54</i>	DNA repair and recombination protein RAD54-like; DEAD-like helicase superfamily	DNA binding / chromatin remodelling	SNF2-related
MH1	E3	96AL_16B06	K07A1.11	<i>rba-1</i>	Isoform 2 of Histone-binding protein RBBP4; Core histone-binding subunit that may target chromatin assembly factors, chromatin remodeling factors and histone deacetylases to their histone substrates in a manner that is regulated by nucleosomal DNA	histone assembly	WD repeats

Hajduskova et al.

MH1	E4	96AL_16B07	K07A1.12	<i>lin-53</i>	protein containing a 7 WD-repeat similar to the mammalian homolog RbAp48; histone binding protein; Core histone-binding subunit that may target chromatin assembly factors, chromatin remodeling factors and histone deacetylases to their histone substrates in a manner that is regulated by nucleosomal DNA	histone binding	WD repeats
MH1	E5	96AL_13D04	T01G9.6	<i>kin-10</i>	Casein kinase II subunit beta	protein kinase	
MH1	E6	96AL_13D11	C34B7.1		divergent MYST acetyltransferase	histone modification; DNA methylation	
MH1	E7	96AL_14D12	DY3.2	<i>lmn-1</i>	Lamin-B1; Provides a framework for the nuclear envelope and probably also interacts with chromatin; bind to histone H2A	chromatin binding	
MH1	E8	96AL_13E03	F16D3.2	<i>rsd-6</i>	RNAi spreading defective, encoding maternal tudor protein.	RNAi machinery	Tudor domain
MH1	E9	96AL_15E06	C12C8.3	<i>lin-41</i>	Ring finger-B box-Coiled coil (RBCC) protein	protein-protein interactions	RING type Zn finger
MH1	E10	96AL_13F02	F02E9.4	<i>sin-3</i>	ortholog of the SIN3 family of histone deacetylase subunits	histone modification; DNA methylation	
MH1	E11	96AL_15F08	C17E4.6		protein of the YL1 family; DNA-binding and may be transcription factor	transcription regulation	
MH1	E12	96AL_15F10	C17E4.6		protein of the YL1 family; DNA-binding and may be transcription factor	transcription regulation	
MH1	F1	96AL_13G07	D10B1.8		SANT/Myb-domain containing protein	DNA binding	SANT/Myb domain
MH1	F2	96AL_14H02	F32H2.1	<i>gei-1</i>	protein containing a RhoGAP domain and a START (STAR-related lipid-transfer) domain	Others	
MH1	F3	AL III-6K7	Y56A3A.16		PHD-finger containing protein	chromatin binding	PHD finger
MH1	F4	96AL_15H05	F30A10.10	<i>usp-48</i>	Ubiquitin Specific Protease	ubiquitin machinery	
MH1	F5	96AL_15H06	C41G7.1	<i>smn-1</i>	human Survival Motor Neuron homolog.	RNA binding	Tudor domain
MH1	F6	96AL_17B02	T23D8.8	<i>cfj-1</i>	DNA-binding protein containing an AT-rich interaction domain (ARID); transcription factor	transcription regulation	ARID (AT-rich interaction) domain
MH1	F7	96AL_20B12	F15D3.1	<i>dys-1</i>	ortholog of human DMD, which when mutated leads to Duchenne muscular dystrophy	Others	ZZ type Zn finger
MH1	F8	96AL_17C05	B0379.3	<i>mut-16</i>	and/or gene expression	chromatin structure / transcription regulation	
MH1	F9	96AL_18D08	T22A3.4	<i>set-18</i>	ortholog of human SMYD1, SMYD2	protein-protein interactions	MYND-type Zn finger
MH1	F10	Supp I-10A5	F28D9.2	<i>sri-5</i>	Serpentine Receptor, class I	Others (signalling)	
MH1	F11	Supp III-8G7	Y119D3B.11	<i>orc-3</i>	PHD-finger containing protein	chromatin binding	PHD finger
MH1	F12	96AL_18G02	B0205.1		SPK-domain containing protein	DNA binding	SPK domain
MH1	G1	96AL_18G04	B0205.3	<i>rpn-10</i>	proteasome Regulatory Particle, Non-ATPase-like; contains two ubiquitin interaction motifs; is a member of the von Willebrand factor	ubiquitin machinery	
MH1	G2	AL I-508	F55A3.3	<i>phi-16</i>	FACT complex subunit spt-16; Component of the FACT complex, a general chromatin factor that acts to reorganize nucleosomes. The FACT complex is involved in multiple processes that require DNA as a template such as mRNA elongation, DNA replication and DNA repair. During transcription elongation the FACT complex acts as a histone chaperone that both destabilizes and restores nucleosomal structure. It facilitates the passage of RNA polymerase II and transcription by promoting the dissociation of one histone H2A-H2B dimer from the nucleosome, then subsequently promotes the reestablishment of the nucleosome following the passage of RNA polymerase II	chromatin remodelling	
MH1	G3	96AL_17H07	F25D7.3	<i>blmp-1</i>	a zinc finger and SET domain-containing protein that is the C. elegans BLIMP1 (B lymphocyte-induced maturation protein 1) ortholog	DNA binding	Zn finger; SET domain
MH1	G4	96AL_20H11	R09B3.4	<i>ubc-12</i>	ubiquitin-conjugating enzyme	ubiquitin machinery	
MH1	G5	96AL_20H12	R09B3.5	<i>mag-1</i>	Drosophila MAGONASHI homolog	Others	
MH1	G6	AL X-1G12	C46H3.1		PHD-finger containing protein	chromatin binding	PHD finger
MH1	G7	96AL_22A10	T15D6.8		putative methyltransferase	histone modification; DNA methylation	
MH1	G8	96AL_23A08	W02A11.4	<i>uba-2</i>	SUMO-activating enzyme subunit	ubiquitin machinery	
MH1	G9	AL X-4D20	C11E4.6		PHD-finger containing protein	chromatin binding	PHD finger
MH1	G10	96AL_22B01	T15D6.11		putative methyltransferase	histone modification; DNA methylation	
MH1	G11	96AL_23B01	B0019.2		SPK-domain containing protein	DNA binding	SPK domain
MH1	G12	96AL_23B03	Y18D10A.1	<i>atf-6</i>	AT hook Transcription Factor family	transcription regulation	AT hook
MH1	H1	96AL_24B04	T04D3.5			others	
MH1	H2	AL I-6G16	K11D2.1		RC1 domain-containing protein 1 (regulator of chromosome condensation)	chromatin structure	
MH1	H3	96AL_21D11	R05D7.2		SPK-domain containing protein family member	DNA binding	SPK domain
MH1	H4	96AL_24D01	Y40B18.6	<i>spr-5</i>	H3K4me2 demethylase that; demethylase containing amine oxidase domain that functions to mediate chromatin remodeling and transcriptional regulation orthologous to human histone demethylase LSD1	histone modification; DNA methylation	
MH1	H5	96AL_22E02	W02D9.3	<i>hmg-20</i>	isoform 1 of High mobility group protein 20A	DNA binding	HMG-box domain
MH1	H6	AL I-7C7	W04A8.7	<i>taf-1</i>	human TATA-binding protein associated factor TAF11 (TAF1250) that possesses histone acetyl transferase (HAT) activity and is a component of the TFIID general transcription factor that recognizes the transcription	transcription regulation / histone modification	bromodomain; Zn finger
MH1	H7	96AL_25C08	F47G4.6	<i>hmg-6</i>	High mobility group box domain	DNA binding	HMG-box domain
MH1	H8	96AL_27C09	Y39G10A.8		histone H3-K79 methyltransferase; In contrast to other lysine histone methyltransferases, it does not contain a SET domain, suggesting the existence of another mechanism for methylation of lysine residues of histones	histone modification; DNA methylation	DOT1 domain
MH1	H9	AL X-5P12	F45E6.3	<i>tbc-13</i>	PHD-finger containing protein	chromatin binding	PHD finger
MH1	H10	96AL_26E08	Y54F5B.4	<i>ubc-16</i>	ubiquitin conjugating enzyme.	ubiquitin machinery	
MH1	H11	96AL_27E05	Y39G10A.8		eukaryotic translation initiation factor 2 gamma	Others (translation)	
MH1	H12	96AL_27E10	Y39G10A.8		eukaryotic translation initiation factor 2 gamma	Others (translation)	
MH2	A1	96AL_26F10	ZK909.2	<i>kin-1</i>	serine/threonine protein kinase that is orthologous to cAMP-dependent protein kinase	protein kinase	
MH2	A2	Suppl-9E5	Y47G6A.6	<i>pcfaf-1</i>	C. elegans PCAF/GCN5-like histone acetyltransferase.	histone modification; DNA methylation	
MH2	A3	AL I-3F21	R06C7.1	<i>wago-1</i>	worm Argonaute protein	RNAi machinery	PIWI/PAZ
MH2	A4	96AL_26G11	F33H2.7	<i>set-10</i>	protein containing trithorax/polycomb SET domain.	histone modification; DNA methylation	SET domain; MYND-type Zn finger
MH2	A5	96AL_25H03	Y105E8A.17	<i>ekl-4</i>	DNA methyltransferase 1 associated protein, Enhancer of Ksr-1 Lethality	histone modification / chromatin remodelling	
MH2	A6	96AL_29E12	Y71G12B.15	<i>ubc-3</i>	E2 ubiquitin-conjugating enzyme orthologous	ubiquitin machinery	
MH2	A7	AL II-1A5	C01B12.2	<i>gmeb-1</i>	GMEB (Glucocorticoid Modulatory Element Binding protein) transcriptional regulator homolog	transcription regulation	SAND domain
MH2	A8	96AL_31A09	C01B12.8		ortholog of human Forkhead-associated (FHA) phosphopeptide binding domain 1	Others (closest ortholog but no evidence, no domain)	
MH2	A9	96AL_31A10	F23F1.1	<i>nfy-1</i>	Nuclear transcription factor Y, subunit gamma	transcription regulation	
MH2	A10	96AL_34A09	W09B6.2	<i>taf-6.1</i>	TAF (TBP-associated transcription factor) family	transcription regulation	
MH2	A11	96AL_32C12	W04H10.3	<i>nhl-3</i>	NHL (ring finger b-box coiled coil) domain containing	DNA binding	RING Zn finger
MH2	A12	96AL_33C03	T07D3.7	<i>alg-2</i>	PAZ and PIWI-domain containing protein that is a member of the highly conserved eukaryotic RDE-1/AGO1/PIWI family of proteins that regulate posttranscriptional gene silencing (PTGS)	RNAi machinery	PAZ/PIWI
MH2	B1	AL I-4G17	F52B5.5	<i>cep-1</i>	transcription factor, p53-like protein	DNA binding	Zn finger
MH2	B2	96AL_36A05	F52C6.12		ubiquitin-conjugating enzyme E2-17 kDa like.	ubiquitin machinery	
MH2	B3	Supp II-10H2	ZK1240.1		Zn finger-containing protein	DNA binding	RING-type Zn finger
MH2	B4	96AL_37A06	ZK1240.2		Zn finger-containing protein	DNA binding	RING-type Zn finger
MH2	B5	96AL_37A07	ZK1240.3		Zn finger-containing protein	DNA binding	RING-type Zn finger
MH2	B6	96AL_36H12	B0281.3		Zn finger-containing protein	DNA binding	RING-type Zn finger
MH2	B7	96AL_37H07	F34D6.4	<i>set-11</i>	histone H3 lysine-9 methyltransferase ortholog	histone modification; DNA methylation	
MH2	B8	AL II-2P24	T10D4.6		others	Others	
MH2	B9	96AL_42A06	C16A11.3		SPK-domain containing protein	DNA binding	SPK domain
MH2	B10	AL II-3B14	C16A11.4		SPK-domain containing protein	DNA binding	SPK domain; Zn finger
MH2	B11	96AL_42B11	H20J04.2	<i>atph-2</i>	AT Hook plus PHD finger transcription factor	transcription regulation	PHD-finger
MH2	B12	96AL_41E08	Y14H12B.2		SPK-domain containing protein	DNA binding	SPK domain; Zn finger
MH2	C1	96AL_41F04	K07D4.3	<i>rpn-11</i>	non-ATPase subunit of the 19S regulatory complex of the proteasome; Metalloprotease component of the 26S proteasome that specifically cleaves 'Lys-63'-linked polyubiquitin chains. The 26S proteasome is involved in the ATP-dependent degradation of ubiquitinated proteins.	ubiquitin machinery	
MH2	C2	96AL_42G06	T05A7.4	<i>hmg-11</i>	High mobility group protein I alpha	DNA binding	HMG box
MH2	C3	AL II-3P2	F10G7.2	<i>tsn-1</i>	component of the RNA-induced silencing complex (RISC); nuclease component Tudor-SN	RNAi machinery	Tudor domain
MH2	C4	96AL_44A05	F58A6.8	<i>mcp-45</i>	major sperm protein	Others	
MH2	C5	AL I-5C1	T23D8.7		Argonaute protein	RNAi machinery	PIWI/PAZ
MH2	C6	96AL_44B09	C34F11.4	<i>mcp-50</i>	major sperm protein	Others	
MH2	C7	96AL_44B11	C34F11.6	<i>mcp-49</i>	major sperm protein	Others	

MH2	C8	Supp I-10A8 D2030.6	<i>prg-1; targets prg-2 as well</i>	Argonaute protein	RNAi machinery	PIWI/PAZ
MH2	C9	96AL_45B08 C17G10.4	<i>cdc-14</i>	cell-division-cycle related; dual-specificity phosphatase (tyrosine-protein phosphatase)	Others (protein phosphatase/cell cycle regulation)	
MH2	C10	Supp II-11111 ZK1248.7	<i>wago-5</i>	Argonaute protein	RNAi machinery	PIWI/PAZ
MH2	C11	96AL_46C06 H12113.1		SPK-domain containing protein family member. Protein kinase	protein kinase	SPK domain
				Retinoblastoma-binding protein homolog 5; a WD40 repeat-containing protein that is the C. elegans homolog of Saccharomyces cerevisiae Swd1; required for di- and trimethylation at H3K4	histone modification; DNA methylation	WD repeats
MH2	C12	96AL_46C08 F21H12.1	<i>rbbp-5</i>	encoding atypical protein kinase C, component of a PDZ-mediated protein complex PAR-6/PAR-3/PKC-3/CDC-42 required for establishing embryonic polarity	protein kinase	
MH2	D1	96AL_44D05 F09F5.1	<i>pkc-3</i>	major sperm protein	Others	
MH2	D2	96AL_43D08 R05F9.3	<i>msp-32</i>	C. elegans Chromodomain protein	DNA binding/structure	chromodomain
MH2	D3	96AL_46D05 C29H12.5	<i>cec-9</i>	major sperm protein	Others	
MH2	D4	96AL_43E01 R05F9.8	<i>msp-33</i>	major sperm protein	Others	
MH2	D5	96AL_43E06 R05F9.13	<i>msp-13</i>	major sperm protein	Others	
MH2	D6	96AL_43E09 ZK546.3		major sperm protein	Others	
MH2	D7	96AL_43E11 ZK546.6	<i>msp-152</i>	major sperm protein	Others	
MH2	D8	AL II-5E23 F18C5.2	<i>wrn-1</i>	Probable Werner syndrome ATP-dependent helicase homolog 1	DNA binding/structure	helicase domains
				putative histone H4K20 methyltransferase; SET-4 is orthologous to Drosophila SUV4-20, and to human SUV420H1; H3K20 represents specific tag for epigenetic transcriptional repression	histone modification; DNA methylation	
MH2	D9	96AL_46G10 C32D5.5	<i>set-4</i>	major sperm protein	Others	
MH2	D10	96AL_45G12 ZK1248.17		major sperm protein	Others	
MH2	D11	96AL_45F05 K05F1.7	<i>msp-63</i>	protein containing trithorax/polycomb SET domain; H3K4 methylation	histone modification; DNA methylation	
MH2	D12	96AL_43H11 ZC8.3	<i>set-30</i>	putative Argonaute	RNAi machinery	
MH2	E1	AL III-1J2 C1481.6	<i>nrde-1</i>	ADA (histone acetyltransferase complex (subunit))	histone modification; DNA methylation	SANT/Myb
MH2	E2	96AL_49B04 F32A5.1	<i>ada-2</i>	Probable U6 snRNA-associated Sm-like protein Lsm4	splicing	
MH2	E3	96AL_49B10 F32A5.7	<i>lsm-4</i>	Argonaute protein	RNAi machinery	PIWI/PAZ
MH2	E4	AL III-5E16 ZK757.3	<i>alg-4</i>	localized to H3/H2A histone acetyltransferase complex	histone modification; DNA methylation	
MH2	E5	AL II-5I8 ZK1127.3		Chromosome instability 4	DNA binding/structure	
MH2	E6	96AL_48E08 ZK1127.7	<i>cin-4</i>	homolog of Serine/Threonine-protein kinase haspin	protein kinase	kinase domain
MH2	E7	Cloned Y18H1A.10		Chromosome instability 4	DNA binding/structure	
MH2	E8	AL II-5I18 ZK1127.7	<i>cin-4</i>	C. elegans Chromodomain protein	DNA binding/structure	chromodomain
MH2	E9	AL II-5J06 T09A5.8	<i>cec-3</i>	Argonaute protein	RNAi machinery	PIWI/PAZ
MH2	E10	Supp III-8B19 C16C10.3	<i>hrde-1</i>	E2 ubiquitin-conjugating enzyme	ubiquitin machinery	
MH2	E11	96AL_49E10 D1022.1	<i>ubc-6</i>	43 kDa receptor-associated protein of the synapse homolog	Others	RING-type Zn finger
MH2	E12	96AL_47G04 K18H9.7	<i>ryp-1</i>	histone deacetylase; Probably responsible for the deacetylation of lysine residues on the N-terminal part of the core histones (H2A, H2B, H3 and H4)	histone modification; DNA methylation	
MH2	F1	96AL_50G04 C08B11.2	<i>hda-2</i>	SWI/SNF nucleosome remodeling complex component	chromatin remodelling	SWI/SNF; ARID
MH2	F2	96AL_50G05 C08B11.3	<i>swsn-7</i>	spliceosome-Associated Protein and actin related protein	splicing	
MH2	F3	96AL_50G08 C08B11.6	<i>arp-6</i>	putative Argonaute	RNAi machinery	
MH2	F4	AL IV-3J8 F45E4.10	<i>nrde-4</i>	Argonaute protein	RNAi machinery	PIWI/PAZ
MH2	F5	AL IV-3O11 C01G5.2	<i>prg-2</i>	Regulator of chromosome condensation; associated with RAN (nuclear import/export) function	chromatin structure	
MH2	F6	96AL_51C10 F35C11.4		Transcription factor	transcription regulation	
MH2	F7	96AL_51D12 C26D10.1	<i>ran-3</i>	related to SAS10-chromatin silencing	chromatin remodelling	
MH2	F8	96AL_53D07 T23G7.1	<i>dpl-1</i>	Mediator of RNA polymerase II transcription subunit 13	transcription regulation	
MH2	F9	96AL_52E03 T01B7.5		TP-dependent DEAD/H box RNA helicase orthologous to human RNA helicase A; Unwinds double-stranded DNA and RNA in a 3' to 5' direction. Transcriptional regulator that controls germline mitosis and development via histone modification	Others (helicases)	
MH2	F10	Supp II-10A24K08F8.6	<i>let-19</i>	Tubulin-tyrosine ligase-like protein 12	Others	TTL domain
MH2	F11	AL II-6M24 T07D4.3	<i>rha-1</i>	Histone-lysine N-methyltransferase PRDM9; H3K4 methyltransferase activity	histone modification; DNA methylation	SET domain; MYND-type Zn finger
MH2	F12	96AL_53G04 D2013.9	<i>tthl-12</i>		histone modification; DNA methylation	
MH2	G1	96AL_52H10 T21B10.5	<i>set-17</i>	SET domain-containing protein 14	Others (nuclear pore)	
MH2	G2	96AL_57B01 R06F6.4	<i>set-14</i>	Nuclear pore complex protein Nup53	transcription regulation	
MH2	G3	96AL_57B02 R06F6.5	<i>npp-19</i>	related to transcription repression	transcription regulation	
MH2	G4	AL II-7I16 R166.1	<i>mab-10</i>	Uncharacterized RING finger protein	DNA binding	RING-type Zn finger
MH2	G5	96AL_55F07 ZK945.4		Zn finger-containing protein	DNA binding	C2H2-type Zn finger
MH2	G6	96AL_55G09 F33H1.4		ubiquitin carboxyl-terminal hydrolase family protein	ubiquitin machinery	
MH2	G7	AL II-7N4 F07A11.4		DAF-12 Interacting Protein	NA binding	
MH2	G8	AL II-7N8 F07A11.6	<i>din-1</i>	proteasome Regulatory Particle S14, Non-ATPase-like	ubiquitin machinery	
MH2	G9	96AL_58G08 ZK20.5	<i>rpn-12</i>	proteasome Regulatory Particle S14, Non-ATPase-like proteins with similarity to the atypical protein kinases of the TRAAP subfamily of PIKK kinases that are found in multisubunit, chromatin-modifying histone acetyltransferase complexes	protein kinase	
MH2	G10	96AL_58G10 C47D12.1	<i>trr-1</i>	Polycomb protein sop-2	transcription regulation	SAM-like
MH2	G11	96AL_60A10 C50E10.4	<i>sop-2</i>	Histone Deacetylase	histone modification; DNA methylation	
MH2	G12	96AL_59B02 F43G6.11	<i>hda-5</i>	Argonaute protein	RNAi machinery	PIWI/PAZ
MH2	H1	AL IV-6A22 T22B3.2	<i>alg-3; targets alg-4 as well</i>	Polycomb protein sop-2	transcription regulation	SAM-like
MH2	H2	96AL_60C02 C50E10.4	<i>sop-2</i>	Probable DNA topoisomerase 2	DNA binding/structure	
MH2	H3	96AL_59C03 K12D12.1	<i>top-2</i>	AT hook-containing High Mobility Group type	DNA binding	AT-hook
MH2	H4	96AL_59D03 Y17G7A.1	<i>hmg-12</i>	zinc finger transcription factor of the C2H2 type	transcription regulation	C2H2-type Zn finger
MH2	H5	96AL_59D08 W03C9.4	<i>lin-29</i>	Argonaute protein	RNAi machinery	PIWI/PAZ
MH2	H6	AL V-1F11 R09A1.1	<i>ergo-1</i>	histone H3 family	chromatin structure	
MH2	H7	96AL_62E06 ZK131.3	<i>his-9</i>	histone H3 family	chromatin structure	
MH2	H8	96AL_62E10 ZK131.7	<i>his-13</i>	SPK-domain containing protein family member.	DNA binding	SPK domain
MH2	H9	96AL_59F12 Y57A10A.1		histone - closest to H3	chromatin structure	
MH2	H10	96AL_61F03 W09H1.2	<i>his-73</i>	histone H3 family	chromatin structure	
MH2	H11	96AL_62F05 F08G2.3	<i>his-42</i>	member of the TBP-associated family (TAF)	Others (helicases)	
MH2	H12	96AL_61F07 F15D4.1	<i>btf-1</i>			
MH3	A1	96AL_59G01 Y57A10A.2		SPK containing protein family member.	DNA binding	SPK domain
MH3	A2	96AL_59G03 Y57A10A.3		SPK containing protein family member.	DNA binding	SPK domain
MH3	A3	96AL_59G05 Y57A10A.4		SPK containing protein family member.	DNA binding	SPK domain
MH3	A4	96AL_59G07 Y57A10A.5		SPK containing protein family member.	DNA binding	SPK domain
MH3	A5	96AL_59G09 Y57A10A.6		SPK containing protein family member.	DNA binding	SPK domain
MH3	A6	96AL_59G11 Y57A10A.7		SPK containing protein family member.	DNA binding	SPK domain
MH3	A7	96AL_59H01 Y57A10A.8		SPK containing protein family member.	DNA binding	SPK domain
MH3	A8	96AL_62G03 Y51H1A.5	<i>hda-10</i>	histone deacetylase.	histone modification; DNA methylation	
MH3	A9	96AL_63C06 Y48B6A.11	<i>jmjd-2</i>	JmJc domain-containing histone demethylase protein 2; Histone demethylase that specifically demethylates H3K9 and H3K36	histone modification; DNA methylation	
MH3	A10	96AL_65C04 Y110A2AR.2	<i>ubc-15</i>	ubiquitin conjugating enzyme	ubiquitin machinery	
MH3	A11	AL V-1G23 T22H9.3	<i>wago-10</i>	Argonaute protein	RNAi machinery	PIWI/PAZ
MH3	A12	96AL_63D07 Y48B6A.14	<i>hmg-1.1</i>	member of the high mobility group (HMG) family of proteins	DNA binding	HMG box
MH3	B1	96AL_64E06 Y53F4B.3		Histone-binding component of a NURF-like (nucleosome remodeling factor-like) complex, which would catalyze ATP-dependent nucleosome sliding and facilitate transcription of chromatin	DNA binding/transcriptional regulation	
MH3	B2	96AL_63F05 F26H11.2	<i>nurf-1</i>	SPT transcription factor family	chromatin remodelling	
MH3	B3	96AL_66B01 F54C4.2	<i>spt-4</i>	AT hook Transcription Factor family	transcription regulation	
MH3	B4	96AL_66B02 F54C4.3	<i>atf-3</i>	transcription cofactor activity	DNA binding	AT hook
MH3	B5	AL III-1C15 C29F9.5			transcription regulation	Zn finger

MH3	B6	96AL_67C11	F23H11.1	<i>bra-2</i>	homolog of the human BMP receptor-associated molecule (BRAM1)	transcription regulation	MYND-type Zn finger
MH3	B7	96AL_68C09	W04B5.1			?	
MH3	B8	96AL_66D04	F40G9.3	<i>ubc-20</i>	Ubiquitin Conjugating enzyme	ubiquitin machinery	
MH3	B9	GP 2D1/3H3	C14B1.4	<i>wdr-5.1</i>	WD-repeat containing protein GMBE (Glucocorticoid Modulatory Element Binding protein) transcriptional regulator	protein-protein interaction	WD repeats
MH3	B10	96AL_69E12	C44F1.2	<i>gmeb-3</i>	homolog	transcription regulation	SAND domain
MH3	B11	96AL_68F08	H05C05.2		SPK-domain containing protein	DNA binding	SPK domain
MH3	B12	96AL_69F09	R13G10.2	<i>amx-1</i>	Amine oxidase family member 1; H3-K4 demethylation activity	histone modification; DNA methylation	
MH3	C1	96AL_69G07	C36A4.8	<i>brc-1</i>	Breast and ovarian cancer susceptibility protein homolog.	DNA binding/ DNA repair/ubiquitin machinery	RING-type Zn finger; PHD
MH3	C2	96AL_70A11	T02C12.3	<i>tfrc-5</i>	Transcription Factor ThreeC subunit (GTF3C homolog)	transcription regulation	
MH3	C3	96AL_73A07	C34E10.5	<i>prmt-5</i>	protein arginine methyltransferase.	histone modification; DNA methylation	potential DNA binding domain
MH3	C4	96AL_73A10	C34E10.8		potential chromatin remodelling protein or helicase	chromatin remodelling	
MH3	C5	96AL_70B01	E03A3.3	<i>his-69</i>	Putative histone H3.3-like type 3	chromatin structure	
MH3	C6	96AL_70C07	C16C10.4		Probable histone deacetylase complex subunit SAP18; Acts in transcription repression.	histone modification; DNA methylation	
MH3	C7	96AL_70C10	C16C10.7	<i>rnf-5</i>	Involved in the tethering of the SIN3 complex to core histone proteins RING finger protein 5	DNA binding	RING-type Zn finger
MH3	C8	96AL_72C04	F26F4.7	<i>nhl-2</i>	ring finger b-box coiled coil domain containing protein; functions together with CGH-1 and in association with the miRISC complex to regulate the efficacy of microRNA-target interactions	RNAi machinery	TRIM motif; RING-type Zn finger
MH3	C9	96AL_72C11	C26E6.3	<i>ntf-9</i>	putative transcription factor	transcription regulation	
MH3	C10	96AL_72D05	C26E6.9	<i>set-2</i>	histone H3K4 methyltransferase	histone modification; DNA methylation	
MH3	C11	Supp III-8E15	C26E6.12		GTP-binding protein, HSR1-related	Others	GTP1/OBG subdomain
MH3	C12	AL V-4H7	Y38A10A.6	<i>smut-1</i>	helicase	DNA binding/structure	helicase domains
MH3	D1	96AL_71G11	C38D4.3	<i>mel-28</i>	protein required for nuclear envelope assembly	Others (nuclear structure)	
MH3	D2	96AL_70H03	R07E5.3	<i>snf-5</i>	homolog of SNF5/Ini1, a component of the SWI/SNF complex	chromatin remodelling	
MH3	D3	96AL_70H09	R07E5.10	<i>pdcd-2</i>	PDCD (mammalian ProgrammeD Cell Death protein) homolog	Others	MYND-type Zn finger
MH3	D4	AL III-2P1	K10D2.1		Required for replication-independent chromatin assembly	chromatin structure	WD repeats
MH3	D5	96AL_73H05	C05D2.5	<i>xnd-1</i>	AT hook motif containing protein family member; X chromosome nondisjunction factor	DNA binding	AT hook
MH3	D6	96AL_72H09	ZC155.2		histone-like	chromatin structure	
MH3	D7	96AL_74A12	B0336.7		zinc finger, C2CH-type family member. LIN37 is a component of the DREAM (MuvB/DRM) complex, which represses cell cycle-dependent genes in quiescent cells and plays a role in the cell cycle-dependent activation of G2/M genes	DNA binding	C2H2-type Zn finger
MH3	D8	96AL_77A04	ZK418.4	<i>lin-37</i>	Chromatin-remodeling complex ATPase chain <i>isw-1</i> ; energy-transducing component of a NURF-like (nucleosome-remodeling factor-like) complex, which would catalyze ATP-dependent nucleosome sliding and facilitate transcription of chromatin	Others	
MH3	D9	96AL_76C08	F37A4.8	<i>isw-1</i>	High mobility group protein 1.2	chromatin remodelling	
MH3	D10	96AL_75D09	F47D12.4	<i>hmg-1.2</i>	High mobility group protein 1.2	DNA binding	HMG box
MH3	D11	GP 2E6	C56G2.1		KH-domain containing protein; A-Kinase Anchor Protein	RNA binding	KH; Tudor
MH3	D12	96AL_75E03	C56G2.1		KH-domain containing protein; A-Kinase Anchor Protein	RNA binding	KH; Tudor
MH3	E1	96AL_74E10	C28H8.9	<i>dpff-1</i>	DPF (transcription factor) Family	transcription regulation	C2H2-type Zn finger; PHD
MH3	E2	Supp:III-8J20	C56G2.15		N-acetyltransferase 6 like. orthologous to the human gene SWI/SNF-related, matrix-associated, actin-dependent regulator of chromatin, subfamily A-like protein 1 (SMARCAL1); SMARCAL1 is involved in the remodeling of chromatin; possesses intrinsic ATP-dependent nucleosome-remodeling activity	histone modification; DNA methylation	
MH3	E3	Supp:III-8E14	C16A3.1		serine/threonine rich protein; CRAMP1L ortholog	chromatin remodelling	
MH3	E4	Cloned	R151.8		Probable double-stranded RNA-specific adenosine deaminase; RNA-editing enzymes that deaminate adenosines to create inosines in double-stranded RNA (dsRNA)	chromatin binding	
MH3	E5	96AL_77E07	T20H4.4	<i>adr-2</i>		RNA binding/ RNAi machinery	
MH3	E6	96AL_75F01	C16A3.3	<i>let-716</i>	Tetratricopeptide repeat-containing	RNA binding and processing	TPR (tetratricopeptide repeat-containing domain)
MH3	E7	96AL_74F05	F25B5.4	<i>ubq-1</i>	Ubiquitin	ubiquitin machinery	
MH3	E8	96AL_76F01	T07E3.3		glutathione S-transferase kappa 1. JmjC domain-containing histone demethylation protein 1; Histone demethylase that specifically demethylates H3K36	Others	
MH3	E9	96AL_75H02	T26A5.5	<i>jhdM-1</i>	SET domain-containing protein predicted to function as a histone lysine N-methyltransferase	histone modification; DNA methylation	
MH3	E10	96AL_75H04	T26A5.7	<i>set-1</i>	transcription factor CBF/NF-Y/archaeal histone	histone modification; DNA methylation	
MH3	E11	96AL_75H05	T26A5.8		FACT complex subunit SSRP1	transcription regulation	histone-fold
MH3	E12	96AL_77H05	T20B12.8	<i>hmg-4</i>	E2 ubiquitin-conjugating enzyme	DNA binding/transcriptional regulation	HMG-box
MH3	F1	96AL_76H12	R01H2.6	<i>ubc-18</i>	abnormal cell lineage, encoding synthetic Multivulva protein with two C2H2 zinc fingers.	ubiquitin machinery	
MH3	F2	96AL_79A05	F44B9.5	<i>lin-36</i>	uncharacterized protein; domains typical for transcription factors/chromatin remodeling complexes/co-chaperones	DNA binding	C2H2-type Zn finger
MH3	F3	96AL_81A04	F54F2.9		Chromo domain-containing protein	chromatin binding	DnaJ domain; SANT/Myb domain; homeodomain-like
MH3	F4	96AL_80A10	ZK1236.2	<i>cec-1</i>	endonuclease Involved in cleaving double-stranded RNA in the RNA interference	DNA binding	chromo domain
MH3	F5	96AL_79B04	K12H4.8	<i>dcr-1</i>	Serine/threonine-protein kinase	RNAi machinery	
MH3	F6	AL:III-4C10	C14B9.4	<i>plk-1</i>	retinoblastoma related pathway actor; component of the DRM complex functioning in transcription repression	protein kinase	
MH3	F7	96AL_81B04	ZK637.7	<i>lin-9</i>	Serine/threonine-protein kinase	transcription regulation	
MH3	F8	AL:III-4E8	C14B9.4	<i>plk-1</i>	DNA binding protein	protein kinase	
MH3	F9	96AL_78C06	ZK783.4	<i>ftt-1</i>	Mediates transcriptional repression by certain nuclear receptors; nuclear receptor corepressor 1	DNA binding	bromodomain; PHD finger
MH3	F10	96AL_79C06	C14B9.6	<i>gei-8</i>	B-box type zinc finger protein; might act directly as a transcription factor to inhibit RNA polymerase I (rRNA) and III (5S RNA) transcription	transcription regulation	SANT/Myb domain
MH3	F11	96AL_78D04	ZK112.2	<i>ncl-1</i>	Zinc finger protein	transcription regulation	B box-type Zn finger
MH3	F12	96AL_78F01	ZK652.6		RING finger protein	DNA binding	C2H2-type Zn finger
MH3	G1	AL III-4N12	F54G8.4	<i>nhl-1</i>	E3 ubiquitin-protein ligase that mediates monoubiquitination of 'K117' of histone H2B. H2B 'K117' ubiquitination gives a specific tag for epigenetic transcriptional activation and is also prerequisite for histone H3 'K4' and 'K79' methylation	protein-protein interaction	Znf_RING
MH3	G2	96AL_79H05	R05D3.4	<i>rfp-1</i>	Histone methyltransferase which is required for the mono- and dimethylation of H3K9. This increases the efficiency of set-25-mediated trimethylation of histone H3K9	histone modification; DNA methylation	
MH3	G3	96AL_79H12	R05D3.11	<i>met-2</i>	AT hook motif containing protein	histone modification; DNA methylation	
MH3	G4	96AL_80H05	K02D10.3		others	Others	
MH3	G5	96AL_81H06	T23G5.6		DNA binding	DNA binding	AT hook
MH3	G6	96AL_80H09	F54F2.2	<i>zfp-1</i>	Zinc finger protein	DNA binding	Znf; PHD
MH3	G7	96AL_81H07	T02C1.1		RING finger protein	protein-protein interaction	Znf_RING
MH3	G8	96AL_80H10	F54F2.2		Zinc finger protein	DNA binding	Znf; PHD
MH3	G9	GP 2F9	C29E4.5	<i>tag-250</i>	Tudor domain containing protein	histone binding	Tudor domain
MH3	G10	96AL_83A05	R10E11.3	<i>usp-46</i>	ubiquitin specific peptidase 46	ubiquitin machinery	
MH3	G11	AL III-5B2	K01G5.2	<i>hpl-2</i>	Chromo domain-containing protein	DNA binding	chromo domain
MH3	G12	96AL_84A08	T20B5.11	<i>rde-4</i>	protein containing two dsRNA-binding motifs; during the initiation phase of RNA interference (RNAi), RDE-4 appears to function in recognition and subsequent cleavage of long-trigger dsRNA molecules into small, interfering RNAs (siRNAs)	RNAi machinery	
MH3	H1	96AL_82B09	F54C8.2	<i>cpar-1</i>	Histone H3-like variant which exclusively replaces conventional H3 in the nucleosome core of centromeric chromatin at the inner plate of the kinetochore. Required for recruitment and assembly of kinetochore proteins, mitotic progression and chromosome segregation. May serve as an epigenetic mark that propagates centromere identity through replication and cell division.	DNA binding/structure	
MH3	H2	96AL_83B12	ZK632.13		Synthetic multivulva class B (synMuvB) protein. SynMuvB proteins are required to repress the induction of vulval development by Ras signaling and probably act by forming the multiprotein DRM complex that repress transcription	transcription regulation	
MH3	H3	96AL_85C01	C44B9.4	<i>lin-52</i>	AT Hook plus PHD finger transcription factor.	transcription regulation	AT hook
MH3	H4	96AL_84D02	M03C11.3	<i>athp-1</i>		Others	
MH3	H5	96AL_84D03	M03C11.4	<i>hat-1/tag-235</i>	Histone acetyltransferase activity; chromatin silencing at telomers	histone modification; DNA methylation	
MH3	H6	Supp:III-8C7	M03C11.8		SWI SNF-related matrix-associated actin-dependent regulator of chromatin subfamily A containing dead H box 1; DNA helicase that possesses intrinsic ATP-dependent nucleosome-remodeling activity and is both required for DNA repair and heterochromatin organization	DNA binding/structure	

MH3	H7	AL X-1A17	R04A9.2	<i>nrde-3</i>	Transports small interfering RNAs (siRNAs) from the cytoplasm to the nucleus. Required for RNA interference (RNAi) in nuclei.	RNAi machinery	PIWI/PAZ
MH3	H8	96AL_82F05	F58A4.3	<i>hcp-3</i>	Histone H3-like variant which exclusively replaces conventional H3 in the nucleosome core of centromeric chromatin at the inner plate of the kinetochore; may serve as an epigenetic mark that propagates centromere identity through replication and cell division	chromatin structure	
MH3	H9	96AL_82F12	F58A4.10	<i>ubc-7</i>	ubiquitin conjugating enzyme.	ubiquitin machinery	
MH3	H10	96AL_82G11	C07A9.7	<i>set-3</i>	SET domain-containing protein predicted to function as a histone lysine N-methyltransferase	histone modification; DNA methylation	
MH3	H11	96AL_83H04	ZK1128.5	<i>swsn-3 = ham-3</i>	chromatin remodeling complex Swp73 SWI/SNF related, actin dependent Regulator of Chromatin, subfamily D (SMARCD3) homolog	chromatin remodelling	
MH3	H12	96AL_89A01	T28A8.6		SPK-containing protein family member.	DNA binding	SPK domain
MH4	A1	96AL_86B02	Y47D3B.9	<i>bed-2</i>	BED-type Zn finger Variant histone H3 which replaces conventional H3 in a wide range of nucleosomes in active genes. Constitutes the predominant form of histone H3 in non-dividing cells and is incorporated into chromatin independently of DNA synthesis. Deposited at sites of nucleosomal displacement throughout transcribed genes, suggesting that it represents an epigenetic imprint of transcriptionally active chromatin.	DNA binding	Zn finger BED-type
MH4	A2	96AL_87B10	Y49E10.6	<i>his-72</i>	pseudogene	chromatin structure	
MH4	A3	96AL_87B11	Y49E10.7		pseudogene	pseudogene?	
MH4	A4	96AL_87B12	Y49E10.8		pseudogene	pseudogene?	
MH4	A5	GP 2H4	T12D8.1	<i>set-16</i>	H3K methyltransferases of the SET1/mixed lineage leukaemia (MLL) family	histone modification; DNA methylation	SET domain
MH4	A6	AL III-6D24	T12D8.7	<i>taf-9</i>	TATA binding protein associated transcription factor	transcription regulation	
MH4	A7	Supp III-8K22	Y55B1B8.3	<i>cec-8</i>	chromodomain-containing protein	DNA binding	chromodomain
MH4	A8	GP 2H2	Y43F4B.3	<i>set-25</i>	putative histone H3 lysine-9 methyltransferase	histone modification; DNA methylation	SET domain
MH4	A9	GP 1E1	F45H11.2	<i>ned-8</i>	Ubiquitin-like protein Nedd8	ubiquitin machinery	
MH4	A10	AL III-6I14	Y111B2A.11	<i>epc-1</i>	enhancer of PolyComb-like; negative regulator of Ras.	transcription regulation	
MH4	A11	96AL_88E07	F53A2.6	<i>dro-1</i>	DR1 transcription factor related mortality factor-related gene; associates to oogenic chromatin, but only to autosomes; represses genes on the X chromosome and promotes germline immortality.	transcription regulation	
MH4	A12	96AL_87G12	Y37D8A.9	<i>mrg-1</i>	WD-repeat containing protein	DNA binding	chromodomain
MH4	B1	GP 1E9	Y87G2A.11		ATP-dependent serine protease that mediates the selective degradation of misfolded and unassembled polypeptides in the peroxisomal matrix	protein-protein interaction	WD repeats
MH4	B2	96AL_86H03	Y75B8A.4		WD-repeat containing protein	Others (protease)	
MH4	B3	GP 3E3	F17C11.10		WD-repeat containing protein	protein-protein interaction	WD repeats
MH4	B4	96AL_88H10	T28A8.3		SPK containing protein family member.	DNA binding	SPK domain
MH4	B5	96AL_88H11	T28A8.4		SPK containing protein family member.	DNA binding	SPK domain
MH4	B6	96AL_88H12	T28A8.5		SPK containing protein family member.	DNA binding	SPK domain
MH4	B7	96AL_89C06	ZK520.2	<i>sid-2</i>	Systemic RNAi-defective; plays a role in RNA-mediated gene silencing by mediating endocytic uptake of double-stranded RNA (dsRNA) ingested from the environment into intestinal cells from the intestinal lumen.	RNAi machinery	
MH4	B8	96AL_91E03	Y71H2AM.17	<i>swsn-3</i>	HMG box family protein like.	DNA binding	HMG box
MH4	B9	GP 4B2	K07H8.3		putative N-acetyltransferase	histone modification; DNA methylation	GNAT domain
MH4	B10	96AL_90G04	Y53G8AR.6		nuclear protein hcc-1.	DNA binding	SAP domain
MH4	B11	96AL_90G05	Y53G8AR.6		nuclear protein hcc-1.	DNA binding	SAP domain
MH4	B12	96AL_90H06	Y53G8AR.2	<i>phf-15</i>	PHD finger protein	DNA binding	Zn PHD finger
MH4	C1	AL IV-1A4	C18H7.9	<i>prmt-4</i>	methyltransferase type 11 and methyltransferase type 12.	histone modification; DNA methylation	
MH4	C2	96AL_95A12	F42A6.5		putative uncharacterized protein	DNA binding/repair	
MH4	C3	96AL_92B02	B05A5.1	<i>tpo-1</i>	protein kinase C-like	protein kinase	
MH4	C4	96AL_92C10	T21D12.3	<i>pqbp-1.1</i>	polyglutamine tract-binding neurodegeneration protein homolog	Others	
MH4	C5	96AL_92E07	T07A9.1	<i>pqbp-1.2</i>	PQBp1 (polyglutamine tract-binding neurodegeneration protein) homolog	Others	
MH4	C6	Supp.IV-9D12	C50A2.2	<i>cec-2</i>	chromodomain-containing protein	DNA binding	chromodomain
MH4	C7	96AL_92E10	T07A9.5	<i>eri-1</i>	3'-5' exonuclease; RNA exonuclease that acts as a negative regulator of RNA interference (RNAi). Probably acts by degrading the 3'-overhangs of short interfering RNAs (siRNAs)	RNAi machinery	
MH4	C8	GP 4C9	K07C5.8	<i>cash-1</i>	WD-repeat containing protein	protein-protein interaction	WD repeats
MH4	C9	96AL_95E05	M57.1		SPK containing protein family member.	DNA binding	SPK domain
MH4	C10	96AL_95E09	B0212.3		SPK containing protein family member.	DNA binding	SPK domain
MH4	C11	AL IV-1O4	F53H1.4		zinc finger, PHD-type family member.	DNA binding	Zn PHD finger
MH4	C12	GP 4E3	R11E3.4	<i>set-15</i>	containing trithorax/polycomb SET domain.	histone modification; DNA methylation	SET domain
MH4	D1	GP 1F3	F39B2.2	<i>uev-1</i>	ubiquitin-conjugating enzyme (UBC or E2) variant that contains the characteristic UBC motif	ubiquitin machinery	
MH4	D2	96AL_108B5	ZK1251.6	<i>msp-76</i>	major sperm protein.	Others	
MH4	D3	AL IV-2C22	R08C7.3	<i>htz-1</i>	Variant histone H2A which replaces conventional H2A in a subset of nucleosomes	DNA structure	
MH4	D4	GP 1H2	F40E12.2		major sperm protein.	protein-protein interaction	ANK repeat
MH4	D5	96AL_99B06	ZK354.4	<i>msp-113</i>	major sperm protein.	Others	
MH4	D6	96AL_99B07	ZK354.5	<i>msp-51</i>	major sperm protein.	Others	
MH4	D7	96AL_99B12	ZK354.11	<i>msp-59</i>	major sperm protein.	Others	
MH4	D8	96AL_97C06	R08C7.10	<i>wapl-1</i>	cohesin interactor, Wings apart-like (Drosophila); regulates heterochromatin structure	chromatin structure	
MH4	D9	96AL_96C09	C35B1.1	<i>ubc-1</i>	Ubiquitin-conjugating enzyme E2	ubiquitin machinery	
MH4	D10	96AL_99C12	F41H10.6	<i>hda-6</i>	histone deacetylase.	histone modification; DNA methylation	
MH4	D11	96AL_97E12	F29B9.2	<i>jmjd-1.2</i>	Histone demethylase required for nervous system development; specifically demethylates dimethylated H3K9me2 and H3K27me2	histone modification; DNA methylation	
MH4	D12	GP 1H7	ZK430.7		WD-repeat containing protein	protein-protein interaction	WD repeats
MH4	E1	96AL_97F1	F29B9.4	<i>psr-1</i>	Dioxyg96AL_se that can both act as a histone arginine demethylase and a lysyl-hydroxylase	histone modification; DNA methylation	
MH4	E2	96AL_97F3	F29B9.6	<i>ubc-9</i>	ubiquitin conjugating enzyme.	ubiquitin machinery	
MH4	E3	GP 1H9	F33G12.2		WD-repeat containing protein	protein-protein interaction	WD repeats
MH4	E4	96AL_99F4	T12E12.2	<i>cec-6</i>	chromodomain-containing protein	DNA binding	chromodomain
MH4	E5	AL IV-2O5	F15E6.1	<i>set-9</i>	protein containing trithorax/polycomb SET domain.	histone modification; DNA methylation	SET domain; PHD Zn finger
MH4	E6	96AL_100A11	C06E7.1	<i>sams-3</i>	Probable S-adenosylmethionine synthase 3	Others (enzymes)	
MH4	E7	AL IV-3B8	F55G1.2	<i>his-59</i>	histone H3	chromatin structure	
MH4	E8	96AL_101B5	F38A5.13	<i>djnj-11</i>	protein containing DnaJ and Myb domains that is orthologous to the mammalian ZRF1/MIDA1/MPP11/DNAJC2 family of ribosome-associated molecular chaperones	chaperones	
MH4	E9	96AL_101B7	F15B10.2	<i>dth-1</i>	DEXH-box Dicer-Related Helicase	RNAi machinery	
MH4	E10	96AL_103C12	F32E10.2	<i>cec-4</i>	chromodomain-containing protein	DNA binding	chromodomain
MH4	E11	96AL_100D3	B0350.2	<i>unc-44</i>	ankyrin-related protein family member	protein-protein interaction	ankyrin repeats
MH4	E12	96AL_100D4	B0350.2	<i>unc-44</i>	ankyrin-related protein family member	protein-protein interaction	ankyrin repeats
MH4	F1	AL IV-3H6	F32E10.5		tudor-domain protein	binding NA, nucleoprotein complexes	tudor domain
MH4	F2	GP 4E12	F32E10.6	<i>cec-5</i>	chromodomain-containing protein	chromatin remodelling	chromodomain
MH4	F3	96AL_101E3	C17H12.13	<i>anat-1</i>	N-acetyltransferase activity	histone modification; DNA methylation	
MH4	F4	96AL_103E3	F45E4.9	<i>hmg-5</i>	HMG (high mobility group) box-containing protein; HMG-5 binds to double-stranded telomeric DNA in vitro	DNA binding	HMG box
MH4	F5	96AL_101F3	T05A12.4		SNF2-related and DNA/RNA helicase, C-terminal family member.	NA binding	RING Zn finger
MH4	F6	96AL_101F10	T05A12.4		SNF2-related and DNA/RNA helicase, C-terminal family member.	NA binding	RING Zn finger
MH4	F7	96AL_101G1C	ZK381.4	<i>pgl-1</i>	P granule abnormality protein, encoding constitutive component of the germline specific P granules	RNA binding	
MH4	F8	96AL_103G4	C46A5.9	<i>hcf-1</i>	encoding host cell factor related; transcriptional regulator that associates with histone modification enzymes and plays a role in cell cycle progression	transcription regulation	
MH4	F9	96AL_103G9	C33H5.6	<i>swd-2.1</i>	WD-repeat containing protein	protein-protein interaction	WD repeats
MH4	F10	AL IV-4A16	F17E9.10	<i>his-32</i>	histone H3	chromatin structure	
MH4	F11	96AL_105B7	D2096.8	<i>nap-1</i>	protein related in sequence to the conserved NAP (Nucleosome Assembly Protein) family of proteins involved in chromatin remodeling	chromatin remodelling	
MH4	F12	96AL_104C1	F20D12.1	<i>csr-1</i>	Argonaute protein required for chromosome segregation, embryonic viability, Slicer activity induced by secondary siRNAs, and (partially) for germline RNAi	RNAi machinery	
MH4	G1	96AL_106C5	C27B7.4	<i>rad-26</i>	helicase	Others (helicases)	
MH4	G2	96AL_105E5	C09G4.4		Caenorhabditis elegans essential complex locus mes-6C, encoding polycomb group silencer embryonic ectoderm development-like, dicistronic, component of histone H3 methyltransferase complex MES-2/MES-6/MES-3	histone modification; DNA methylation	
MH4	G3	96AL_105E6	C09G4.5	<i>mes-6</i>	WD repeat-containing protein that is orthologous to Drosophila Extra sex combs (Esc); as a member of a Polycomb-like chromatin repressive complex with MES-2 and MES-3	histone modification; DNA methylation	
MH4	G4	96AL_105E8	F42A9.2	<i>lin-49</i>	bromodomain protein; regulates expression of homeobox genes; may play an analogous role to the trithorax Group (trxG) proteins	transcription regulation	bromodomain

MH4	G5	96AL_107E2	F56D5.4		pseudogene	pseudogene?		
MH4	G6	AL IV-4J18	F59B8.2	<i>idh-1</i>	Isocitrate dehydrogenase	Others (enzymes)		
MH4	G7	96AL_110A7	R11A8.4	<i>sir-2.1</i>	NAD-dependent protein deacetylase; putative histone H3 deacetylase	histone modification; DNA methylation		
MH4	G8	96AL_109B11	C04G2.4	<i>misp-36</i>	major sperm protein.	Others		
MH4	G9	GP 2B1	F28C6.3	<i>cpf-1</i>	WD-repeat containing protein	protein-protein interaction	WD repeats	
					Putative RNA polymerase II transcriptional coactivator; General coactivator that functions cooperatively with TAFs and mediates functional interactions between upstream activators and the general transcriptional machinery	transcription regulation		
MH4	G10	96AL_108C8	T13F2.2		major sperm protein.	Others		
MH4	G11	96AL_108D4	T13F2.10	<i>misp-79</i>	WD-repeat containing protein	protein-protein interaction	WD repeats	
MH4	G12	GP 2B2	F46C5.9		WD40- and FYVE-domain containing protein that is orthologous to mammalian WDFY2	protein-protein interaction	WD repeats	
MH4	H1	GP 2B5	D2013.2	<i>wdfy-2</i>	ankyrin and KAP P-loop family member.	Others		
MH4	H2	96AL_111D1C	F36H1.2	<i>kdin-1</i>	major sperm protein.	Others		
MH4	H3	96AL_108E2	K07F5.1	<i>misp-81</i>	major sperm protein.	Others		
MH4	H4	96AL_108E3	K07F5.2	<i>misp-10</i>	major sperm protein.	Others		
MH4	H5	96AL_109E3	K08F4.8	<i>misp-38</i>	major sperm protein.	Others		
MH4	H6	96AL_108E4	K07F5.3	<i>misp-56</i>	major sperm protein.	Others		
MH4	H7	AL IV-5J14	M7.1	<i>let-70</i>	Ubiquitin-conjugating enzyme E2	ubiquitin machinery		
MH4	H8	96AL_108F8	F32B6.6	<i>misp-77</i>	major sperm protein.	Others		
MH4	H9	96AL_108G11	C47E12.4	<i>ppp-1</i>	inorganic Pyrophosphatase.	Others		
MH4	H10	96AL_111G3	F01G4.1	<i>psa-4 = swsn-4</i>	ortholog of SWI2/SNF2, a component of the SWI/SNF complex	chromatin remodelling	bromodomain	
					protein similar to prefoldin 4 chaperone; Binds specifically to cytosolic chaperonin (c-CPN) and transfers target proteins to it. Binds to nascent polypeptide chain and promotes folding in an environment in which there are many competing pathways for nonnative proteins	chaperones		
MH4	H11	96AL_112B8	B0035.4	<i>pfid-4</i>	histone H3	DNA structure		
MH4	H12	96AL_112C9	F54E12.1	<i>his-55</i>				
MH5	A1	96AL_112C10	F54E12.2		helicase	Others (helicases)		
MH5	A2	96AL_113D6	C29E6.2	<i>trpo-1</i>	TRPA cation channel homolog.	Others		
MH5	A3	96AL_114D4	F28D1.1	<i>wdr-46</i>	WD repeat protein	protein-protein interaction	WD repeats	
MH5	A4	96AL_112E2	F22B3.2	<i>his-63</i>	histone H3	chromatin structure		0
MH5	A5	AL IV-6J23	C25G4.4	<i>tag-347</i>	SAND family member; early sperm-fate marker	transcription regulation	SAND domain	
					zinc-finger protein; Required for fem-3 3'-UTR-mediated repression in the regulation of the sperm/oocyte switch	RNA binding	C2H2 Zn finger	
MH5	A6	96AL_112F5	M04B2.1	<i>mep-1</i>	involved in maintaining euchromatin-heterochromatin boundaries; thought to form a complex that enhances transcription from repetitive DNA sequences by modulating chromatin structure	chromatin binding; transcription regulation		
MH5	A7	96AL_112F7	M04B2.3	<i>gfl-1</i>	involved in maintaining euchromatin-heterochromatin boundaries; thought to form a complex that enhances transcription from repetitive DNA sequences by modulating chromatin structure	transcription regulation		
MH5	A8	96AL_113F12	K08E4.1	<i>spt-5</i>	SPT transcription factor component.	transcription regulation		
					involved in maintaining euchromatin-heterochromatin boundaries; thought to form a complex that enhances transcription from repetitive DNA sequences by modulating chromatin structure	chromatin structure; transcription regulation	bromodomain	
MH5	A9	96AL_113G6	F11A10.1	<i>lex-1</i>	DNA-binding SAP containing protein; The SAP motif is found in a variety of nuclear proteins involved in transcription, DNA repair, RNA processing or apoptotic chromatin degradation	DNA binding	SAP domain	
MH5	A10	AL IV-7A1	C39E9.12		SPK containing protein family member.	DNA binding	SPK domain	
MH5	A11	96AL_117A8	C08F11.7		Synthetic multivulva class B (synMuvB) protein. SynMuvB proteins are required to repress the induction of vulval development by Ras signaling and probably act by forming the multiprotein DRM complex that repress transcription	transcription regulation		
MH5	A12	AL IV-7E9	JC8.6	<i>lin-54</i>	F-box protein with WD repeats	ubiquitin machinery	F-box domain; WD repeats	
MH5	B1	GP 2B9	T01E8.4	<i>mec-15</i>	pseudogene	Others (cell cycle)		
MH5	B2	96AL_117E1	B0513.6		putative cell cycle and apoptosis regulatory protein	protein kinase		
MH5	B3	96AL_117F10	Y37A1B.1	<i>lst-3</i>	tyrosine protein kinase.	DNA binding		0
MH5	B4	96AL_116F11	Y38H8A.3		FEZ family zinc finger protein	DNA binding		
MH5	B5	96AL_96AL_1	Y38H8A.5	<i>fezf-1</i>	CFP1 (CpG-binding protein, CXXC Finger Protein 1) homolog	Others		
MH5	B6	96AL_117G1	F52B11.1	<i>cpf-1</i>	neuropeptide-like protein.	histone modification; DNA methylation	SET	
MH5	B7	96AL_116G7	Y45F10A.5	<i>nlp-17</i>	protein containing trithorax/polycomb SET domain.	chaperones		
MH5	B8	AL IV-7P18	Y51H4A.12	<i>set-26</i>	hsp70A, a member of the heat shock family of proteins	histone modification; DNA methylation	SET	
MH5	B9	AL IV-8A12	F26D10.3	<i>hsp-1</i>	probable histone methyltransferase	histone modification; DNA methylation	SET	
MH5	B10	96AL_122A6	Y41D4B.12	<i>set-23</i>	Probable histone methyltransferase involved in chromatin modification and/or remodeling in meiotic germ cells. May act redundantly with mes-3 and mes-4 proteins	histone modification; DNA methylation	SET	
MH5	B11	96AL_122B8	C26E6.9	<i>set-2</i>	RAD54B homolog (DNA repair protein); helicase	Others (helicases)		
MH5	B12	96AL_120D2	Y116A8C.13		protein containing ubiquitin-like (UBL) and ubiquitin-associated (UBA) domains that is a member of the Radiation Sensitivity 23 (RAD23) family of proteasomal ubiquitin receptors	ubiquitin machinery		
MH5	C1	GP 2B12	ZK20.3	<i>rad-23</i>	SPK containing protein family member.	DNA binding	SPK domain	
MH5	C2	96AL_121F1	Y73B3B.1		hsp70A, a member of the heat shock family of proteins	chaperones		
MH5	C3	AL IV-8O17	F26D10.3	<i>hsp-1</i>	DNA topoisomerase II family member.	chromatin structure		
MH5	C4	96AL_128D1C	Y46H3C.4		PHD and JmjC domain-containing protein	histone modification; DNA methylation	PHD; JmjC	
MH5	C5	GP 2C3	F43G6.6	<i>jmjd-1.1</i>	GCN5-related N-acetyltransferase family member	histone modification; DNA methylation		0
MH5	C6	GP 3C4	T10B5.4		SNF2-related and DNA/RNA helicase	DNA binding/structure		0
MH5	C7	GP 3C5	F59A7.8		zinc-finger protein	DNA binding	Zn finger C2H2	
MH5	C8	96AL_131E5	F37B4.10		protein with similarity to the KAT8 NLS3 non-enzymatic subunit of the mammalian KAT8/MOF histone acetyltransferase complex	histone modification; DNA methylation		
MH5	C9	96AL_136A12	F54D11.2	<i>sumv-2</i>	one of two C. elegans homologs of human MTA1 (metastasis-associated protein), part of a nucleosome remodeling and histone deacetylation (NURD) complex	histone modification; DNA methylation		
MH5	C10	96AL_134B7	T27C4.4	<i>lin-40</i>	linker histone H1.4.	chromatin structure		
MH5	C11	96AL_136D6	C18G1.5	<i>hil-4</i>	spermine oxidase.	Others		
MH5	C12	96AL_138B11	C24G6.6	<i>hpo-15</i>	systemic RNA Interference Defective. Plays a role in RNA-mediated gene silencing by acting cell-autonomously as a channel for the transport of double-stranded RNA (dsRNA) between cells.	RNAi machinery		
MH5	D1	96AL_137C2	C04F5.1	<i>sid-1</i>	zinc finger, HIT-type.	DNA binding	Zn finger HIT-type	
MH5	D2	96AL_138D5	C04.7	<i>zhit-1</i>	DEAD box RNA helicase; MUT-14 activity is required redundantly with its paralog SMUT-1, for germline RNAi and endogenous siRNA formation	RNAi machinery		
MH5	D3	96AL_138E6	C14C11.6	<i>mut-14</i>	N-acetyltransferase 12	histone modification; DNA methylation	acetyltransferase domain	
MH5	D4	96AL_137F9	B0238.10		wago-8, Argonaute homolog that is partially required for the amplification phase of RNAi responses;	RNAi machinery	PAZ/PIWI	
MH5	D5	96AL_139F7	K12B6.1	<i>sago-1</i>	Probable corepressor protein, which probably participates in the transcriptional repression of the presenilin protein hop-1. Probably acts via the formation of a multiprotein complex that deacetylates and demethylates specific sites on histones	histone modification; DNA methylation		
MH5	D6	96AL_144D11	D1014.8	<i>spr-1</i>	Probable corepressor protein, which probably participates in the transcriptional repression of the presenilin protein hop-1. Probably acts via the formation of a multiprotein complex that deacetylates and demethylates specific sites on histones	histone modification; DNA methylation		
MH5	D7	96AL_144D12	D1014.9	<i>spr-1</i>	MYST family histone acetyltransferase-like; Probable catalytic subunit of the Tip60	histone modification; DNA methylation		
MH5	D8	96AL_141E5	VC5.4	<i>mys-1</i>	chromatin-remodeling complex	histone modification; DNA methylation		
MH5	D9	96AL_144E12	K07C11.2	<i>air-1</i>	Aurora/plp1-related protein kinase 1	protein kinase		
MH5	D10	96AL_141G8	F09G2.9	<i>atf-2</i>	AT-hook motif containing protein.	DNA binding	AT hook	
MH5	D11	GP 3D4	T23B12.1	<i>phf-30</i>	PHD-finger containing protein	chromatin binding	PHD finger	
					guanine nucleotide exchange factor (GEF) that is similar to Drosophila Claret and human RP3; chromosome condensation	chromatin structure		
MH5	D12	96AL_147B4	F07C3.4	<i>glo-4</i>	histone H3	chromatin structure		
MH5	E1	96AL_145E3	F45F2.13	<i>his-6</i>	histone acetyltransferase	histone modification; DNA methylation		
MH5	E2	96AL_148F3	R07B5.9	<i>lsy-12</i>	AAA+ ATPase orthologous to the RUVBL1 family of ATPases; ruvb-1 functions as a component of the TOR signaling pathway	Others		
MH5	E3	96AL_148H3	C27H6.2	<i>ruvb-1</i>	member of the PIWI/STING/Argonaute/Zwille/elf2c family of proteins	RNAi machinery		
MH5	E4	96AL_148H11	K08H10.7	<i>rde-1</i>	protein containing trithorax/polycomb SET domain.	histone modification; DNA methylation	SET domain	
MH5	E5	96AL_150A6	Y32F6A.1	<i>set-22</i>	proline hydroxylase; EGL-9 functions in a conserved hypoxia-sensing pathway to negatively regulate HIF-1 (hypoxia inducible factor) by hydroxylating prolyl HIF-1 residues	Others		
MH5	E6	96AL_150A12	F22E12.4	<i>egl-9</i>		?		
MH5	E7	96AL_152A12	K03B8.4		class 4 histone deacetylase (HDAC)	histone modification; DNA methylation		
MH5	E8	96AL_150B12	C35A5.9	<i>hda-11</i>	HIT zinc finger family protein like.	DNA binding	Zn finger HIT-type	
MH5	E9	Supp V-14G1	ZK856.9	<i>zhit-3</i>	Serine/threonine-protein kinase	protein kinase		
MH5	E10	96AL_149E9	C12D8.10	<i>akt-1</i>	JmjC domain containing protein; encoding GCN5-related N-acetyltransferase	histone modification; DNA methylation	JmjC domain	
MH5	E11	96AL_151E4	C06H2.3	<i>jmjd-5</i>	Ubiquitin-like protein 1-40S ribosomal protein S27a	ubiquitin machinery		
MH5	E12	GP 2C12	H06I04.4	<i>ubl-1</i>				

MHS	F1	96AL_152F7	T27F2.1	<i>skp-1</i>	ortholog of the SKI-binding protein (SKIP); <i>skp-1</i> is predicted to function as a transcriptional cofactor	transcription regulation	
MHS	F2	96AL_149G4	B0024.12	<i>gna-1</i>	glucosamine 6-phosphate N-acetyltransferases	histone modification; DNA methylation	
MHS	F3	96AL_151H11	F47G9.4		Probable RING finger protein 207 homolog	DNA binding	Zn finger RING
MHS	F4	GP 2D6	T10F2.4	<i>prp-19</i>	Pre-mRNA-processing factor 19 homolog; yeast PRP (splicing factor) related	splicing	WD repeats
MHS	F5	96AL_153D3	F57F5.5	<i>pkc-1</i>	serine/threonine protein kinase that is orthologous to mammalian protein kinase C epsilon	protein kinase	
MHS	F6	96AL_156D7	M04G12.4	<i>sami-1</i>	zinc finger, C2H2-type	DNA binding	C2H2 Zn finger
MHS	F7	96AL_155E3	F54F3.1	<i>nid-1</i>	C.elegans homolog of the nidogen (entactin) protein	Others	
MHS	F8	96AL_156E7	Y2H9A.1	<i>mes-4</i>	Histone-lysine N-methyltransferase	histone modification; DNA methylation	
MHS	F9	96AL_153G9	ZK863.6	<i>dpy-30</i>	Dosage compensation protein	Others	
MHS	F10	96AL_159C6	C53A5.3	<i>hda-1</i>	Histone deacetylase 1	histone modification; DNA methylation	
MHS	F11	96AL_157D1	C55B12.3	<i>set-10</i>	encodes two isoforms of an F-box and WD-repeat-containing protein that is a component of an E3 ubiquitin ligase	ubiquitin machinery	WD repeats
MHS	F12	GP 3E12	C47E8.8	<i>set-5</i>	protein containing trithorax/polycomb SET domain.	histone modification; DNA methylation	SET; SPK domain
MHS	G1	96AL_162B1	F28F8.7		ELM2 (Egl-27 and MTA1 homology 2) domain is a small domain of unknown function. It is found in the MTA1 protein that is part of the NuRD complex	DNA binding	ELM2 domain
MHS	G2	96AL_163G4	T10C6.13	<i>his-2</i>	histone H3	chromatin structure	
MHS	G3	AL V-11G22	Y102A5C.18	<i>eft-1</i>	E2F-like (mammalian transcription factor)	transcription regulation	
MHS	G4	96AL_171C1	C25F9.5		SNF2-related domain	transcription regulation	SNF2-related domain
MHS	G5	96AL_172G1	Y113G7B.14		pseudogene	pseudogene	
MHS	G6	96AL_172G4	Y113G7B.17	<i>prmt-1</i>	protein arginine N-methyltransferase PRMT1.	histone modification; DNA methylation	
MHS	G7	96AL_175A6	Y97E10AR.4		SPK-domain containing protein family member.	DNA binding	SPK domain
MHS	G8	96AL_175A7	Y97E10AR.3		SPK-domain containing protein family member.	DNA binding	SPK domain
MHS	G9	96AL_173B11	B0250.9	<i>dhcr-7</i>	7-dehydrocholesterol reductase.	Others (enzymes)	
MHS	G10	AL V-1H20	Y46H3C.4		topoisomerase II family member.	chromatin structure	
MHS	G11	96AL_176A12	R04A9.7		serine/threonine protein kinase-related and tyrosine protein kinase and protein kinase	protein kinase	
MHS	G12	AL X-1G3	F13C5.2		bromodomain-containing protein like.	chromatin structure	bromodomain
MHS	H1	AL X-1K7	T04G9.1		AT hook motif containing protein.	DNA binding	AT hook
MHS	H2	96AL_178F12	ZC53.6		Histone-lysine N-methyltransferase, H3 lysine-79 specific	histone modification; DNA methylation	
MHS	H3	96AL_177G3	ZK402.3		SPK-domain containing protein family member.	DNA binding	SPK domain
MHS	H4	GP 2F9	C29E4.5	<i>tag-250</i>		histone binding	Tudor domain
MHS	H5	96AL_177G6	ZK402.5		SPK-domain containing protein family member.	DNA binding	SPK domain
MHS	H6	AL X-2C18	C12D12.5	<i>sox-2</i>	putative HMG-box transcription factor orthologous to human SOX1, SOX2, and SOX3	transcription regulation	
MHS	H7	96AL_182D3	F48D6.1	<i>taf-11.1</i>	putative TATA binding protein associated transcription factor; transcription initiation from RNA polymerase II promoter	transcription regulation	
MHS	H8	96AL_182E2	C52B9.8		SWI/SNF-related matrix-associated actin-dependent regulator of chromatin a4.	chromatin remodelling	
MHS	H9	AL X-2I11	C24A8.3	<i>pqn-15</i>	prion-like Q/N-rich domain protein.	Others	
MHS	H10	96AL_183F4	ZC8.3	<i>set-30</i>	protein containing trithorax/polycomb SET domain; histone methyltransferase activity (H3-K4 specific)	histone modification; DNA methylation	SET domain
MHS	H11	96AL_183F5	ZC8.3	<i>set-30</i>	protein containing trithorax/polycomb SET domain; histone methyltransferase activity (H3-K4 specific)	histone modification; DNA methylation	SET domain
MHS	H12	96AL_180G5	K09C4.3	<i>hsp-2</i>	heat-shock protein	pseudogene?	
MH6	A1	AL X-2O6	F47F2.1		putative Ser/Thr-protein kinase	protein kinase	
MH6	A2	96AL_182H9	C07A12.5	<i>spr-3</i>	zinc finger family member, probable transcriptional regulator; suppressor of presenilin defect.	transcription regulation	
MH6	A3	SuppX-8A23	T03G11.1	<i>pqn-62</i>	prion-like Q/N-rich domain protein; SAP motif-containing protein	DNA binding	SAP motif
MH6	A4	96AL_185A1	F49E10.5	<i>ctbp-1</i>	CTBP transcriptional co-repressor homolog.	transcription regulation	
MH6	A5	96AL_187A10	C54D1.5	<i>lam-2</i>	laminin gamma-1.	Others (cell. structures)	
MH6	A6	96AL_187C4	K03A1.1	<i>his-40</i>	histone H3	chromatin structure	
MH6	A7	96AL_184E11	T22B7.1	<i>egl-13</i>	SOX domain transcription factor; HMG box	transcription regulation	HMG box
MH6	A8	96AL_187E10	C10A4.8	<i>mnm-2</i>	M Neuron Morphology abnormal, encoding zinc finger, C2H2-type.	DNA binding	Zn finger C2H2
MH6	A9	96AL_184F7	T22B7.1	<i>egl-13</i>	SOX domain transcription factor; HMG box	transcription regulation	HMG box
MH6	A10	GP 3G9	W01C8.3	<i>set-19</i>	protein containing trithorax/polycomb SET domain.	histone modification; DNA methylation	SET
MH6	A11	96AL_184F9	W01C8.4	<i>set-20</i>	protein containing trithorax/polycomb SET domain.	histone modification; DNA methylation	SET
MH6	A12	96AL_187F3	K08A8.2	<i>sox-2</i>	putative HMG-box transcription factor orthologous to human SOX1, SOX2, and SOX3	transcription regulation	HMG box
MH6	B1	Supp X-8L14	F14B8.5		others	Others	
MH6	B2	96AL_188A12	K09F5.5	<i>set-12</i>	protein containing trithorax/polycomb SET domain.	histone modification; DNA methylation	SET domain
MH6	B3	96AL_190A7	C28G1.1	<i>ubc-23</i>	ubiquitin conjugating enzyme.	ubiquitin machinery	
MH6	B4	AL X-4C5	C47C12.3	<i>ref-2</i>	zinc finger C2H2-type, transcription factor	transcription regulation	Zn finger C2H2
MH6	B5	96AL_190B1	C06E2.3	<i>ubc-21</i>	ubiquitin conjugating enzyme.	ubiquitin machinery	
MH6	B6	96AL_190D6	F47E1.3		zinc finger, C2H2-type.	DNA binding	Zn finger C2H2
MH6	B7	96AL_188E4	F45E1.6	<i>his-71</i>	Variant histone H3 which replaces conventional H3 in a wide range of nucleosomes in active genes	chromatin structure	
MH6	B8	96AL_189E5	D2021.1	<i>utx-1</i>	putative histone H3 di/trimethyllysine-27 (H3K27me2/me3) demethylase	histone modification; DNA methylation	
MH6	B9	96AL_189F1	F18E9.5	<i>jmjd-3.1</i>	histone H3 trimethyllysine-27 (H3K27me3) demethylase	histone modification; DNA methylation	
MH6	B10	GP 3A1	C33H5.7	<i>swd-2.2</i>	Set1 WD40 repeat protein	protein-protein interaction	WD40 repeats
MH6	B11	96AL_188G6	F22F1.1	<i>hil-3</i>	histone H1.3	chromatin structure	
MH6	B12	96AL_188G8	F22F1.3		transcription cofactor activity	transcription regulation	
MH6	C1	96AL_190G12	E01H11.1	<i>pkc-2</i>	protein kinase C.	protein kinase	
MH6	C2	96AL_195A3	C49F5.5		putative histone acetyltransferase activity	histone modification; DNA methylation	Zn finger
MH6	C3	96AL_192D6	F46F6.2	<i>pkn-1</i>	protein kinase N1.	protein kinase	
MH6	C4	96AL_195E3	W06D11.4		Histone-lysine N-methyltransferase, H3K79-specific	histone modification; DNA methylation	
MH6	C5	96AL_195E6	F17A2.3	<i>phf-32</i>	PHD zinc finger protein	chromatin binding	PHD finger
MH6	C6	96AL_194F5	C34E11.1	<i>rsd-3</i>	RNAi Spreading Defective	RNAi machinery	
MH6	C7	96AL_194F8	F54F7.1	<i>taf-7.1</i>	putative TATA binding protein associated transcription factor	transcription regulation	
MH6	C8	96AL_193G3	F38B2.1	<i>ifa-1</i>	Intermediate filament protein	Others (cell. structures)	
MH6	C9	96AL_192G9	F13E6.3	<i>phf-31</i>	PHD finger family	chromatin binding	PHD finger
MH6	C10	96AL_194G2	F54F7.7		Histone-lysine N-methyltransferase, H3K79-specific	histone modification; DNA methylation	
MH6	C11	96AL_192H3	T01C1.3	<i>mbr-1</i>	helix-turn-helix transcription factor	transcription regulation	homeodomain-like
MH6	C12	96AL_194H9	T08D10.2	<i>lsd-1</i>	ortholog of the human histone demethylase LSD1	histone modification; DNA methylation	
MH6	D1	96AL_194H12	C49F5.2	<i>set-6</i>	protein containing trithorax/polycomb SET domain.	histone modification; DNA methylation	SET domain
MH6	D2	96AL_197A1	K09A11.1		zinc finger family member.	DNA binding	Zn finger
MH6	D3	96AL_197A5	K09A11.5	<i>phf-33</i>	PHD-finger family protein like.	chromatin binding	PHD finger
MH6	D4	96AL_198A2	ZK108E.3		putative methyltransferase	histone modification; DNA methylation	Methyltransferase FkbM
MH6	D5	96AL_199A3	F23D12.5	<i>jmjd-3.2</i>	putative histone H3 di/trimethyllysine-27 (H3K27me2/me3) demethylase	histone modification; DNA methylation	
MH6	D6	96AL_199A6	M163.3	<i>his-24</i>	linker histone H1.1, essential for chromatin silencing and germline development: HIS-24 is retained in granular structures in the cytoplasm and this promotes germline development	chromatin structure/remodelling	
MH6	D7	96AL_197B5	F46G10.3	<i>sir-2.3</i>	and influences histone H3 methylation by the polycomb group genes MES-2/3/4/6.	histone modification; DNA methylation	
MH6	D8	96AL_197B9	F46G10.7	<i>sir-2.2</i>	similarity to the Saccharomyces cerevisiae Sir2p NAD-dependent histone deacetylase	histone modification; DNA methylation	
MH6	D9	96AL_198B8	F48F7.1	<i>alg-1</i>	similarity to the Saccharomyces cerevisiae Sir2p NAD-dependent histone deacetylase	RNAi machinery	
MH6	D10	GP 3A8	T13F2.3	<i>pis-1</i>	Argonaut ortholog	Others	BRCT domain
MH6	D11	96AL_196C11	T22H6.6	<i>gei-3</i>	ortholog of mammalian Pax transcription activation domain interacting protein PTIP	transcription regulation	HMG box
MH6	D12	96AL_197C10	C29F7.6	<i>jmjd-3.3</i>	member of the high mobility group (HMG) protein family	histone modification; DNA methylation	
MH6	E1	GP 3A11	R13.4	<i>miz-1</i>	putative histone H3 di/trimethyllysine-27 (H3K27me2/me3) demethylase	transcription regulation	Zn finger
MH6	E2	96AL_196D1	L14G8.1	<i>chd-3</i>	Miz-type Zn finger transcription factor	chromatin remodelling	chromodomain
MH6	E3	GP 4A5	F02D10.7	<i>set-8</i>	Chromodomain protein, DNA binding helicase Mi-2 like	histone modification; DNA methylation	SET
MH6	E4	GP 4F8	D1053.2		protein containing trithorax/polycomb SET domain.	histone modification; DNA methylation	SET
MH6	E5	96AL_198E5	F28H6.4		Histone-lysine N-methyltransferase, H3 lysine-79 specific	histone modification; DNA methylation	DOT1
MH6	E6	96AL_197F8	F54B11.6	<i>bra-1</i>	SPK-domain containing protein	DNA binding	SPK domain
MH6	E7	96AL_196H1K	K08H2.6	<i>hpl-1</i>	BMP receptor associated protein	NA/protein binding	Zn finger MYND
MH6	E8	GP 1B12	K06A5.8		Heterochromatin protein 1 homolog	chromatin structure	
MH6	E9	Supp I-9F2	ZK973.2	<i>cec-10</i>	protein containing WD40 repeats	protein-protein interaction	WD40 repeats
MH6	E10	96AL_201A12	F53H4.6		C. elegans chromodomain protein	chromatin remodelling	chromodomain
MH6	E11	96AL_202A6	F22H10.5		putative helicases	Others (helicases)	
					putative kinase	protein kinase	

MH6	E12	GP 4B1	C10E2.3	<i>hda-4</i>	histone deacetylase; Responsible for the deacetylation of lysine residues on the N-terminal part of the core histones (H2A, H2B, H3 and H4)	histone modification; DNA methylation	
MH6	F1	AL X-7C6	F53H4.5	<i>gmeh-2</i>	SAND family member.	transcription regulation	SAND domain
MH6	F2	AL X-4L16	C17G1.4	<i>nra-3</i>	Zn finger, PHD-type	chromatin binding	PHD finger
MH6	F3	AL X-7K21	K09A9.4	<i>usp-33</i>	Ubiquitin carboxyl-terminal hydrolase	ubiquitin machinery	
MH6	F4	96AL_S1A3	B0207.4	<i>air-2</i>	Serine/threonine-protein kinase which mediates both meiotic and mitotic chromosome segregation. Required for histone H3 'Ser-10' phosphorylation	protein kinase; histone modification; DNA methylation	
MH6	F5	96AL_S1A11	Y17F9B.7	<i>plk-2</i>	Ser/Thr-protein kinase	protein kinase	
MH6	F6	96AL_S1C3	Y47G6A.6	<i>pcaf-1</i>	C. elegans PCAF/GCN5-like histone acetyltransferase.	histone modification; DNA methylation	
MH6	F7	96AL_S1C6	Y71G12B.1	<i>chaf-2</i>	Chromatin Assembly Factor	chromatin structure	
MH6	F8	96AL_S1C12	Y119C1B.8	<i>tag-332 = bet-1</i>	BET-family protein that colocalizes with chromosomes; Bet-family proteins are evolutionarily conserved, have two bromodomains, which recognize acetylated histone	chromatin binding	bromodomain
MH6	F9	96AL_S2B3	T06D10.2	<i>chaf-1</i>	chromatin assembly like. RNA-dependent RNA polymerase (RdRP) homolog required for somatic (but not germline)	chromatin structure	
MH6	F10	96AL_S3A1	F26A3.8			RNAi machinery	
MH6	F11	96AL_S3A7	C41G7.4	<i>set-32</i>	a divergent histone H3 lysine-9 (H3K9) methyltransferase homolog with a SET domain	histone modification; DNA methylation	SET
MH6	F12	cloned	Y43F11A.5	<i>set-24</i>	protein containing trithorax/polycomb SET domain	histone modification; DNA methylation	SET
MH6	G1	96AL_S3C9	Y71A12B.9	<i>usp-3</i>	ubiquitin-specific protease	ubiquitin machinery	
MH6	G2	96AL_S3H3	Y74C9A.4	<i>rcor-1</i>	RCOR (REST CO-Repressor) homolog; similar to co-repressor of REST RE1-silencing transcription factor.	transcription regulation	SANT; Zn finger GATA
MH6	G3	96AL_S4B3	B0205.9		SPK-domain containing protein	DNA binding	SPK domain
MH6	G4	96AL_S5C9	Y92H12A.2		E3 ubiquitin-protein ligase	ubiquitin machinery	
MH6	G5	96AL_S6B1	ZK1320.12	<i>taf-8</i>	putative TATA binding protein associated transcription factor.	transcription regulation	
MH6	G6	Supp:II-1001:Y52E8A.2				DNA binding	Zn finger RING; PHD finger
MH6	G7	Supp:II-10A1C:Y48E1B.13		<i>csp-1</i>	caspase	Others (caspase)	
MH6	G8	96AL_S7B3	C13B4.2	<i>usp-14</i>	ubiquitin-specific protease	ubiquitin machinery	
MH6	G9	96AL_S7E2	Y17G7B.2	<i>ash-2</i>	C. elegans ortholog of Drosophila Ash2, a trithorax group protein that is a member of the conserved H3K4 trimethylation (H3K4me3) complex	histone modification; DNA methylation	
MH6	G10	96AL_S8B9	Y51H1A.4	<i>ing-3</i>	plant homeodomain-containing protein closely related to human ING3; PHD-type zinc finger mediates the binding to H3K4me3	chromatin binding	PHD finger
MH6	G11	96AL_S9A8	F10B5.7	<i>rff-3</i>	RNA-dependent RNA polymerase family member, mutants enhance RNA interference and resistance to viral infections.	RNAi machinery	
MH6	G12	96AL_S9E1	K12H6.11	<i>set-13</i>	protein containing trithorax/polycomb SET domain.	histone modification; DNA methylation	SET
MH6	H1	cloned	T07C4.11	<i>jmjd-4</i>	JmJc-domain containing protein	histone modification; DNA methylation	JmJc
MH6	H2	96AL_S14B12	Y47D3A.16	<i>rsk-1</i>	putative ribosomal protein S6 kinase (S6K) required additively with IFG-1 for normally high levels of protein synthesis	protein kinase	
MH6	H3	96AL_S14D1	Y71H2AM.8	<i>set-27</i>	protein containing trithorax/polycomb SET domain.	histone modification; DNA methylation	SET
MH6	H4	96AL_S15C3	BE0003N10.3		putative ubiquitin-protein transferase activity	ubiquitin machinery	
MH6	H5	96AL_S15E6	Y111B2A.16	<i>taf-7.2</i>	putative TATA binding protein associated transcription factor.	transcription regulation	
MH6	H6	96AL_S15H2	Y67D2.7		transcriptional regulator protein HCNGP like	transcription regulation	
MH6	H7	96AL_S18A1	F40F12.7		CREB binding protein like family member.	transcription regulation	Zn finger TAZ type
MH6	H8	96AL_S18H5	K03H1.10	<i>cbp-2</i>	CREB binding protein like family member.	transcription regulation	Zn finger TAZ type
MH6	H9	96AL_S20B6	VT23B5.1		ncRNA	others	
MH6	H10	96AL_S20C3	Y24D9A.2	<i>set-21</i>	protein containing trithorax/polycomb SET domain.	histone modification; DNA methylation	SET
MH6	H11	Supp:IV-9A24	Y37E11B.4	<i>taf-2</i>	putative TATA binding protein associated transcription factor	transcription regulation	
MH6	H12	Supp:IV-9G04	Y55F3AM.14		zinc finger C2H2 type protein.	DNA binding	Zn finger C2H2
MH7	A1	96AL_S23D3	C27B7.1	<i>spr-2</i>	C. elegans ortholog of the Drosophila and mammalian SET proteins; SPR-2 is predicted to be a member of the SET protein complex that functions in chromatin remodeling, DNA repair, and transcriptional regulation	chromatin remodelling / transcription regulation	
MH7	A2	96AL_S24A6	Y94H6A.6	<i>ubc-9</i>	ubiquitin conjugating enzyme	ubiquitin machinery	
MH7	A3	96AL_S28A6	F26F12.7	<i>let-418/evl-11, chd-4</i>	homolog of Mi-2/CHD3, a component of the nucleosome remodeling and histone deacetylase (NURD) complex; LET-418 is similar to DNA helicases	histone modification / chromatin remodelling	chromodomain; PHD finger
MH7	A4	96AL_S29A10	C01B7.6	<i>rpm-1/rpm-3/sam-1/sad-3/syd-3</i>	E3 ubiquitin-protein ligase	ubiquitin machinery	
MH7	A5	Supp:V-14E24	Y113G7B.23	<i>psa-1/swsn-1</i>	SWI3/SNF-related matrix-associated actin-dependent regulator of chromatin-like protein	DNA binding	SANT/Myb domain
MH7	A6	96AL_S30F4	K04A8.6	<i>dre-1</i>	F-box protein	ubiquitin machinery	F-box domain
MH7	A7	Supp:V-15E2C	D2023.4		thialysine N-(epsilon)-acetyltransferase, belonging to the GCN5-related N-acetyltransferase superfamily	histone modification; DNA methylation	GNAT domain
MH7	A8	96AL_S37C6	T07C12.14	<i>suds-3</i>	SUDS (vertebrate Suppressor of Defective Silencing) homolog	Others	
MH7	A9	96AL_S38D4	F59A7.4	<i>hil-6</i>	Putative histone H1.6	chromatin structure	
MH7	A10	96AL_S40C6	F55G7.2		DOT1 histone methyltransferase family	histone modification; DNA methylation	DOT1
MH7	A11	Supp:X-8G5	M163.2	<i>ztf-14</i>	Zinc finger putative Transcription Factor family	transcription regulation	
MH7	A12	Supp:X-8A4	F28H6.1	<i>akt-2</i>	homolog of the serine/threonine kinase Akt/PKB	protein kinase	
MH7	B1	96AL_S42B9	Y40A1A.1		protein kinase	protein kinase	
MH7	B2	Supp:X-8F5	F45B8.4	<i>pag-3</i>	C2H2 zinc-finger protein orthologous to Drosophila SENSELESS, and to human GF11	DNA binding	C2H2-type Zn finger
MH7	B3	VL_10002-F1	B0205.7	<i>kin-3</i>	ortholog of the catalytic subunit of casein kinase II alpha; serine/threonine kinase	protein kinase	
MH7	B4	VL_10012-B5	ZK909.2	<i>kin-1</i>	serine/threonine protein kinase that is orthologous to cAMP-dependent protein kinase	protein kinase	
MH7	B5	VL_10012-G1	ZK909.2	<i>kin-1</i>	serine/threonine protein kinase that is orthologous to cAMP-dependent protein kinase	protein kinase	
MH7	B6	VL_10013-E1	Y51H1A.4	<i>ing-3</i>	Proteins are expected to have molecular functions (NADH dehydrog96AL_se (ubiquinone) ac	chromatin binding	PHD-finger
MH7	B7	AL II-9E3	W03H9.1		Zn finger, PHD-type	chromatin binding	PHD-finger
MH7	B8	VL_10018-F9	B0207.4	<i>air-2</i>	aurora/tp1-related serine/threonine protein kinase	protein kinase	
MH7	B9	VL_10018-H5	Y48E1B.13	<i>csp-1</i>	caspase	Others (caspase)	
MH7	B10	VL_10020-C5	C13B4.2	<i>usp-14</i>	ubiquitin-specific protease 14 (Usp14), a highly conserved thiol protease that hydrolyzes the peptide bond at the C-terminal glycine of ubiquitin	ubiquitin machinery	
MH7	B11	VL_10020-C1	Y48E1B.13	<i>csp-1</i>	caspase	Others (caspase)	
MH7	B12	VL_10021-G6	F09E5.1	<i>pkc-3</i>	atypical protein kinase	protein kinase	
MH7	C1	VL_10022-F1	E01H11.1	<i>pkc-2</i>	protein kinases similar to the classical protein kinase C family	protein kinase	
MH7	C2	VL_10022-G5	R06A4.7	<i>mes-2</i>	ET domain-containing protein that is orthologous to the Drosophila Polycomb group protein Enhancer of zeste [E(Z)]; as a member of a Polycomb-like chromatin repressive complex	histone modification; DNA methylation	
MH7	C3	AL IV-3G8	C17H12.1	<i>dyci-1</i>	with MES-3 and MES-6 dynein intermediate chain	protein-protein interaction	WD repeats
MH7	C4	VL_10036-G4	Y54G2A.31	<i>ubc-13</i>	ubiquitin conjugating enzyme.	ubiquitin machinery	
MH7	C5	VL_10037-B1	Y87G2A.9	<i>ubc-14</i>	putative ubiquitin conjugating enzyme E2G 2.	ubiquitin machinery	
MH7	C6	VL_10051-F4	F40F12.7			DNA binding	Zn finger
MH7	C7	VL_10114-C8	C15F1.8			?	
MH7	C8	VL_10154-B1	F45B8.4	<i>pag-3</i>	C2H2 zinc-finger protein orthologous to Drosophila SENSELESS, and to human GF11	DNA binding	C2H2-type Zn finger
MH7	C9	Supp III-8F21	Y54H5A.1			chromatin binding	WD40, histone-binding protein RBBP4 N-terminal domain
MH7	C10	VL_11002-D3	Y37E11B.4	<i>taf-2</i>	member of the peptidase M1 family, a predicted aminopeptidase with similarity to human TBP-associated factor 2	transcription regulation	
MH7	C11	VL_11010-D1	Y47D3A.26	<i>smc-3</i>	SMC (structural maint96AL_nce of chromosomes) family	chromatin structure	
MH7	C12	VL_11010-E3	Y47D3A.16	<i>rsk-1</i>	putative ribosomal protein S6 kinase (S6K); Serine/threonine protein kinase family	protein kinase	
MH7	D1	AL IV-3C1	C06E7.3	<i>sams-4</i>	S-adenosyl methionine synthase	Others	
MH7	D2	VL_11013-D6	C01G8.9	<i>let-526</i>	component of the SWI/SNF complex	DNA binding	ARID (AT-rich interaction) domain
MH7	D3	GP 2G4	R10E11.1	<i>cbp-1</i>	homolog of the mammalian transcriptional cofactors CBP and p300 that have been shown to possess histone acetyltransferase activity	histone modification / transcription regulation	bromodomain; Zn finger
MH7	D4	cloned	F57C7.1	<i>bet-2</i>	PHD-finger containing protein	chromatin binding	PHD finger
MH7	D5	VL_11014-D1	F47G4.6	<i>hmg-6</i>	High mobility group box domain	DNA binding	HMG box cold-shock domain; CCHC Zn finger
MH7	D6	VL_11014-G3	F02E9.2	<i>lin-28</i>	heterochronic gene; miRNA interaction	NA binding	finger
MH7	D7	VL_11019-C1	Y54E10BR.8	<i>ztf-23</i>	Zinc finger putative Transcription Factor family	DNA binding	C2H2-type Zn finger
MH7	D8	VL_11019-G7	C41G7.4	<i>set-32</i>	SET-domain containing protein; histone H3 lysine-9 (H3K9) methyltransferase	histone modification; DNA methylation	SET
MH7	D9	VL_11020-H1	F33H2.7	<i>set-10</i>	SET (trithorax/polycomb)-domain containing	histone modification; DNA methylation	MYND-type Zn finger

MH7	D10	VL_11021-C3 Y74C9A.4	<i>rcor-1</i>		chromatin binding	SANT/Myb; Zn finger
MH7	D11	VL_11021-F5 Y47G6A.19		metallocarboxypeptidase	Others	
MH7	D12	VL_11021-H6 B0205.9		SPK-domain containing protein	DNA binding	SPK domain
MH7	E1	VL_11022-A2 Y71F9B.7	<i>plk-2</i>	Serine/threonine-protein kinase	protein kinase	
MH7	E2	VL_11022-A1 Y47G6A.6	<i>pcof-1</i>	C. elegans PCAF/GCN5-like histone acetyltransferase	histone modification; DNA methylation	
MH7	E3	Cloned C04F12.1	<i>vsr-1</i>	Argonaute protein	RNAi machinery	PIWI
MH7	E4	Cloned Y110A7A.13	<i>chp-1</i>	CHORD containing protein; germline RNAi	RNAi machinery	CHORD domain
MH7	E5	VL_11023-C6 Y71F9B.10	<i>sop-3</i>	Mediator of RNA polymerase II transcription subunit 1.1; Component of the Mediator complex, a coactivator involved in the regulated transcription of nearly all RNA polymerase II-dependent genes.	transcription regulation	
MH7	E6	VL_11023-D1 Y119C1B.8	<i>tag-332 = bet-1</i>	BET-family protein that colocalizes with chromosomes; Bet-family proteins are evolutionarily conserved, have two bromodomains, which recognize acetylated histone	chromatin binding	bromodomain
MH7	E7	Cloned Y37D8A.11	<i>cec-7</i>	C. elegans Chromodomain protein	histone modification; DNA methylation	chromodomain
MH7	E8	VL_11023-H1 K12C11.4	<i>dapk-1</i>	death-associated protein (DAP) kinase	protein kinase	ANK repeats
MH7	E9	Cloned K03D10.3	<i>mys-2</i>	MYST acetyltransferase	histone modification; DNA methylation	chromodomain
MH7	E10	VL_11025-B9 K05F1.2	<i>msp-142</i>	major sperm protein	Others	MSP
MH7	E11	Cloned R06C1.1	<i>hda-3</i>	histone deacetylase	histone modification; DNA methylation	histone-deacetylase domain
MH7	E12	VL_11031-H3 Y9D1A.1			others	
MH7	F1	Cloned C25A1.10	<i>dao-5</i>	nucleolar phosphoprotein related to Saccharomyces cerevisiae SRP40 and the vertebrate Nopp140 proteins that may play a role in rRNA gene transcription and nucleolar structural organization	rRNA-related	SRP40 domain
MH7	F2	VL_11036-D6 Y17G7B.2	<i>ash-2</i>	trithorax group protein that is a member of the conserved H3K4 trimethylation (H3K4me3) complex	histone modification; DNA methylation	
MH7	F3	Cloned H15N14.1	<i>adr-1</i>	ADAR (adenosine deaminase acting on RNA)	RNAi machinery	
MH7	F4	Cloned C43E11.11	<i>cogc-5</i>	Conserved Oligomeric Golgi (COG) Component	Others (cell. structures)	
MH7	F5	Cloned C18E3.7	<i>ppw-1</i>	PAZ/PIWI domain-containing protein; mutants are resistant to RNA interference in the germline.	RNAi machinery	PAZ/PIWI domain
MH7	F6	VL_11040-F5 B0035.10	<i>his-45 = his-55, F54E12.1 + many more</i>	histone 3	chromatin structure	
MH7	F7	Cloned B0261.1		DNA-binding protein	DNA binding	SANT/Myb domain
MH7	F8	HR B0261.1		DNA-binding protein	DNA binding	SANT/Myb domain
MH7	F9	Cloned Y73B3B.2	<i>set-28</i>	SET-domain containing protein	histone modification; DNA methylation	SET
MH7	F10	VL_11054-H2 Y71A12B.9	<i>usp-3</i>	Ubiquitin Specific Protease	ubiquitin machinery	
MH7	F11	VL_11054-H5 Y111B2A.22	<i>ssl-1</i>	SWI2/SNF2 family ATPase; may participate in a TRR-1/MYS-1/EPC-1/SSL-1 histone acetyltransferase complex	chromatin remodelling; histone modification	SWI/SNF
MH7	F12	VL_11055-F5 D2023.4		N-acetyltransferase	histone modification; DNA methylation	acetyltransferase domain
MH7	G1	Cloned Y110A7A.18	<i>ppw-2</i>	encoding PAZ/PIWI domain-containing.	RNAi machinery	PAZ/PIWI domain
MH7	G2	VL_11068-F5 F59A7.4	<i>hil-6</i>	Putative histone H1.6	chromatin structure	
MH7	G3	VL_11071-D1 K04A8.6	<i>dre-1</i>	F-box protein	ubiquitin machinery	F-box domain
MH7	G4	VL_11071-F1 Y113G7B.23	<i>psa-1/swsn-1</i>	SWI3/SNF-related matrix-associated actin-dependent regulator of chromatin-like protein	chromatin remodelling	SANT/Myb domain
MH7	G5	VL_11071-H9 F38B7.5	<i>duo-1</i>	deubiquitylating with USP/UBP and OTU domains; ubiquitin specific protease	ubiquitin machinery	USP domain
MH7	G6	VL_11077-B9 F55G7.2		Histone-lysine N-methyltransferase, H3 lysine-79 specific	histone modification; DNA methylation	
MH7	G7	VL_11081-E2 W10G6.2	<i>sgk-1</i>	serine/threonine protein kinase	protein kinase	
MH7	G8	VL_11201-B2 Y48E1B.13	<i>csp-1</i>	Caspase-related protein 1A	Others (caspase)	SPK domain
MH7	G9	VL_11303-F8 Y57A10A.3		SPK-domain containing protein	DNA binding	SPK domain
MH7	G10	VL_11304-E2 Y57A10A.6			others	
MH7	G11	JAP-MS box2 B0041.7	<i>xnp-1/slr-8</i>	Transcriptional regulator ATRX homolog; modifies gene expression by affecting chromatin; helicase	Others (helicases)	
MH7	G12	JAP-MS box2 C25F9.5			DNA binding	SNF2-related
MH7	H1	JAP-MS box2 Y111B2A.22	<i>ssl-1</i>	encoding SWI2/SNF2 family ATPase; may participate in a TRR-1/MYS-1/EPC-1/SSL-1 histone acetyltransferase complex	chromatin remodelling	SWI/SNF
MH7	H2	JAP-MS box2 F26F12.7	<i>let-418/evl-11, chd-4</i>	homolog of Mi-2/CHD3, a component of the nucleosome remodeling and histone deacetylase (NURD) complex; LET-418 is similar to DNA helicases	histone modification / chromatin remodelling	chromodomain; PHD finger
MH7	H3	JAP-MS box2 F19B2.5		transcription factor family member	DNA binding	SNF2-related
MH7	H4	JAP-MS box2 Y43F8B.14			DNA binding	SNF2-related
MH7	H5	JAP-MS box2 M04C3.1			DNA binding	SNF2-related
MH7	H6	Cloned Y71F9A1.18	<i>pme-1</i>	poly(ADP-ribosyl) transferase; homolog of PARP1 (chromatin associated enzyme)	chromatin binding	
MH7	H7	Cloned T21B4.4	<i>adar-1</i>	adenosine receptor like family member; closest homolog to Dnm11 (DNA-methyltransferase)	histone modification; DNA methylation	
MH7	H8	Cloned T23B5.1	<i>prmt-3</i>	protein arginine N-methyltransferase	histone modification; DNA methylation	
MH7	H9	Cloned C15H11.5	<i>set-31/tag-338</i>	protein containing trithorax/polycomb SET domain	histone modification; DNA methylation	chromodomain, SET
MH7	H10	Cloned R07B5.9	<i>lsy-12/mys-3</i>	MYST histone acetyltransferase	histone modification; DNA methylation	
MH7	H11	Cloned ZK380.5		RNAi-related	RNAi machinery	
MH7	H12	Cloned ZK616.4	<i>swsn-6/psa-13</i>	actin-like 6; Actin-related protein 4 (Arp4) is a component of chromatin-remodeling enzyme complexes; SWI/SNF	chromatin remodelling	
MH8	A1	Cloned Y92H12BR.6	<i>set-29</i>	protein containing trithorax/polycomb SET domain	histone modification; DNA methylation	SET
MH8	A2	Cloned Y37E3.15	<i>npp-13</i>	encoding nuclear Pore complex Protein nucleoporin 93; closely related to Nup35	Others (cell. structures)	
MH8	A3	Cloned Y39G10AR.18		homolog of DOT1L H3K79 methyltransferase	histone modification; DNA methylation	DOT1-like domain
MH8	A4	Cloned H12I13.1		SPK containing protein family member	DNA binding / kinase	SPK; kinase-like
MH8	A5	Cloned Y110A2AR.2	<i>ubc-15</i>	E2 ubiquitin-conjugating enzyme	ubiquitin machinery	
MH8	A6	Cloned Y41D4B.10	<i>dsf-3</i>	putative delta/Serrate/Lag-2 protein (Notch ligand)	Others (signalling)	DSL; EGF-like
MH8	A7	Cloned Y45F10C.1		encoding SPK containing protein family member	chromatin binding	SET, PHD, SPK
MH8	A8	Cloned F07B7.12	<i>targets rpm-1 as well</i>	regulator of chromosome condensation, RCC1 and PHR	chromatin remodelling	
MH8	A9	Cloned Y108F1.3	<i>set-33</i>	a putative histone H3 lysine-9 methyltransferase that is predicted to function in transcriptional repression; SET-33 is paralogous to SET-6, SET-15, SET-21, and SET-32	histone modification; DNA methylation	SET
MH8	A10	Cloned Y48G8AL.1	<i>herc-1/hpo-23</i>	regulator of chromosome condensation and HECT domain protein; homolog of human E6-AP ubiquitin-protein ligase	ubiquitin machinery	HECT (E6AP-type E3 ubiquitin-protein ligase) domain
MH8	A11	Cloned C18E3.2	<i>swsn-2.2</i>	homolog of Swp73/BAF60, a component of the SWI/SNF complex	chromatin remodelling	SWIB
MH8	A12	Cloned T04D1.4	<i>chd-7/tag-192</i>		chromatin remodelling	chromodomain; helicase domain
MH8	B1	Cloned Y46H3C.4	<i>targets K08E5.1 and top-2 as well</i>	beta-1 of topoisomerase II	chromatin remodelling	
MH8	B2	Cloned Y73B3B.1		ortholog of human plastin-3 isoform 2	chromatin remodelling	SPK
MH8	B3	Cloned CE7X_3.2			Others	Myc motif
MH8	B4	Cloned C04A2.3	<i>egl-27</i>	homolog of human MTA1, part of an ATP-dependent complex with nucleosome remodelling and histone deacetylation activities	chromatin remodelling	SANT; Zn finger
MH8	B5	Cloned F15D4.1	<i>btf-1</i>	member of the TBP-associated family (TAF)	DNA binding/helicase	
MH8	B6	Cloned T22B7.1	<i>egl-13</i>	transcription factor	transcription regulation	SOX domain
MH8	B7	Cloned B0564.11	<i>rde-11</i>	RNAi-defective	RNAi machinery	Zn finger
MH8	B8	Cloned C34B7.4	<i>mys-4</i>	MYST histone acetyltransferase; component of NuA4-like HAT complex	histone modification; DNA methylation	PHD finger
MH8	B9	Cloned M01E5.6	<i>sepa-1</i>	putative transcription cofactor	transcription regulation	KIX domain
MH8	B10	Cloned ZK1098.8	<i>mut-7</i>	exonuclease 3'-5' domain-containing protein 3 homolog	RNAi machinery	3'-5' exonuclease domain
MH8	B11	Cloned Y73E7A.9	<i>adpr-1</i>	ortholog of human isoform 1 of WD and tetratricopeptide repeats protein 1	chromatin binding	WD repeats
MH8	B12	Cloned F53H10.2	<i>saeg-1</i>	ortholog of human isoform 4 of Transcriptional-regulating factor 1	chromatin remodelling	SANT/Myb; Zn finger
MH8	C1	Cloned F21G4.4	<i>phf-34</i>	PHD-finger containing protein	chromatin binding	PHD finger

MH8	C2	Cloned	Y54E10A.11		FANCL homolog; E3 ubiquitin-protein ligase listerin	ubiquitin machinery	
MH8	C3	Cloned	W02D3.9	<i>unc-37</i>	transcription factor; transducin-like WD-repeat protein orthologous to Drosophila Groucho	transcription regulation	WD repeats
MH8	C4	Cloned	F59E12.9			others	
MH8	C5	Cloned	T01H8.1	<i>rskn-1</i>	Putative ribosomal protein S6 kinase alpha-1; Serine/threonine kinase	transcription regulation	N-acetyltransferase domain
MH8	C6	Cloned	Y49F6A.1	<i>wago-11</i>	Argonaute protein	RNAi machinery	PIWI/PAZ
					Catalytic histone acetyltransferase subunit of the RNA polymerase II elongator complex, which is a component of the RNA polymerase II (Pol II) holoenzyme and is involved in transcriptional elongation. Elongator may play a role in chromatin remodeling. May also have a methyltransferase activity	transcription regulation	
MH8	C7	Cloned	ZK863.3	<i>elpc-3</i>		RNAi machinery	PIWI/PAZ
MH8	C8	Cloned	F55A12.1	<i>wago-2</i>	Argonaute protein	chromatin binding	PHD finger
MH8	C9	Cloned	T06A10.4	<i>lsy-13</i>	PHD-finger containing protein	DNA binding	Zn finger C2H2
MH8	C10	Cloned	ZK337.2		Zn finger protein	RNA binding	
MH8	C11	Cloned	F56D12.5	<i>vig-1</i>	RNA-binding protein orthologous to Drosophila VIG	DNA binding	SPK
MH8	C12	Cloned	F59H5.1		SPK-containing protein		
					Probable 26S proteasome non-ATPase regulatory subunit 9; acts as a chaperone during the assembly of the 26S proteasome	ubiquitin machinery	
MH8	D1	Cloned	C44B7.1	<i>psmd-9</i>		RNAi machinery	
MH8	D2	Cloned	F52G2.2	<i>rsd-2</i>	RNAi Spreading Defective, required for systemic RNAi	RNAi machinery	
MH8	D3	Cloned	Y47G6A.4	<i>rde-10</i>	RNAi defective	transcription regulation	Zn PHD finger
MH8	D4	Cloned	C11G6.1	<i>taf-3</i>	putative TATA binding protein associated transcription factor	transcription regulation	C2H2 Zn finger
MH8	D5	Cloned	Y47D3A.6	<i>tra-1</i>	Sex-determining transformer protein 1	chromatin remodelling	SWIB (SWI/SNF)
MH8	D6	Cloned	T24G10.2		SWIB domain-containing protein	chromatin binding	PHD finger
MH8	D7	Cloned	Y54F10BM.14	<i>phf-5</i>		transcription regulation	
MH8	D8	Cloned	Y56A3A.4	<i>taf-12</i>	TATA binding protein associated transcription factor	chromatin binding	kinase-specific; PHD finger
MH8	D9	Cloned	C09E10.2	<i>dgk-1</i>	diacylglycerol kinase theta	histone modification; DNA methylation	Xn finger CXXC-type
MH8	D10	Cloned	Y7588A.6		methyltransferase activity	histone modification; DNA methylation	JmjC; ARID; PHD
					retinoblastoma Binding protein Related, demethylase specific for tri- and dimethylated lysine 4 on histone 3	NA binding	
MH8	D11	Cloned	ZK593.4	<i>rbr-2</i>		transcription regulation	Zn finger
MH8	D12	Cloned	K08F4.2			DNA binding	Zn finger
MH8	E1	Cloned	F54H5.4	<i>klf-3</i>	Kruppel-Like Factor (zinc finger protein)	ubiquitin machinery	Zn RING finger
MH8	E2	Cloned	Y116A8C.22	<i>athp-3</i>	AT hook motif containing protein	protein-protein interaction	WD repeats
MH8	E3	Cloned	C39F7.2	<i>trim-9</i>	E3 ubiquitin-protein ligase	chromatin binding	PHD finger
MH8	E4	Cloned	ZC302.2	<i>wdr-5.3</i>	WD repeat-containing protein	DNA binding	HMG domain
MH8	E5	Cloned	F33E11.6	<i>phf-10</i>	PHD-finger containing protein	protein-protein interaction	WD repeats
MH8	E6	Cloned	F40E10.2	<i>sox-3</i>	SOX (mammalian SRY box) related protein	chromatin binding	SANT domain
MH8	E7	Cloned	K04G11.4	<i>wdr-5.2</i>	WD repeat-containing protein	chromatin binding	SANT domain
					100% hom with F10E7.11	NA binding	cold-shock domain; CCHC Zn finger
MH8	E8	Cloned	T07F8.4		SANT-domain containing protein		
MH8	E9	Cloned	F10E7.11		SANT-domain containing protein		
MH8	E10	AL I-9L05	F02E9.2	<i>lin-28</i>	heterochronic gene; miRNA interaction		

Overview of all newly generated RNAi clones:

MH1	B8	cloned	C06A5.3		PSIP1 protein ortholog	protein-protein interactions	PWWP domain (Pro-Trp-Trp-Pro motif)
MH2	E7	Cloned	Y18H1A.10		homolog of Serine/Threonine-protein kinase haspin	protein kinase	kinase domain
MH3	E4	Cloned	R151.8		serine/threonine rich protein; CRAMP1L ortholog	chromatin binding	
MH6	F12	Cloned	Y43F11A.5	<i>set-24</i>	protein containing trithorax/polycomb SET domain	histone modification; DNA methylation	SET
MH6	H1	Cloned	T07C4.11	<i>jmjd-4</i>	JmJc-domain containing protein	histone modification; DNA methylation	JmjC
MH7	D4	Cloned	F57C7.1	<i>bet-2</i>	PHD-finger containing protein	chromatin binding	PHD finger
MH7	E3	Cloned	C04F12.1	<i>vsr-1</i>	Argonaute protein	RNAi machinery	PIWI
MH7	E4	Cloned	Y110A7A.13	<i>chp-1</i>	CHORD containing protein; germline RNAi	RNAi machinery	CHORD domain
MH7	E7	Cloned	Y37D8A.11	<i>cec-7</i>	C. elegans Chromodomain protein	histone modification; DNA methylation	chromodomain
MH7	E9	Cloned	K03D10.3	<i>mys-2</i>	MYST acetyltransferase	histone modification; DNA methylation	chromodomain
MH7	E11	Cloned	R06C1.1	<i>hda-3</i>	histone deacetylase	histone modification; DNA methylation	histone-deacetylase domain
					nucleolar phosphoprotein related to Saccharomyces cerevisiae SRP40 and the vertebrate Nopp140 proteins that may play a role in rRNA gene transcription and nucleolar structural organization	rRNA-related	SRP40 domain
MH7	F1	Cloned	C25A1.10	<i>dao-5</i>		RNAi machinery	
MH7	F3	Cloned	H15N14.1	<i>adr-1</i>	ADAR (adenosine deaminase acting on RNA)	Others (cell. structures)	
MH7	F4	Cloned	C43E11.11	<i>cogc-5</i>	Conserved Oligomeric Golgi (COG) Component	RNAi machinery	PAZ/PIWI domain
					PAZ/PIWI domain-containing protein; mutants are resistant to RNA interference in the germline.	DNA binding	SANT/Myb domain
MH7	F5	Cloned	C18E3.7	<i>ppw-1</i>		histone modification; DNA methylation	SET
MH7	F7	Cloned	B0261.1		DNA-binding protein	RNAi machinery	PAZ/PIWI domain
MH7	F9	Cloned	Y73B3B.2	<i>set-28</i>	SET-domain containing protein	chromatin binding	
MH7	G1	Cloned	Y110A7A.18	<i>ppw-2</i>	encoding PAZ/PIWI domain-containing.	histone modification; DNA methylation	chromodomain, SET
MH7	H6	Cloned	Y71F9AL.18	<i>pme-1</i>	poly(ADP-ribosyl) transferase; homolog of PARP1 (chromatin associated enzyme)	chromatin binding	
MH7	H7	Cloned	T21B4.4	<i>ador-1</i>	adenosine receptor like family member; closest homolog to Dnmt1 (DNA-methyltransferase)	histone modification; DNA methylation	
MH7	H8	Cloned	T23B5.1	<i>prmt-3</i>	protein arginine N-methyltransferase	histone modification; DNA methylation	
MH7	H9	Cloned	C15H11.5	<i>set-31/tag-338</i>	protein containing trithorax/polycomb SET domain	histone modification; DNA methylation	
MH7	H10	Cloned	R07B5.9	<i>lsy-12/mys-3</i>	MYST histone acetyltransferase	histone modification; DNA methylation	
MH7	H11	Cloned	ZK380.5		MYST-related	RNAi machinery	
					actin-like 6; Actin-related protein 4 (Arp4) is a component of chromatin-remodeling enzyme complexes; SWI/SNF	chromatin remodelling	
MH7	H12	Cloned	ZK616.4	<i>swsn-6/psa-13</i>		histone modification; DNA methylation	SET
MH8	A1	Cloned	Y92H12BR.6	<i>set-29</i>	protein containing trithorax/polycomb SET domain	Others (cell. structures)	
MH8	A2	Cloned	Y37E3.15	<i>npp-13</i>	encoding nuclear Pore complex Protein nucleoporin 93; closely related to Nup35	histone modification; DNA methylation	DOT1-like domain
MH8	A3	Cloned	Y39G10AR.18		homolog of DOT1L H3K79 methyltransferase	protein kinase	SPK; kinase-like
MH8	A4	Cloned	H12113.1		SPK containing protein family member	ubiquitin machinery	
MH8	A5	Cloned	Y110A2AR.2	<i>ubc-15</i>	E2 ubiquitin-conjugating enzyme	Others (signalling)	DSL; EGF-like
MH8	A6	Cloned	Y41D4B.10	<i>dsl-3</i>	putative delta/Serrate/Lag-2 protein (Notch ligand)	chromatin binding	SET, PHD, SPK
MH8	A7	Cloned	Y45F10C.1		encoding SPK containing protein family member	chromatin remodelling	
					targets <i>rpm-1</i> as well	histone modification; DNA methylation	SET
MH8	A8	Cloned	F07B7.12		regulator of chromosome condensation, RCC1 and PHR		
					a putative histone H3 lysine-9 methyltransferase that is predicted to function in transcriptional repression; SET-33 is paralogous to SET-6, SET-15, SET-21, and SET-32	ubiquitin machinery	HECT (E6AP-type E3 ubiquitin-protein ligase) domain
MH8	A9	Cloned	Y108F1.3	<i>set-33</i>		chromatin remodelling	
					regulator of chromosome condensation and HECT domain protein; homolog of human E6-AP ubiquitin-protein ligase	chromatin remodelling	SWIB
MH8	A10	Cloned	Y48G8AL.1	<i>herc-1/hpo-23</i>		chromatin remodelling	chromodomain; helicase domain
MH8	A11	Cloned	C18E3.2	<i>swsn-2.2</i>	homolog of Swp73/BAF60, a component of the SWI/SNF complex		
					targets <i>K08E5.1</i> and <i>top-2</i> as well	chromatin remodelling	SPK
MH8	B1	Cloned	Y46H3C.4		beta-1 of topoisomerase II	Others	Myc motif
MH8	B2	Cloned	Y73B3B.1		ortholog of human platin-3 isoform 2		
MH8	B3	Cloned	CE7X_3.2				

MH8	B4	Cloned	C04A2.3	<i>egl-27</i>	homolog of human MTA1, part of an ATP-dependent complex with nucleosome remodelling and histone deacetylation activities	chromatin remodelling	SANT; Zn finger
MH8	B5	Cloned	F15D4.1	<i>btf-1</i>	member of the TBP-associated family (TAF)	DNA binding/helicase	
MH8	B6	Cloned	T22B7.1	<i>egl-13</i>	transcription factor	transcription regulation	SOX domain
MH8	B7	Cloned	B0564.11	<i>rde-11</i>	RNAi-defective	RNAi machinery	Zn finger
MH8	B8	Cloned	C34B7.4	<i>mys-4</i>	MYST histone acetyltransferase; component of NuA4-like HAT complex	histone modification; DNA methylation	PHD finger
MH8	B9	Cloned	M01E5.6	<i>sepa-1</i>	putative transcription cofactor	transcription regulation	KIX domain
MH8	B10	Cloned	ZK1098.8	<i>mut-7</i>	Exonuclease 3'-5' domain-containing protein 3 homolog	RNAi machinery	3'-5' exonuclease domain
MH8	B11	Cloned	Y73E7A.9	<i>adpr-1</i>	ortholog of human isoform 1 of WD and tetratricopeptide repeats protein 1	chromatin binding	WD repeats
MH8	B12	Cloned	F53H10.2	<i>saeg-1</i>	ortholog of human isoform 4 of Transcriptional-regulating factor 1	chromatin remodelling	SANT/Myb; Zn finger
MH8	C1	Cloned	F21G4.4	<i>phf-34</i>	PHD-finger containing protein FANCL homolog; E3 ubiquitin-protein ligase listerin	chromatin binding	PHD finger
MH8	C2	Cloned	Y54E10A.11			ubiquitin machinery	
MH8	C3	Cloned	W02D3.9	<i>unc-37</i>	transcription factor; transducin-like WD-repeat protein orthologous to Drosophila Groucho	transcription regulation	WD repeats
MH8	C4	Cloned	F59E12.9			others	
MH8	C5	Cloned	T01H8.1	<i>rskn-1</i>	Putative ribosomal protein S6 kinase alpha-1; Serine/threonine kinase	transcription regulation	N-acetyltransferase domain
MH8	C6	Cloned	Y49F6A.1	<i>wago-1</i>	Argonaute protein	RNAi machinery	PIWI/PAZ
MH8	C7	Cloned	ZK863.3	<i>elpc-3</i>	Catalytic histone acetyltransferase subunit of the RNA polymerase II elongator complex, which is a component of the RNA polymerase II (Pol II) holoenzyme and is involved in transcriptional elongation. Elongator may play a role in chromatin remodeling. May also have a methyltransferase activity	transcription regulation	
MH8	C8	Cloned	F55A12.1	<i>wago-2</i>	Argonaute protein	RNAi machinery	PIWI/PAZ
MH8	C9	Cloned	T06A10.4	<i>lsy-13</i>	PHD-finger containing protein	chromatin binding	PHD finger
MH8	C10	Cloned	ZK337.2		Zn finger protein	DNA binding	Zn finger C2H2
MH8	C11	Cloned	F56D12.5	<i>vig-1</i>	RNA-binding protein orthologous to Drosophila VIG	RNA binding	
MH8	C12	Cloned	F59H5.1		SPK-containing protein	DNA binding	SPK
MH8	D1	Cloned	C44B7.1	<i>psmd-9</i>	Probable 26S proteasome non-ATPase regulatory subunit 9; acts as a chaperone during the assembly of the 26S proteasome	ubiquitin machinery	
MH8	D2	Cloned	F52G2.2	<i>rsd-2</i>	RNAi Spreading Defective, required for systemic RNAi	RNAi machinery	
MH8	D3	Cloned	Y47G6A.4	<i>rde-10</i>	RNAi defective	RNAi machinery	
MH8	D4	Cloned	C11G6.1	<i>taf-3</i>	putative TATA binding protein associated transcription factor	transcription regulation	Zn PHD finger
MH8	D5	Cloned	Y47D3A.6	<i>tra-1</i>	Sex-determining transformer protein 1	transcription regulation	C2H2 Zn finger
MH8	D6	Cloned	T24G10.2		SWIB domain-containing protein	chromatin remodelling	SWIB (SWI/SNF)
MH8	D7	Cloned	Y54F10BM.14	<i>phf-5</i>		chromatin binding	PHD finger
MH8	D8	Cloned	Y56A3A.4	<i>taf-12</i>	TATA binding protein associated transcription factor	transcription regulation	
MH8	D9	Cloned	C09E10.2	<i>dgk-1</i>	diacylglycerol kinase theta	chromatin binding	kinase-specific; PHD finger
MH8	D10	Cloned	Y75B8A.6		methytransferase activity retinoblastoma Binding protein Related, demethylase specific for tri-and dimethylated lysine 4 on histone 3	histone modification; DNA methylation	Xn finger CXXC-type
MH8	D11	Cloned	ZK593.4	<i>rbr-2</i>		histone modification; DNA methylation	JmjC; ARID; PHD
MH8	D12	Cloned	K08F4.2			NA binding	
MH8	E1	Cloned	F54H5.4	<i>klf-3</i>	Kruppel-Like Factor (zinc finger protein)	transcription regulation	Zn finger
MH8	E2	Cloned	Y116A8C.22	<i>athp-3</i>	AT hook motif containing protein	DNA binding	Zn finger
MH8	E3	Cloned	C39F7.2	<i>trim-9</i>	E3 ubiquitin-protein ligase	ubiquitin machinery	Zn RING finger
MH8	E4	Cloned	ZC302.2	<i>wdr-5.3</i>	WD repeat-containing protein	protein-protein interaction	WD repeats
MH8	E5	Cloned	F33E11.6	<i>phf-10</i>	PHD-finger containing protein	chromatin binding	PHD finger
MH8	E6	Cloned	F40E10.2	<i>sax-3</i>	SOX (mammalian SRY box) related protein	DNA binding	HMG domain
MH8	E7	Cloned	K04G11.4	<i>wdr-5.2</i>	WD repeat-containing protein	protein-protein interaction	WD repeats
MH8	E8	Cloned	T07F8.4	100% hom with F10E7.11	SANT-domain containing protein	chromatin binding	SANT domain
MH8	E9	Cloned	F10E7.11	100% hom with T07F8.4	SANT-domain containing protein	chromatin binding	SANT domain

CATEGORIES:

histone modification; DNA methylation
 RNAi machinery
 transcription regulation
 DNA/chromatin/histone binding, chromatin structure
 Chromatin remodelling
 ubiquitin machinery
 Protein-protein interactions; protein kinases; chaperones
 RNA binding/splicing
 Others (helicases, enzymes, translation, cell. structures, signalling)

Table S2 Efficiency of worm recovery from individual plates by the LPsampler.

		Mixture A	Mixture B	Mixture C
	# of <i>gcy-5p::gfp</i> worms	10	20	30
	# of <i>unc-119p::gfp</i> worms	40	30	20
remainders in well after LP sampler uptake	replicate #1A	1	0	0
	replicate #2A	0	0	0
	replicate #3A	1	0	2
	average %	1,33	0	1,33
transferred to new plate into corresponding well	replicate #1B	48	49	42
	replicate #2B	39	40	45
	replicate #3B	48	45	46
	average %	90	89,33	88,67
recovered worms after sorting for <i>gcy-5::gfp</i>	replicate #1C	10	18	27
	replicate #2C	10	18	28
	replicate #3C	7	16	22
	average %	90	86,67	85,56
recovered worms after sorting for <i>unc-119::gfp</i>	replicate #1D	31	23	18
	replicate #2D	39	28	17
	replicate #3D	38	29	16
	average %	90	88,89	85